12-2008

The application of a two-dimensional sediment transport model in a Cumberland Plateau mountainous stream reach with complex morphology and coarse substrate

Daniel Hale Johnson
University of Tennessee - Knoxville

To the Graduate Council:

I am submitting herewith a thesis written by Daniel Hale Johnson entitled "The application of a two-dimensional sediment transport model in a Cumberland Plateau mountainous stream reach with complex morphology and coarse substrate." I have examined the final electronic copy of this thesis for form and content and recommend that it be accepted in partial fulfillment of the requirements for the degree of Master of Science, with a major in Civil Engineering.

John S. Schwartz, Major Professor

We have read this thesis and recommend its acceptance:

Eric C. Drumm, Daniel C. Yoder

Accepted for the Council:
Carolyn R. Hodges

Vice Provost and Dean of the Graduate School

(Original signatures are on file with official student records.)

To the Graduate Council:

I am submitting herewith a thesis written by Daniel Hale Johnson entitled "The application of a two-dimensional sediment transport model in a Cumberland Plateau mountainous stream reach with complex morphology and coarse substrate." I have examined the final electronic copy of this thesis for form and content and recommend that it be accepted in partial fulfillment of the requirements for the degree of Master of Science, with a major in Civil Engineering.

_____

John S. Schwartz, Major Professor

We have read this thesis
and recommend its acceptance:

_____

Eric C. Drumm

_____

Daniel C. Yoder

Accepted for the Council:

_____

Carolyn R. Hodges, Vice Provost
and Dean of the Graduate School

(Original signatures are on file with official student records.)

The application of a two-dimensional sediment transport model in a Cumberland Plateau mountainous stream reach with complex morphology and coarse substrate

A Thesis
Presented for the
Master of Science
Degree
The University of Tennessee, Knoxville

Daniel Hale Johnson
December 2008

Abstract

Among river engineers there is growing recognition that the success of a stream restoration project is dependent on the accurate prediction of sediment transport along a reach. To aid the design process, several numerical one- and multi-dimensional models have been developed to quantify in-stream sediment transport and hydraulic characteristics, and multiple sampling techniques have been proposed to establish the upstream sediment supply. However, the governing physical boundaries and variables (i.e., Manning's 'n' variable, energy slope, and upstream sediment supply) required to initiate a sediment transport simulation are time consuming and difficult to measure in the field, and the estimation of these variables based on best professional judgment can lead to inaccurate predictions of sediment transport, resulting in the design of unstable projects. Thus, there exists a demand to understand the model sensitivity to key input parameters (i.e., Manning's n value and sediment rating curves), and their effects on sediment transport simulations, especially when input parameters must be estimated and results can not be verified easily.

The goal of this study was to evaluate the performance of CCHE2D, a two-dimensional sediment transport model, in a Cumberland Plateau mountainous stream reach with complex morphology and coarse substrate. The model was utilized to simulate sediment transport through a single hydrograph. Bed elevation change along a reach (100-m scale), was evaluated by comparing the deviation between simulated and measured elevations at multiple monitoring points before and after the simulated flood

event. The study objective included testing the sensitivity of overall bed change at a reach, local, and point scales to two key model inputs parameters, the Manning's n value and sediment supply.

Despite the relative stability observed along the site, simulated results show the model overestimated aggradation at a reach, local, and point scales. Statistical analysis of simulated results showed that bed elevation change was most sensitive to the bedload rating curve and Manning's n value input parameters. Importantly, the site-specific bedload rating curve and measured roughness coefficient have the potential to reduce the error between simulated and measured results if accurate simulations of sediment transport can be achieved by a computational model.

Acknowledgements

I would like to thank my advisors, UT faculty, fellow graduate students, family, and friends for their support and participation through this process. I would like to thank Dr. Schwartz for taking on the responsibility of yet another graduate student and serving as my major advisor. Dr. Schwartz allowed me to explore the application of a two-dimensional model, answered countless questions, and provided direction and insight during my research. I'd like to thank Dr. Drumm for providing a perspective based on his experience outside the discipline of fluid mechanics and sediment transport. Dr. Yoder's analysis of my methods and research objectives has ultimately resulted in a higher quality product. Dr. Yoder's focus on a defined research question, study design, and objectives helped establish a path for success during this research.

I would like to thank the University of Tennessee's faculty and staff. Larry Roberts and Ken Thomas assisted with the construction of the bedload traps. Ken provided skilled insight on the trap design and Larry acquired the materials and assisted with the fabrication. Despite the numerous graduate students and associated tasks, both were always willing to answer questions and provide insight into this research. In addition, the shop provided a location where a graduate student could step away from the strains and struggles of developing a thesis. Nancy Roberts provided insight and a helpful hand with the dry sieving analysis and other lab procedures.

I would like to thank the graduate students who assisted with various field operations, post processing of field data, and discussions concerning my research. Tom

Zimmerman, Joe Parker, and William Cantrell assisted with the collection of topographic data along Ligias Creek. Joe Parker and William Cantrell assisted with various field activates on numerous weekdays and several weekends. Without Will's and Joe's help this project would not be a success. Kyle Neff gave support with statistics and an insight into the development of a thesis that only a PhD student could provide. Patrick Massey and Patrick White were sponsored under the OSM contract and also provided assistance with field data collection, processing of suspended sediment data, and processing of the bedload sample.

I would like to thank Carolyn Ritchey, my girlfriend, for supporting my decision to obtain an advanced degree and supporting me through the trials and tribulations that are associated with the development of a thesis. My mom, Maggie Johnson, obtained her Doctor of Philosophy in the spring of 2008; her constant encouragement and insight allowed me to overcome the struggles associated with the graduate degree. I would like to thank all of my family and friends for providing the encouragement and support through out this process. Finally, I would like to thank the United States Department of the Interior Office of Surface Mining (OSM) for the 2nd Applied Science Program Grant, (2007), which funded my education and a portion of this study.

Table of Contents

List of Tables

List of Figures

Chapter 1: Introduction

Computational modeling in river engineering has the potential to increase our understanding of channel hydrodynamic and sediment transport processes (Jia et al., 2002; Jin & Steffler, 1993; Langendoen, 2001; Wu & Wang, 2004). Modeling is advantageous because: it offers real scale spatially dense results; it allows for the simulation of past, current, and future conditions governed by multiple boundary conditions; it provides significant cost advantages over the production of a physical model; and it provides a tool to address questions that have previously been restricted by time, scale, and resources (Lane et al., 1999; Wu, 2008). However, results produced by a computational model are dependent on how well the physical processes are mathematically described through governing equations, boundary conditions, and empirical formulas, on how accurately the differential governing equations are discretized using numerical schemes, on how effectively the discretized algebraic equations are solved using direct or iterative solutions methods, and on whether the numerical solution procedures are correctly coded using computer languages. The results will not be accurate if the physical boundary conditions (i.e., the topography and flow resistance) are not described accurately or if the numerical schemes and empirical formulas do no accurately represent the hydrodynamics and sediment transport processes occurring within the channel. Computational modeling must be validated using analytical solutions, flume and laboratory data, and data measured in the field for the results to be accepted and useful (Duan et al., 2007; Jia & Wang, 1999).

Numerous one- and multi-dimensional computational models have been developed to simulate the complex sediment transport and hydrodynamic processes within a stream channel (Appendix A; Langendoen, 2000 & 2001). These models are classified based on their formulation in the spatial and temporal continua (one-dimensional, two-dimensional, or three-dimensional, and steady versus unsteady flow simulation) and their application to sediment transport (suspended load, bedload, or total load simulation) (Papanicolaou et al., 2008). One-dimensional (1D) models (i.e., 3STD1, CONCEPTS, and HEC-6) simulate flow and sediment transport in the stream-wise, longitudinal channel direction without solving the details over the cross section. For this reason, these models are most applicable to the evaluation of long-term and reach scale processes in channels with longitudinal flow fields, limited hydraulic complexity, and minimal variation in channel geometry in the stream-wise direction (Formann et al., 2007; Waddle et al., 2000). Two-dimensional (2D) models (i.e., CCHE2D, DELFT2D, FLUVIAL 12, and MIKE 21) have greater application than 1D models, since structured grids are utilized to define bed topography and the capability to simulate the transverse velocity component; however, the increased complexity necessitates significantly more data input compared to 1D models (Lane et al., 1999). 2D models are most applicable to evaluate hydraulic changes induced by complex morphology at the local scale (100 m to 10 m) and over shorter periods. Three dimensional (3D) models (i.e., CCHE3D, Delft 3D, and MIKE3) allow for the simulation of complex flow fields and variations in velocity in the vertical direction (Dworak, 2005; Wu, 2008), but 3D models impose high demands on data collection and computational time. Combined with high resolution topographic data 3D models can provide a detailed analysis of local to point scale

processes (1 m to 0.01 m) and very short time periods. 2D sediment transport models provide for the simulation of the lateral and longitudinal velocity components, critical to the evaluation of sediment transport, but do not require the computational capacity of 3D models. For this reason the two-dimensional sediment transport model (CCHE2D) was applied in this study.

The ability of CCHE2D to simulate hydraulic (Jia et al., 2002; Jin & Steffler, 1993; Wu, 2004; Wu & Wang, 2006) and sediment transport (Duan et al., 2001; Wu, 2002; Wu et al., 2004) processes has been validated in multiple flume studies (Appendix B). However, few studies have utilized measured model inputs (i.e., sediment rating curves and the Manning's n value) to validate and test the ability of the model to simulate the complex sediment transport processes that occur in a natural channel; the highly variable data intensive model inputs make model calibration and verification of model output very difficult (Formann et al., 2007; Jia et al., 2006; Jiang et al., 2004; Scott & Jia, 2005; Wu, 2004). Due to these challenges, practitioners are often estimating critical input parameters and accepting simulated results without proper model calibration and validation data (Chen et al., 2007; Jia & Wang, 1999; Jia et al., 2006; Scott & Jia, 2005). Thus, there exists a demand to understand the sensitivity of the model to input parameters (i.e., Manning's n value and sediment rating curves) and their effects on sediment transport simulations, especially when input parameters must be estimated and results can not be verified (Duan et al., 2007; Jia & Wang, 1999).

The goal of this study was to evaluate the performance of CCHE2D, a two-dimensional sediment transport model, in a complex stream reach with coarse substrate. The model was utilized to simulate a single hydrograph, bed elevation change along a

reach (100 m scale), and was evaluated by comparing the deviation between simulated and measured bed elevation change at multiple monitoring points before and after the simulated flood event. The study objective included testing the sensitivity of overall bed change at a reach, local, and point scales to two key model inputs parameters, the Manning's n value and sediment supply. The sensitivity analysis was performed by quantitatively comparing observed and simulated bed elevation changes at various monitoring points based on the adjustment of the Manning's n value and sediment rating curve at the upstream model boundary. Understanding the sensitivity of these input parameters will support model use by practitioners, particularly in the area of stream restoration, by providing valuable information to direct time limited resources and measurements that may result in a more accurate simulation of sediment transport and corresponding bed elevation change along a reach.

Chapter 2: Methods

2.1 Study design

A single storm event was modeled using CCHE2D to test the performance of the two-dimensional sediment transport model along a complex channel reach of Ligias Creek. The following sections detail the data collection, field data post processing, model development and model simulations. Field activities were conducted on Ligias Creek, beginning on January 24th, 2008 and ending on May 5th, 2008. Field activities included a topographic survey, flow measurements, bed sediment characterization, suspended sediment sampling, and bedload sediment measurement. Post processing activities included dry sieving the bedload sample and post processing data in Autodesk™ Land Desktop and Microsoft™ excel. All model simulations were performed using CCHE2D-GUI version 3.15 and CCHE2D mesh generator version 3.07. Table 1 illustrates the data collected for this study.

Ligias Creek is located in the Cumberland Plateau mountain near Briceville, TN The upstream extent of the project is located at approximately 36° 12' 23.90" North and 84° 18' 51.63" West. The downstream extent of the project is located at approximately 36° 12' 23.15" North and 84° 19' 02.77" West. It is a complex stream dominated by coarse substrate. Site aerial images and pictures are included in Appendix C.

Table 1: Summary of data collected

Variable required to simulate a 2D sediment transport model	Action or measurement	Dates
Channel and bed topography (2D mesh)	Topographic Survey	Jan. 24th to March 3rd
Roughness coefficient (Energy slope)	Upstream Stage Recorder Installed	March 28th
Downstream Boundary Condition (Water surface elevation)	Downstream Stage Recorder Installed	January
Upstream suspended sediment supply	Suspended Load measurements	Jan. 8th to March 8th
Upstream bedload supply	Bedload Trap Sample	March 4th at 16:42:03
Bed gradation	Wolman Pebble count	Feb. 14th
Upstream Boundary Condition (Discharge)	Measured in-stream velocities	Jan. 8th to March 8th
	Measured bed change (Monitoring Points)	March 6th

2.2 Field measurements and processing

Model development required topographic surveys, flow measurements and the development of a stage-discharge curve, bed sediment characterization, development of a suspended sediment rating curve, bedload collection during the modeled storm event and a particle size distribution analysis of the bedload sample, and computation of a bedload rating curve.

2.2.1 Topographic survey

Channel topographic data was collected using standard topographic surveying techniques along 257 m of Ligias Creek, prior to the modeled storm event. A Trimble™

3600 series total station and Trimble™ Recon Pocket PC were utilized to collect the channel topographic data. The survey began at the downstream extent and proceeded in the upstream direction. A benchmark was established near the downstream modeling boundary at an elevation of 30.4878 m. 3,234 points were collected along multiple transects perpendicular to the direction of flow. The average transect spacing was approximately 3 meters. Major breaks in slope were identified in the field and recorded to provide a more accurate interpolated surface within the CCHE2D mesh generator. Areas with a large change in elevation were identified and defined with a higher density of points.

AutoDesk™ Land Desktop 2007 (Land Desktop) was utilized to process the survey data. The process was performed as follows: a JOB (.job) file was transferred from the Trimble Recon Pocket PC to a desktop computer using Microsoft™ ActiveSync, then converted to an ASCII formatted file and imported into Land Desktop. Land Desktop was used to visually inspect, process, and review the survey data. After review, the data were exported as an ASCII file in the following format (point number, northing, easting, elevation, point description). Appendix D describes in detail the process associated with importing the ASCII file into the CCHE2D mesh generator.

2.2.2 Flow measurements

A Global Water™ stage recorder (model number WL-16) was installed near the downstream extent of the project reach prior to the beginning of the project. This stage recorder provided stage readings at least every 20 minutes throughout the project duration.

An identical stage recorder was installed at the upstream extent of the project reach on March 28th, 2008. The upstream stage recorder was installed to provide the data necessary to calculate an energy slope along the reach. The energy slope was calculated as the difference between the measured upstream and downstream water surface elevations divided by the flow length between the two stage recorders, which was 209 m. Both the upstream and downstream stage recorders were programmed to take readings every 10 minutes from the time of installation of the upstream stage recorder.

The data collected from both stage recorders and the corresponding calculated energy slope were utilized to calibrate the one-dimensional hydraulic model, HEC-RAS. Once calibrated, the HEC-RAS model was used to simulate discharges and corresponding stage heights in excess of values measured in the field. Stage-discharge relationships were developed according to standard USGS procedures (Buchanon & Somers, 1969). The process of calibrating the HEC-RAS model and development of the stage-discharge relationship is discussed in detail in Appendix E.

2.2.3 Bed sediment characteristics

A pebble count was performed, following the procedure outline by Wolman (1954), at a cross section that contained substrate representative of the project reach. Sampling consisted of measuring the intermediate axis of one hundred sand to gravel sized particles selected from the bed along a representative transverse section. The results were utilized to define the bed gradation along the reach length. Results are included in Appendix F.

2.2.4 Suspended sediment

Measured suspended load data, provided by Massey (2008), were utilized to develop a suspended load rating curve as a function of discharge. Additional information concerning suspended sediment sampling and post processing can be found in Appendix G and in Massey (2008).

2.2.5 Bedload sediment measurement

Bedload was sampled with constructed portable bedload traps; trap construction is discussed in detail in Appendix H. The traps were installed during four storm events, but only one bedload sample was collected, on March 4th, 2008. This sample was characterized via a dry sieve analysis at the Civil Engineering Geotechnical Laboratory at the University of Tennessee, Knoxville to define the particle size distribution of the sample. The standard procedures for a particle-size analysis of soils (ASTM D421 and ASTM D422) were followed. A mechanical sieve shaker was utilized to determine the particle size distribution of the bedload sample. Particles smaller then 3.75 mm have the potential of passing through the trap netting uninhibited; for this reason, and based on available sieve sizes, a sieve size of 4.75 mm was the smallest sieve utilized during the dry sieve testing.

2.2.6 Bedload rating curve

The collected bedload sample did not provide adequate data to develop a bedload rating curve, thus a bedload rating curve was developed using the Meyer-Peter and Muller (MPM) empirical transport formula (Sturm, 2001). As discussed in Appendix E,

HEC-RAS was utilized to predict the water surface elevations at the upstream cross section and energy slope along the reach at discharges that exceeded measured values. The data set, measured and simulated, included energy slope, downstream and upstream stages, and a corresponding discharge at each time interval throughout the hydrograph. The energy slope along the reach was measured, however the energy slope was not measured upstream of the model boundary. For this reason, an assumption was made that the energy slope at the upstream model boundary was equivalent to the energy slope along the reach. This information, in conjunction with the critical diameter for initiation discussed in the following paragraph, was used to calculate the volumetric transport rate per unit width in square feet per second (ft^2/s) through the duration of the simulated storm event using the MPM formula. The results were converted to kilograms per meter per second (kg/m/s) and applied at the upstream boundary condition. Calculations are illustrated in Appendix I.

A hiding coefficient was implemented to account for the coarse, widely graded, sediment bed exhibited along Ligias Creek (Langendoen, 2000 and 2008). The critical diameter for each size class within CCHE2D was calculated via Equation 1.

$$d_{c,k} = d_k \left(\frac{\bar{d}}{d_k} \right)^{\chi} \tag{1}$$

where,

$d_{c,k}$ = critical diameter for initiation of size class k

$\bar{d}$ = mean size of the bed material

χ = hiding coefficient

When χ is equal to a value of 1, the mean size of the sediment is the critical diameter for all size fractions and all fractions tend to move at the same flow strength. When χ is equal to a value of 0, each size fraction behaves independently of the others, and the d_k for each size fraction is used to calculate flow strength at which motion begins. Based on personal correspondence with Eddy Langendoen (2008), a hiding coefficient equal to a value of 0.7 was implemented to represent the bimodal gravel substrate defining the bed gradation.

2.3 Model development and simulation

To evaluate the performance of CCHE2D, multiple simulations were performed with various input parameters (i.e., the Manning's n value and sediment rating curves), with the selection of these parameters targeted to equate simulated and measured bed elevation change at a reach scale. After evaluating the performance, additional model simulations were conducted with additional parameters to understand the sensitivity of the simulation of bed elevation change at a reach, local and point scales to these parameters. The bedload rating curve, calculated with the MPM formula, and the suspended load rating curve, developed based on measured results, are defined by 100% suspended and 100% bedload; 80% suspended load and bedload refers to scaling the suspended load and bedload discharges by 80% at each time step.

The general procedure of a numerical simulation (i.e., generating the mesh, specify the boundary conditions, assigning the flow and sediment parameters, performing the simulation, and visualizing the results), and its application to this specific study is discussed in detail in the following paragraphs.

2.3.1 CCHE2D - mesh generator

A computational mesh is required to represent the physical domain defined by the topography of a site. The computational mesh for Ligias Creek was generated with the CCHE2D mesh generator version 3.07 and the topographic survey data, processed in Land Desktop and formatted as described in Appendix D. An outer boundary condition was created based on the extents of the survey data. Once a boundary had been created an algebraic mesh was generated. The algebraic mesh consisted of interior mesh nodes based on the specified maximum number of both I and J lines. J lines are defined as perpendicular to the flow direction, and I lines are parallel to the flow direction for all model simulations within the scope of this project. Based on CPU constraints, a value of 100 was specified for I_{max} and a value of 125 was specified for J_{max}. The iteration number was set to a value of 10. Once the mesh was generated, the mesh evaluation tool was implemented to determine the minimum and maximum cell length in both the I and J directions.

After the mesh grid was generated, random interpolation was performed to create the topographic surface. The resulting surface was saved as a geometry file (.geo) and the associated workspace file was saved with a (.mesh_wsp) extension.

2.3.2 CCHE2D GUI (Graphical User Interface)

The geometry file created in the mesh generator was then opened utilizing CCHE-GUI version 3.15. The graphical user interface or GUI allowed for interaction with the CCHE code and algorithms via graphical icons and pull down menus. The following sections detail the definition of the flow initial conditions, bed material properties, flow parameters, sediment parameters, sediment boundary conditions, and inlet and outlet boundary conditions.

2.3.2.1 Flow initial conditions

The initial bed elevations were imported into the GUI via the geometry file created in the mesh generator. The initial water surface elevations recorded at the upstream and downstream stage recorders, prior to the simulated storm event, were rounded to the nearest meter and utilized to establish the upstream and downstream initial water surface elevations in the model. The upstream initial water surface elevation was set equal to 30.0 m and the downstream initial water surface elevation was set equal to 29.0 m. Values between the upstream and downstream boundaries were interpolated in the J direction or perpendicular to the flow direction

2.3.2.2 Bed material properties

The bed roughness value was one of the variables that was modified between simulation runs as part of the sensitivity analysis objective. However, the chosen bed roughness value was assigned to the whole domain in all simulations. The bed erodibility

was set equal to a value of 1.0 for the whole domain. This value allows the bed to erode throughout the domain. The maximum deposition and erosion thickness were set equal to 90.0 m and -90.0 m respectively. These values allow each node to increase in elevation up to 90.0 m, above the initial bed elevation, and erode up to -90.0 m below the initial bed elevation. Very large erosion and deposition thicknesses were specified to indicate that no limit exist corresponding to the simulated aggradation and degradation along the reach. One bed layer was utilized to define the entire domain; the thickness of this layer was set to equal a value of 10.0 m. The bed gradation was defined by the Wolman pebble count results. The bed erodibility, maximum deposition and erosion thickness, and bed gradation and thickness remained constant through all simulations.

2.3.2.3 Flow Parameters

The total simulation period was 2 days, 10 hours, and 42 minutes or 211,320 seconds. This time series represented the storm event which produced measured bedload and corresponding bed elevation change along the reach. The time step increment, measured in seconds, was decreased until the model was successful in performing a simulation without producing a "floating overflow" or "floating invalid" error. A time step of 1 or 2 seconds allowed the model to complete a simulation without errors. To reduce computational time, a time step of 2 seconds was utilized in a majority of the simulations.

In addition the turbulence closure is defined in the flow parameter menu. The parabolic eddy viscosity model was utilized for all simulations. The turbulent viscosity

coefficient was set to a value of 1.0. Thus, the turbulent viscosity is equal to the value computed from the parabolic eddy viscosity model turbulent closure scheme. Khan (2003) suggest that a value of 1.0 is sufficient for most applications.

Unsteady flow sediment transport simulations require a great deal of time due to the interpolation of discharge, suspended sediment concentration (kg/m^3) and bedload (kg/m/s) between time steps. To increase the computational efficiency, unsteady flow was computed as quasi-steady for all simulation runs. The discharge and sediment are considered constant and simulations are performed as steady flow during a quasi-steady time step. A value of 20 or 40 was used for the number of time steps to reach steady state conditions. To reduce computational time, at time step of 20 was utilized in a majority of the simulations. An unsteady flow hydraulic simulation, utilizing the discharge and stage hydrographs for a duration of 3600 seconds or 1 hour, provided a starting condition for the quasi-steady simulation. The quasi-steady simulation was performed for the remainder of the storm event.

2.3.2.4 Sediment parameters

Ten sediment size classes were defined in CCHE2D based on a qualitative analysis of the pebble count and bedload sample data and associated particle size distributions. Each size class is defined by a mean diameter. A mean diameter of 2 mm was assigned to represent suspended sediment. The remaining nine size classes were defined to accurately represent the bed gradation and bed material available for transport. Each size class is defined in the "Set Sediment Samples" simulation menu. These size

classes were incorporated into the definition of the bed gradation, suspended load rating curve, and bedload rating curve for each model simulation. The minimum mixing layer thickness, used to confine the bed erosion process, was set to a value of 0.05 m (Zhang, 2006). "Total load as bedload plus suspended load" was selected as the transport mode; and the Wu et al. (2001) formula was utilized for the sediment transport computations. The adaptation length for bedload was set as the average grid length and the adaptation factor for suspended load is based on Armanini and di Silvio (1988). Values in the geometry file (.geo) were specified as containing the Manning's n values. Bank erosion was not simulated for this project, because banks erosion was not observed along the project reach.

2.3.2.5 Sediment and hydraulic boundary conditions

The upstream sediment boundary conditions included a suspended sediment boundary condition file (.sbc) and a bedload boundary condition file (.bbc). Incoming sediment was defined as a function of time for each predefined size class for both conditions. A time step of 20 minutes was implemented in both the bedload and suspended load boundary condition files. Suspended sediment discharge has the units of (kg/m^3) and bedload has the units of (kg/m/s).

All simulations involved specifying a discharge hydrograph at the upstream extent of the project reach and a stage hydrograph at the downstream boundary condition. The stage discharge curve, discussed in Appendix E, was implemented to calculate discharge at each stage during the simulated storm event. The calculated discharge at each stage

was then associated with a time via the time series and stage recorded at the downstream stage recorder during the storm event. The downstream boundary condition was defined by a stage hydrograph. The stage hydrograph was created based on data collected from the downstream stage recorder during the simulated storm event. This data was associated with time to produce the stage hydrograph.

2.4 Model performance and evaluation

A monitoring survey was performed in addition to the topographic survey in order to evaluate model performance. On March, 6th 2008, after the actual storm event that was ultimately simulated, field crews returned to the study site and resurveyed seventeen predetermined points, here after referred to as monitoring points, along the reach. Monitoring points were identified in locations that were isolated from the effects of wood debris or in-stream structures (i.e., minimized point locations in recirculation zones), that had the potential to represent reach scale bed elevation changes (i.e., aggradation or degradation along the reach), and that were located along the main flow path. The monitoring points are shown in Figure 1. The monitoring survey data allowed for the calculation of actual bed elevation change due to the simulated storm event. Model output at the monitoring point locations was then compared with measured data, and deviations between simulated and measured results were computed.

The seventeen monitoring points were identified within CCHE2D by formatting the monitoring survey data as a (.mesh_xyz) file and importing them into the CCHE2D-GUI. The data probe tool was utilized to identify the nodes surrounding each monitoring

point; each monitoring point was defined by at least four surrounding nodes. Points located directly on a J or I line included the identification of six surrounding nodes. Groups of aggregated monitoring points were utilized to further test the correlation between the model simulations and measured results. Five groups were identified based on the spatial proximity of the points along the reach; the monitoring points comprising each group are presented in Table 2 and shown in Figure 1.

Measured and simulated reach scale bed elevation change was calculated as the average of bed elevation change at each of the 17 monitoring points. Measured and simulated bed elevation change for each group was calculated as the average of the bed elevation change at each of the monitoring points defined within a group. Simulated point scale bed elevation change or bed elevation change at each monitoring point was calculated as the average bed elevation change of the surrounding nodes.

2.4.1 Statistical analysis

The SAS™ JMP statistical software was used to analyze the significance of the different independent variables (bedload, suspended load, and the Manning' n value) on

Table 2: Monitoring point groups

Group 1	Group 2	Group 3	Group 4	Group 5
MP-1883	MP-1490	MP-843	MP-378	MP-199
MP-1873	MP-1463	--	MP-373	--
MP-1871	MP-1464	--	MP-237	--
MP-1869	MP-1424	--	--	--
MP-1868	MP-1425	--	--	--
MP-1859	--	--	--	--
MP-1866	--	--	--	--

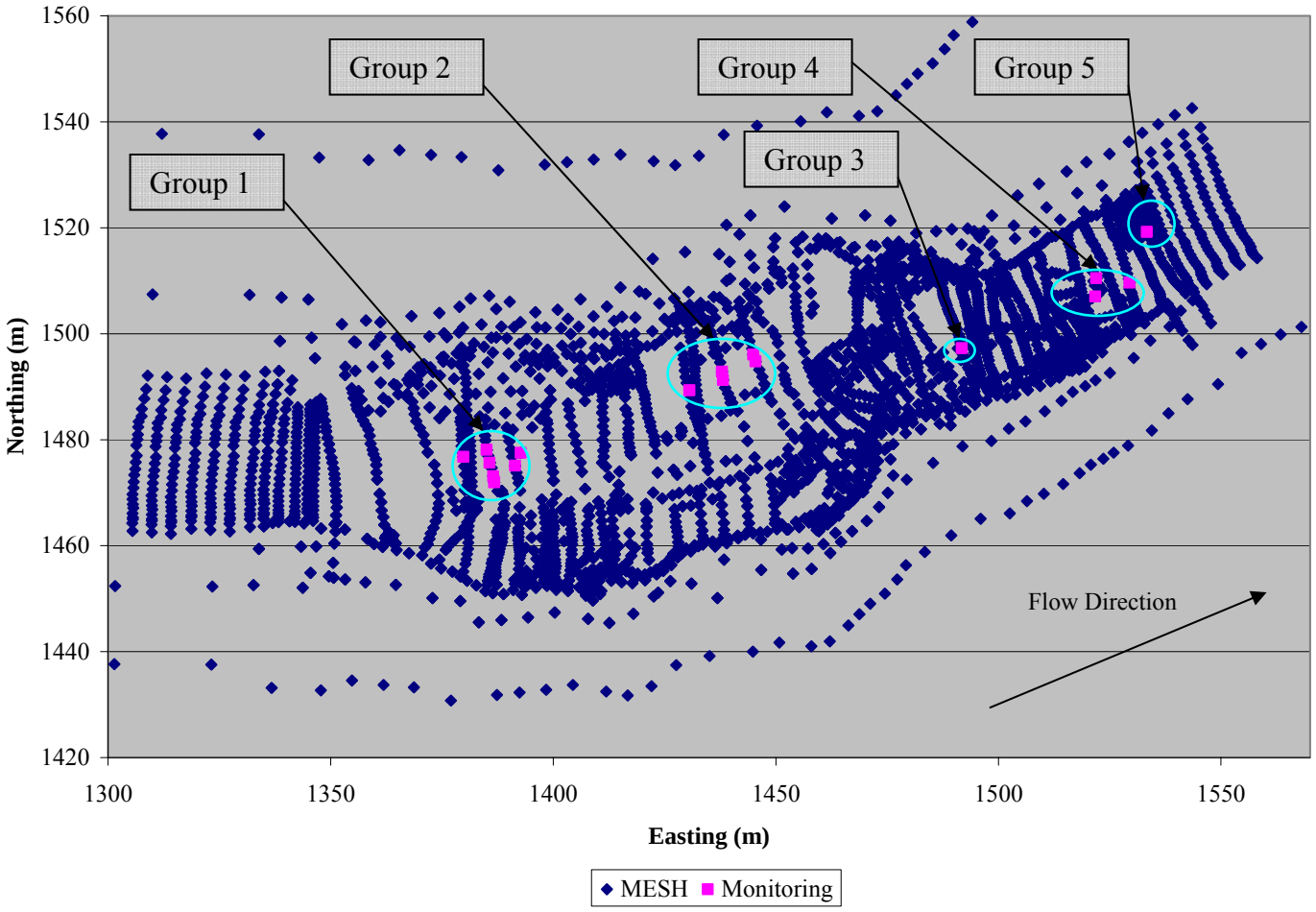

Figure 1: Monitoring points and point groups

simulated bed elevation change at a reach, local, and point scale. Four multivariate analyses were performed utilizing the results produced by successful model simulations. The independent variables remained constant throughout the four analyses; these included the suspended load rating curve, the bedload rating curve, and the Manning's n value. The first analysis included 72 dependent variables, defined by the bed elevation change at each node surrounding a monitoring point. The second analysis included the reach scale bed elevation change results produced by successful model simulations. The third analysis included the group scale bed elevation change results. The final analysis included the bed elevation change at each monitoring point.

Chapter 3: Results

3.1 Field measurements and processing

3.1.1 Flow measurement

Validation of the HEC-RAS model is included in Appendix E. Simulated water surface elevations matched within 0.5% of measured water surface elevations at the upstream and downstream stage recorders. The simulated and measured energy slope, upstream and downstream stage, and discharge data are included in Appendix E.

3.1.2 Bed sediment characteristics

A summary of the pebble count results is presented in Table 3. The pebble count data set is included in Appendix F. The sampled particle sizes ranged from 2 mm to 180 mm, with a median diameter of 66 mm.

Table 3: Summary of pebble count results

Summary of Pebble Count	
	Millimeters
Minimum size	2
Maximum size	180
d_{16}	28
d_{50}	66
d_{84}	105
d_{90}	115

3.1.3 Suspended sediment

Suspended sediment loads are often estimated from an empirical relation between suspended sediment load and stream flow (Crawford, 1991). This relation is often defined as a power function, and is referred to as a suspended sediment rating curve. Based on measured suspended load samples two power functions were developed to define the suspended load concentration with respect to discharge, as illustrated in Equations 2 and 3. Figure 2 illustrates the measured suspended load concentrations (ppm) plotted versus discharge (i.e., the suspended load rating curve) and the corresponding power relationships.

$$q_s = 122.21(Q)^{0.5074} \quad \text{for } 13.6 \text{ m}^3/\text{s} < Q \tag{2}$$

$$q_s = 18.995(Q)^{1.221} \quad \text{for } 0.0 \text{ m}^3/\text{s} < Q < 13.6 \text{ m}^3/\text{s} \tag{3}$$

where,

q_s = Total suspended sediment concentration (ppm)

Q = discharge (m^3/s)

Equations 2 and 3 were used to develop the upstream suspended sediment rating curve. The suspended load rating curve and associated flow discharge values are plotted versus time in Figure 3. The corresponding suspended sediment hydrograph file (.sbc), employed at the upstream model boundary, is included in Appendix J.

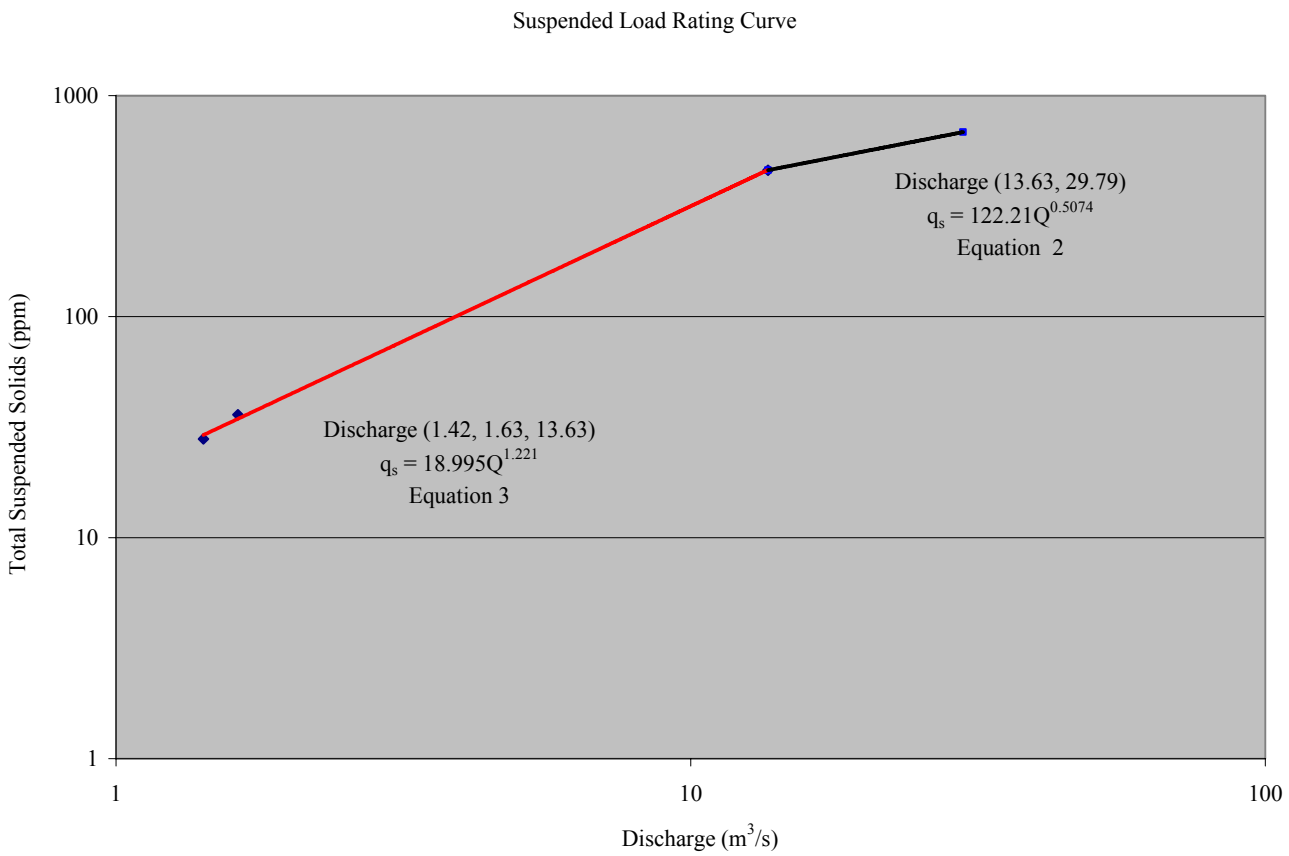

Figure 2: Suspended sediment measurements plotted versus discharge

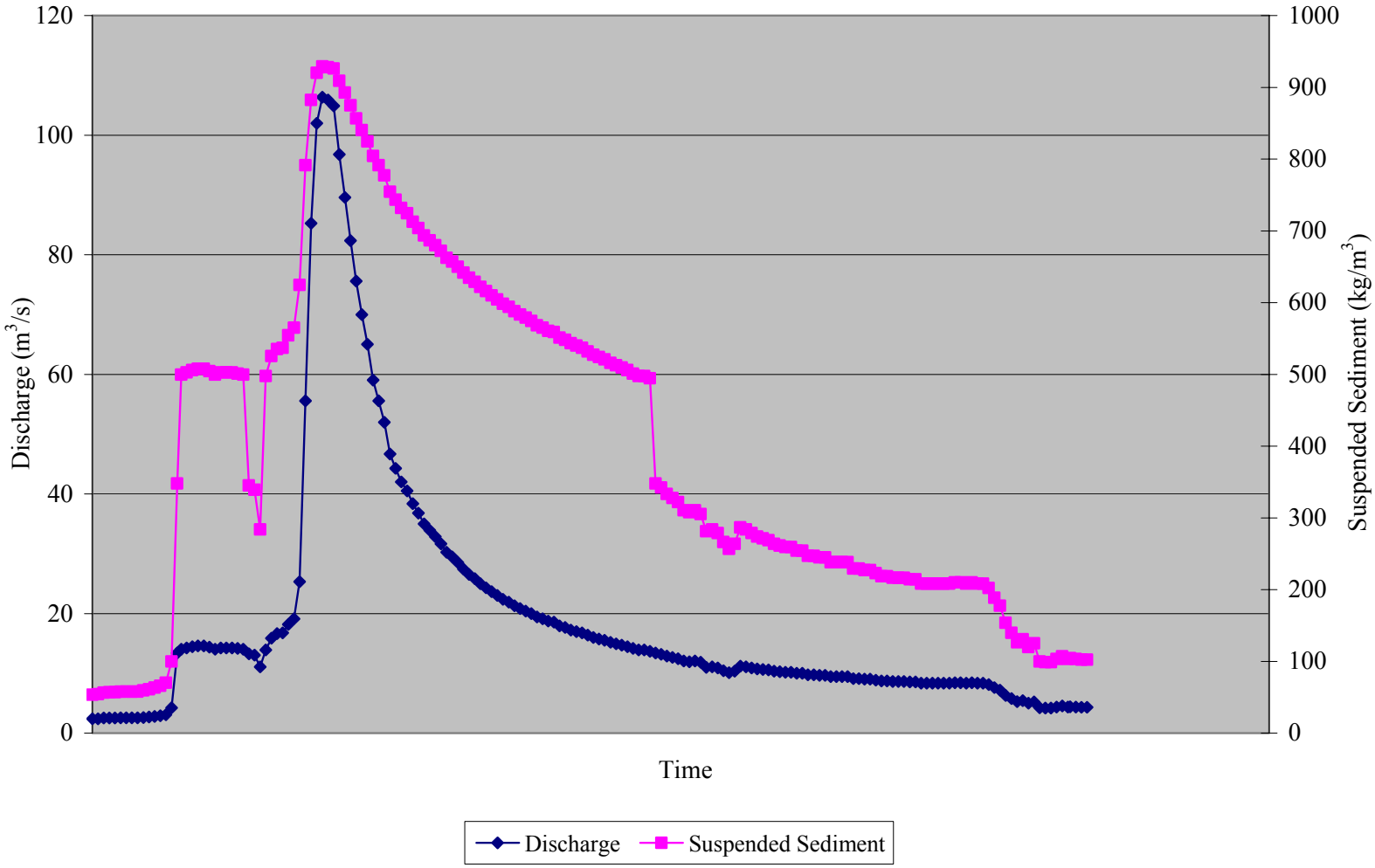

Figure 3: Suspended sediment and discharge plotted versus time

3.1.4 Bedload sediment measurement

A summary of the bedload sampling results is illustrated in Table 4. The portable bedload traps were deployed during three storm events but bedload was only trapped during one of those storm events. The resulting cumulative particle size distribution for the three bedload traps is presented in Table 5, summary presented in Table 6. A majority of the bedload sample was less then 4.75 mm, and the median measured particle size diameter was 4.63 mm. Table 7 illustrates the measured bedload sample mass for each size class defined in CCHE2D. The particle size distribution for each trap and the cumulative results are graphed and illustrated in Figure 4, a wide range of sediment particle sizes were collected.

3.1.5 Bedload rating curve

A hiding coefficient, equal to a value of 0.7, was implemented to account for the bimodal bed gradation and the influence of hiding and exposure effects on sediment transport. The mean particle diameter was calculated as 69 mm based on the pebble count data, presented in Appendix F. The resulting critical diameter of nine of the ten

Table 4: Bedload sampling results

Peak Stage/Discharge Date and Time	Max Stage (m)	Downstream Stage Elevation (m)	Discharge (m^3/s)	Bedload Measured (Yes/No)
02/17/2008 21:43:00	1.13	28.84	4.96	No
03/01/2008 13:09:03	1.25	28.95	7.04	No
03/04/2008 16:42:03	2.54	30.24	76.50	Yes
04/04/2008 20:35:03	1.52	29.22	14.65	No

Table 5: Bedload trap sample, cumulative particle size distribution results

Sieve Size (in)	Sieve Size (mm)	Weight Retained (oz)	Weight Retained (kg)	% Retained	Cumulative % Retained	% Passing
--	181	13.00	0.37	0.31	0.31	99.69
--	128	502.80	14.25	11.97	12.28	87.72
--	90.5	311.85	8.84	7.42	19.70	80.30
--	64	215.12	6.10	5.12	24.82	75.18
2	50	53.13	1.51	1.26	26.09	73.91
1 1/2	37.5	168.97	4.79	4.02	30.11	69.89
1	25	158.50	4.49	3.77	33.88	66.12
3/4	19	87.30	2.47	2.08	35.96	64.04
5/8	16	49.60	1.41	1.18	37.14	62.86
1/2	12.5	82.10	2.33	1.95	39.10	60.90
3/8	9.5	123.10	3.49	2.93	42.03	57.97
1/4	6.3	169.10	4.79	4.03	46.05	53.95
No.4	4.75	110.80	3.14	2.64	48.69	51.31
Pan	--	2155.60	61.11	51.31	100.00	0.00

Table 6: Summary of cumulative particle size distribution

	Millimeters	Meters
d_{16}	1.48	0.001
d_{50}	4.63	0.005
d_{84}	109.20	0.109
d_{90}	138.09	0.138

Table 7: Cumulative measured mass by CCHE2D size class

Median diameter of size class (mm)	(oz)	(kg)
2.00		
8.25	141.1	4.00
17.25	65.3	1.85
28.50	161.4	4.58
41.50	131.9	3.74
54.00	99.4	2.82
67.50	227.9	6.46
82.75	283.6	8.04
109.25	407.3	11.55
154.50	257.9	7.31

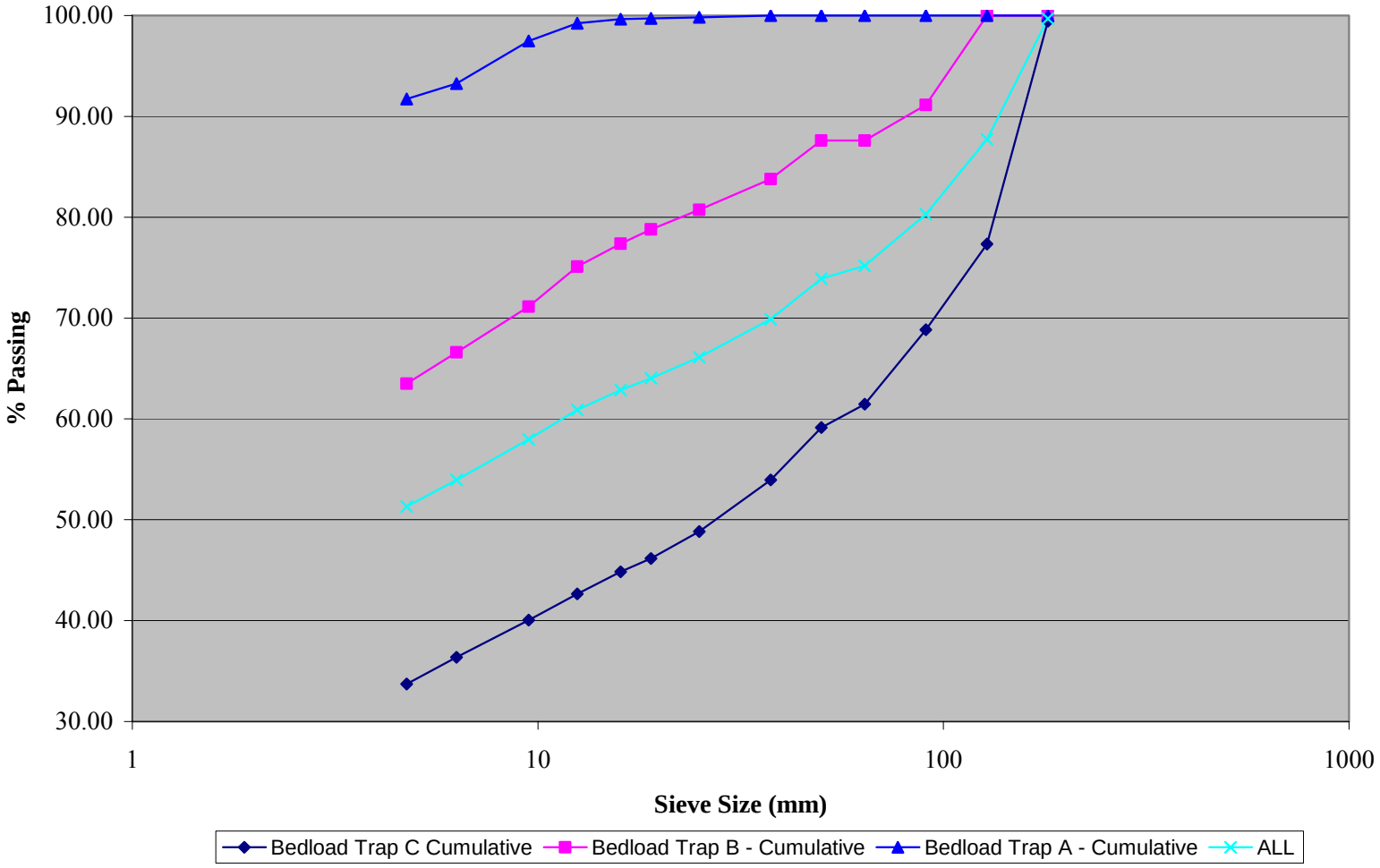

Figure 4: Bedload trap sample, particle size distribution graph

predefined sediment size classes is illustrated in Table 8. Note the calculated critical diameter for initiation is greater then the particle size defining each size class for particle sizes less than or equal to 67.5 mm. The calculated critical diameter for initiation is less than the particle size defining each size class for particle sizes greater than 67.5 mm. The bedload rating curve data and supporting material are included in Appendix I.

3.2 Model development and simulation

Successful model simulation results are presented in Table 9. A successful model simulation is defined as a simulation run which completed the numerical computation without producing a "floating overflow" or "floating invalid" error, and without stopping due to excessive amounts of bed change between a quasi-steady step. Unsuccessful model simulations are presented in Table 10. Figure 5 illustrates successful and

Table 8: Hiding coefficient, critical diameter for initiation

Size (mm)	d_c	round (mm)
8.25	36.49	36
17.25	45.52	46
28.5	52.92	53
41.5	59.24	59
54	64.11	64
67.5	68.55	69
82.75	72.87	73
109.25	79.20	79
154.5	87.88	88
hiding coefficient		
0.7		
	mm	
D_{50}	69	(median diameter)

Table 9: Successful model simulations

Description	Manning's n value
0% suspended, 0% Bedload	0.01
0% suspended, 0% Bedload	0.015
0% suspended, 0% Bedload	0.02
0% suspended, 0% Bedload	0.025
0% suspended, 0% Bedload	0.03
0% suspended, 0% Bedload	0.035
0% suspended, 0% Bedload	0.040
0% suspended, 0% Bedload	0.041
0% suspended, 0% Bedload	0.042
0% suspended, 0% Bedload	0.043
0% suspended, 0% Bedload	0.044
0% suspended, 0% Bedload	0.045
0% suspended, 0% Bedload	0.050
0% suspended, 0% Bedload	0.055
0% Suspended, 1% Bedload	0.025
0% Suspended, 1% Bedload	0.035
0% Suspended, 10% Bedload	0.025
0% Suspended, 20% Bedload	0.025
0% Suspended, 30% Bedload	0.025
0% Suspended, 40% Bedload	0.025
0% Suspended, 5% Bedload	0.025
0% Suspended, 5% Bedload	0.035
0% suspended, 5% Bedload	0.055

Description	Manning's n value
10% suspended, 0% Bedload	0.025
10% suspended, 10% Bedload	0.055
10% suspended, 10% Bedload	0.065
100% suspended, 0% Bedload	0.020
100% suspended, 0% Bedload	0.025
100% suspended, 0% Bedload	0.035
100% suspended, 0% Bedload	0.045
100% suspended, 0% Bedload	0.055
20% suspended, 0% Bedload	0.025
25% Suspended, 5% Bedload	0.050
30% suspended, 0% bedload	0.025
40% suspended, 0% bedload	0.025
5% suspended, 5% Bedload	0.025
5% suspended, 5% Bedload	0.035
5% suspended, 5% Bedload	0.045
50% suspended, 50% Bedload	0.010
50% suspended, 50% Bedload	0.025
50% suspended, 50% Bedload	0.050
50% suspended, 50% Bedload	0.055

Table 10: Unsuccessful model simulations

Description	Time step (s), Time steps to reach steady state (#)	Manning's n value	Message
0% Suspended, 0% Bedload	2 (s) time step, 20 steps to reach steady state	0.020	Stopped (i.e., Bed change between time steps is to great)
0% Suspended, 0% Bedload	2 (s) time step, 20 steps to reach steady state	0.020	Stopped at 104th step
0% Suspended, 0% Bedload	2 (s) time step, 40 steps to reach steady state	0.025	Stopped at 91th step
0% Suspended, 0% Bedload	2 (s) time step, 20 steps to reach steady state	0.025	Stopped at 131th step
0% Suspended, 0% Bedload	2 (s) time step, 40 steps to reach steady state	0.025	Stopped at 91th step
0% Suspended, 0% Bedload	2 (s) time step, 20 steps to reach steady state	0.055	Stopped
0% Suspended, 0% Bedload	2 (s) time step, 20 steps to reach steady state	0.055	Stopped at 89th step
0% Suspended, 1% Bedload	2 (s) time step, 20 steps to reach steady state	0.015	Stopped at 139th step
0% Suspended, 1% Bedload	2 (s) time step, 20 steps to reach steady state	0.045	Stopped 79th step
0% Suspended, 1% Bedload	2 (s) time step, 20 steps to reach steady state	0.055	Stopped at 83th step
0% Suspended, 1% Bedload	2 (s) time step, 20 steps to reach steady state	0.055	Stopped
0% Suspended, 10% Bedload	2 (s) time step, 20 steps to reach steady state	0.025	Floating overflow at 133th step
0% Suspended, 10% Bedload	2 (s) time step, 20 steps to reach steady state	0.045	Stopped 61th step
0% Suspended, 2% Bedload	2 (s) time step, 20 steps to reach steady state	0.025	Stopped at 109th step
0% Suspended, 2% Bedload	2 (s) time step, 20 steps to reach steady state	0.045	Stopped at 90th step
0% Suspended, 2% Bedload	2 (s) time step, 20 steps to reach steady state	0.065	Stopped at 80th step
0% Suspended, 2.5% Bedload	2 (s) time step, 20 steps to reach steady state	0.025	Stopped at 105th step
0% Suspended, 5% Bedload	2 (s) time step, 20 steps to reach steady state	0.025	Floating overflow at 133th step
0% Suspended, 5% Bedload	2 (s) time step, 20 steps to reach steady state	0.045	Stopped at 62th step
0% Suspended, 5% Bedload	2 (s) time step, 20 steps to reach steady state	0.060	Stopped at 76th step
0% Suspended, 5% Bedload	2 (s) time step, 20 steps to reach steady state	0.065	Stopped at 90th step
0% Suspended, 5% Bedload	2 (s) time step, 20 steps to reach steady state	0.075	Stopped
10% Suspended, 10% Bedload	2 (s) time step, 20 steps to reach steady state	0.025	Stopped
10% Suspended, 10% Bedload	2 (s) time step, 20 steps to reach steady state	0.035	Floating overflow at 143th step
10% Suspended, 10% Bedload	2 (s) time step, 20 steps to reach steady state	0.045	Stopped at 107th step
100% Suspended, 0% Bedload	2 (s) time step, 20 steps to reach steady state	0.010	Stopped
25% Suspended, 25% Bedload	2 (s) time step, 20 steps to reach steady state	0.010	Stopped at 140th step
25% Suspended, 25% Bedload	2 (s) time step, 20 steps to reach steady state	0.025	Floating overflow at 133th step
25% Suspended, 25% Bedload	2 (s) time step, 20 steps to reach steady state	0.035	Floating overflow at 83th step
5% Suspended, 5% Bedload	2 (s) time step, 20 steps to reach steady state	0.055	Stopped at 86th step
50% Suspended, 50% Bedload	2 (s) time step, 20 steps to reach steady state	0.075	Stopped at 68th step
25% Suspended, 1% Bedload	2 (s) time step, 20 steps to reach steady state	0.05	Stopped at 109th step

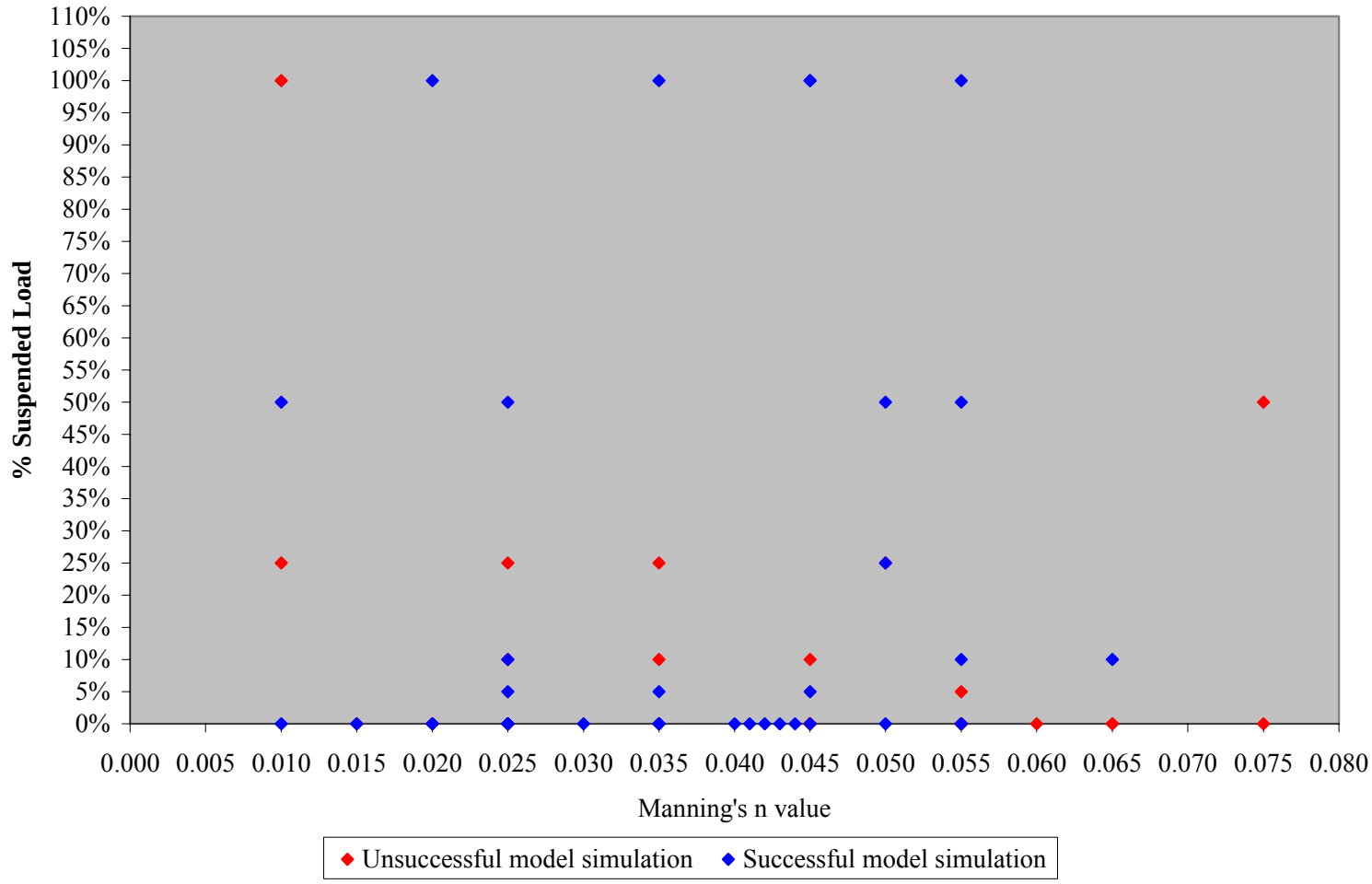

Figure 5: Successful and Unsuccessful model simulations plotted versus % suspended load and the Manning's n value

unsuccessful model simulations plotted as a function of the percentage suspended load and the Manning's n value input parameters utilized in each simulation. Figure 6 illustrates successful and unsuccessful model simulations plotted as a function of the percentage bedload and the Manning's n value input parameters. 42 simulations were successfully executed, while 32 unsuccessful model simulations were recorded. A successful simulation could not be completed with a Manning's n values higher than 0.065, nor with a sediment rating curve of 25% suspended load and 25% bedload. Simulated reach, local and point results are presented in Tables 11, 12, and 13.

3.2.1 CCHE2D Mesh Generator

Table 14 illustrates the results of the mesh evaluation. The minimum and maximum cell lengths parallel to the flow direction are 0.851 m and 1.072 m, respectively. The minimum and maximum cell lengths perpendicular to the flow direction are 1.551 m and 2.849 m, respectively.

3.2.2 CCHE2D GUI –Sediment parameters

The ten sediment size classes and associated mean diameter for each size class, defined within CCHE2D, are included in Table 15. The bed gradation is defined in Table 16 as a percentage of each predefined size class. The largest portion of the pebble count data, 23%, falls within size class nine. The particle size range included in size class nine is 90.5 mm to 128.0 mm.

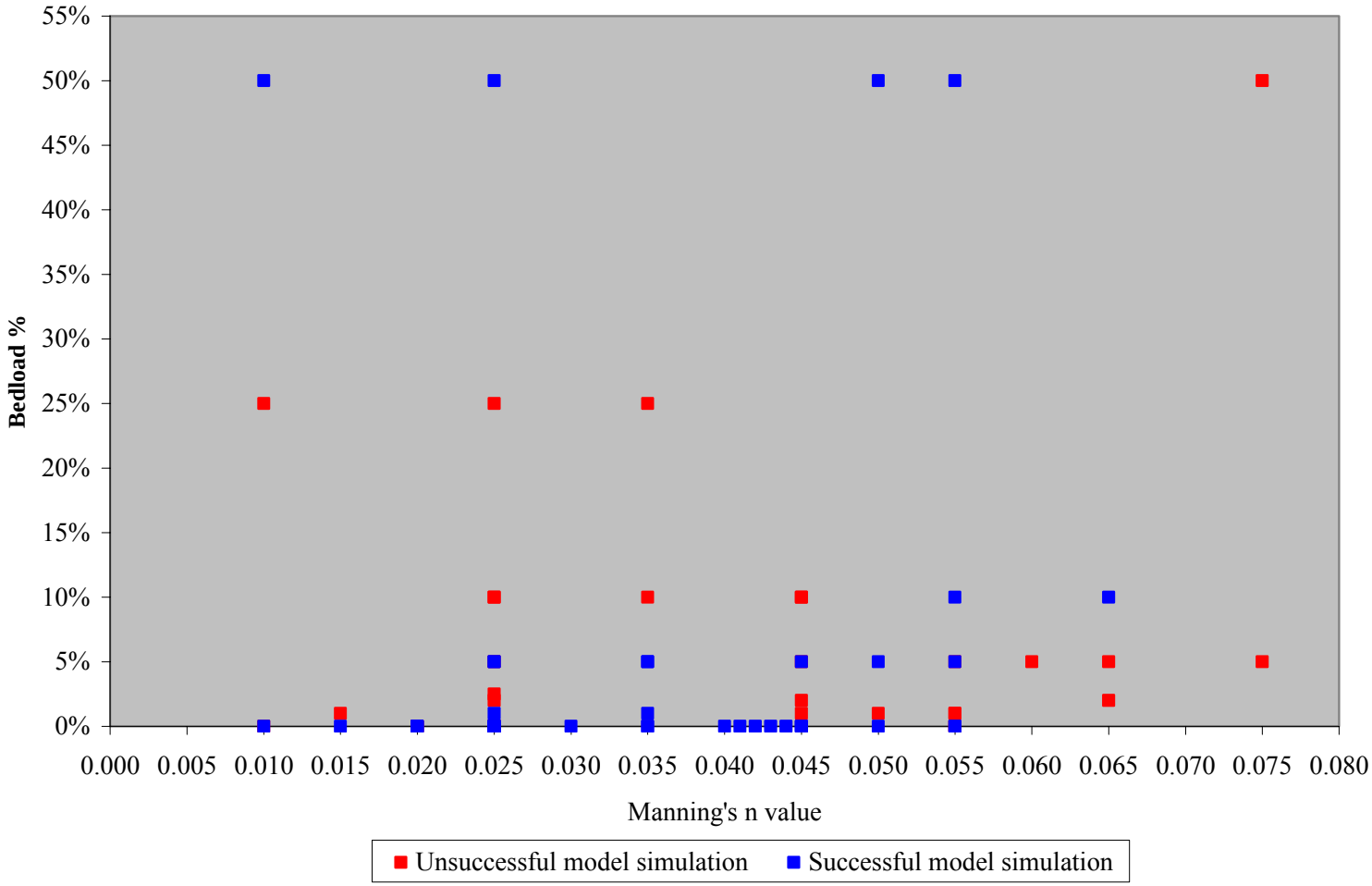

Figure 6: Successful and unsuccessful model simulations plotted as a function of % bedload & the Manning's n value

Table 11: Reach scale bed elevation change

Description	Manning's n value	(Simulated - Measured) bed elevation change (m)
0% suspended, 0% Bedload	0.01	0.153
0% suspended, 0% Bedload	0.015	0.074
0% suspended, 0% Bedload	0.02	0.013
0% suspended, 0% Bedload	0.025	0.049
0% suspended, 0% Bedload	0.03	0.031
0% suspended, 0% Bedload	0.035	0.020
0% suspended, 0% Bedload	0.040	0.006
0% suspended, 0% Bedload	0.041	0.001
0% suspended, 0% Bedload	0.042	-0.021
0% suspended, 0% Bedload	0.043	-0.023
0% suspended, 0% Bedload	0.044	-0.032
0% suspended, 0% Bedload	0.045	-0.037
0% suspended, 0% Bedload	0.050	-0.054
0% suspended, 0% Bedload	0.055	-0.077
0% Suspended, 1% Bedload	0.025	0.034
0% Suspended, 1% Bedload	0.035	0.076
0% Suspended, 10% Bedload	0.025	0.031
0% Suspended, 20% Bedload	0.025	0.182
0% Suspended, 30% Bedload	0.025	0.140
0% Suspended, 40% Bedload	0.025	0.167
0% Suspended, 5% Bedload	0.025	0.067
0% Suspended, 5% Bedload	0.035	0.041
0% suspended, 5% Bedload	0.055	0.014

Description	Manning's n value	(Simulated - Measured) bed elevation change (m)
10% suspended, 0% Bedload	0.025	0.078
10% suspended, 10% Bedload	0.055	0.139
10% suspended, 10% Bedload	0.065	0.137
100% suspended, 0% Bedload	0.020	0.152
100% suspended, 0% Bedload	0.025	0.125
100% suspended, 0% Bedload	0.035	0.137
100% suspended, 0% Bedload	0.045	0.165
100% suspended, 0% Bedload	0.055	0.183
20% suspended, 0% Bedload	0.025	0.790
25% Suspended, 5% Bedload	0.050	0.120
30% suspended, 0% bedload	0.025	0.065
40% suspended, 0% bedload	0.025	0.096
5% suspended, 5% Bedload	0.025	0.062
5% suspended, 5% Bedload	0.035	0.060
5% suspended, 5% Bedload	0.045	0.105
50% suspended, 50% Bedload	0.010	0.378
50% suspended, 50% Bedload	0.025	0.224
50% suspended, 50% Bedload	0.050	0.266
50% suspended, 50% Bedload	0.055	0.220

Table 12: Local scale bed elevation change

Description	Manning's n value	(Simulated - Measured) bed elevation change (m)				
		Group 1	Group 2	Group 3	Group 4	Group 5
0% suspended, 0% Bedload	0.010	0.259	0.257	-0.042	-0.096	-0.158
0% suspended, 0% Bedload	0.015	0.171	0.077	-0.047	-0.057	-0.107
0% suspended, 0% Bedload	0.020	0.197	-0.066	-0.058	-0.208	-0.150
0% suspended, 0% Bedload	0.025	0.224	0.004	-0.051	-0.168	-0.196
0% suspended, 0% Bedload	0.030	0.235	-0.025	-0.062	-0.224	-0.245
0% suspended, 0% Bedload	0.035	0.241	-0.047	-0.080	-0.260	-0.241
0% suspended, 0% Bedload	0.040	0.198	-0.050	-0.072	-0.246	-0.224
0% suspended, 0% Bedload	0.041	0.189	-0.049	-0.073	-0.259	-0.218
0% suspended, 0% Bedload	0.042	0.171	-0.050	-0.070	-0.325	-0.254
0% suspended, 0% Bedload	0.043	0.170	-0.053	-0.078	-0.326	-0.263
0% suspended, 0% Bedload	0.044	0.155	-0.053	-0.079	-0.341	-0.264
0% suspended, 0% Bedload	0.045	0.141	-0.053	-0.080	-0.339	-0.262
0% suspended, 0% Bedload	0.050	0.108	-0.051	-0.082	-0.355	-0.279
0% suspended, 0% Bedload	0.055	0.044	-0.048	-0.086	-0.347	-0.244
0% Suspended, 1% Bedload	0.025	0.199	0.007	-0.050	-0.200	-0.208
0% Suspended, 1% Bedload	0.035	0.290	-0.033	-0.080	-0.147	-0.048
0% Suspended, 10% Bedload	0.025	0.252	-0.057	-0.070	-0.238	-0.163
0% Suspended, 20% Bedload	0.025	0.438	0.197	-0.071	-0.245	-0.149
0% Suspended, 30% Bedload	0.025	0.430	0.051	-0.074	-0.220	-0.151
0% Suspended, 40% Bedload	0.025	0.490	0.042	-0.078	-0.197	-0.136
0% Suspended, 5% Bedload	0.025	0.208	-0.003	-0.054	-0.011	-0.221
0% Suspended, 5% Bedload	0.035	0.251	-0.033	-0.078	-0.213	-0.171
0% suspended, 5% Bedload	0.055	0.269	-0.038	-0.085	-0.356	-0.292

Description	Manning's n value	(Simulated - Measured) bed elevation change (m)				
		Group 1	Group 2	Group 3	Group 4	Group 5
10% suspended, 0% Bedload	0.025	0.237	0.019	-0.083	-0.075	-0.122
10% suspended, 10% Bedload	0.055	0.453	0.124	-0.083	-0.348	-0.301
10% suspended, 10% Bedload	0.065	0.459	0.107	-0.083	-0.343	-0.302
100% suspended, 0% Bedload	0.020	0.327	0.077	-0.090	0.010	-0.034
100% suspended, 0% Bedload	0.025	0.267	0.057	-0.106	0.019	0.029
100% suspended, 0% Bedload	0.035	0.349	0.071	-0.090	-0.099	-0.073
100% suspended, 0% Bedload	0.045	0.388	0.171	-0.059	-0.184	-0.150
100% suspended, 0% Bedload	0.055	0.458	0.122	-0.050	-0.188	-0.100
20% suspended, 0% Bedload	0.025	1.062	0.793	0.195	0.471	0.422
25% Suspended, 5% Bedload	0.050	0.354	0.088	-0.066	-0.219	-0.155
30% suspended, 0% bedload	0.025	0.207	-0.032	-0.120	-0.006	-0.051
40% suspended, 0% bedload	0.025	0.241	0.051	-0.098	-0.050	-0.065
5% suspended, 5% Bedload	0.025	0.226	0.001	-0.069	-0.089	-0.197
5% suspended, 5% Bedload	0.035	0.272	0.000	-0.082	-0.199	-0.200
5% suspended, 5% Bedload	0.045	0.326	0.079	-0.073	-0.210	-0.196
50% suspended, 50% Bedload	0.010	0.621	0.378	-0.052	0.113	-0.088
50% suspended, 50% Bedload	0.025	0.487	0.110	-0.070	0.019	-0.124
50% suspended, 50% Bedload	0.050	0.655	0.268	-0.080	-0.347	-0.279
50% suspended, 50% Bedload	0.055	0.653	0.118	-0.081	-0.352	-0.286

Table 13: Point Scale bed elevation change

Description	Manning's n value	Point Scale (Simulated - Measured) bed elevation change (m)																
		MP-199	MP-237	MP-373	MP-378	MP-843	MP-1424	MP-1425	MP-1463	MP-1464	MP-1490	MP-1859	MP-1866	MP-1868	MP-1869	MP-1871	MP-1873	MP-1883
0% suspended, 0% Bedload	0.010	-0.158	-0.146	-0.109	-0.034	-0.042	0.312	0.359	0.261	0.243	0.108	0.396	0.431	0.358	0.370	0.182	0.121	-0.043
0% suspended, 0% Bedload	0.015	-0.107	-0.133	-0.035	-0.003	-0.047	0.045	0.276	-0.004	0.118	-0.050	0.331	0.145	0.359	0.340	0.083	0.060	-0.122
0% suspended, 0% Bedload	0.020	-0.150	-0.307	-0.212	-0.106	-0.058	-0.140	0.116	-0.141	-0.086	-0.078	0.318	0.226	0.387	0.355	0.103	0.036	-0.046
0% suspended, 0% Bedload	0.025	-0.196	-0.334	-0.108	-0.063	-0.051	-0.010	0.103	-0.067	0.008	-0.012	0.360	0.325	0.350	0.367	0.143	0.070	-0.048
0% suspended, 0% Bedload	0.030	-0.245	-0.377	-0.162	-0.133	-0.062	-0.022	0.028	-0.033	-0.032	-0.068	0.362	0.347	0.347	0.351	0.171	0.102	-0.037
0% suspended, 0% Bedload	0.035	-0.241	-0.388	-0.226	-0.166	-0.080	-0.034	-0.011	-0.021	-0.060	-0.112	0.328	0.384	0.299	0.351	0.188	0.137	-0.002
0% suspended, 0% Bedload	0.040	-0.224	-0.433	-0.156	-0.149	-0.072	-0.031	-0.022	-0.007	-0.070	-0.120	0.244	0.354	0.207	0.269	0.171	0.144	-0.003
0% suspended, 0% Bedload	0.041	-0.218	-0.441	-0.176	-0.159	-0.073	-0.029	-0.024	-0.003	-0.071	-0.116	0.225	0.341	0.188	0.252	0.167	0.135	0.015
0% suspended, 0% Bedload	0.042	-0.254	-0.459	-0.302	-0.215	-0.070	-0.032	-0.028	-0.002	-0.070	-0.118	0.206	0.319	0.152	0.231	0.155	0.125	0.011
0% suspended, 0% Bedload	0.043	-0.263	-0.428	-0.324	-0.225	-0.078	-0.032	-0.029	-0.007	-0.075	-0.121	0.206	0.318	0.135	0.218	0.165	0.134	0.017
0% suspended, 0% Bedload	0.044	-0.264	-0.469	-0.326	-0.228	-0.079	-0.032	-0.031	-0.005	-0.076	-0.121	0.189	0.306	0.104	0.194	0.153	0.125	0.016
0% suspended, 0% Bedload	0.045	-0.262	-0.454	-0.336	-0.228	-0.080	-0.031	-0.031	-0.005	-0.077	-0.120	0.175	0.293	0.077	0.172	0.143	0.114	0.016
0% suspended, 0% Bedload	0.050	-0.279	-0.501	-0.332	-0.232	-0.082	-0.030	-0.032	-0.002	-0.075	-0.116	0.134	0.246	0.034	0.129	0.109	0.081	0.024
0% suspended, 0% Bedload	0.055	-0.244	-0.508	-0.314	-0.219	-0.086	-0.028	-0.032	0.003	-0.072	-0.112	0.089	0.202	-0.043	0.052	0.041	0.014	-0.046
0% Suspended, 1% Bedload	0.025	-0.208	-0.338	-0.141	-0.122	-0.050	-0.033	0.195	-0.080	-0.005	-0.040	0.347	0.314	0.320	0.341	0.102	0.040	-0.071
0% Suspended, 1% Bedload	0.035	-0.048	-0.319	-0.042	-0.081	-0.080	-0.029	0.027	-0.033	-0.045	-0.087	0.349	0.445	0.418	0.407	0.207	0.171	0.035
0% Suspended, 10% Bedload	0.025	-0.163	-0.355	-0.230	-0.129	-0.070	-0.136	0.107	-0.074	-0.111	-0.071	0.392	0.306	0.471	0.414	0.113	0.044	0.026
0% Suspended, 20% Bedload	0.025	-0.149	-0.356	-0.242	-0.136	-0.071	0.171	0.255	0.200	0.134	0.223	0.569	0.570	0.555	0.567	0.353	0.259	0.195
0% Suspended, 30% Bedload	0.025	-0.151	-0.342	-0.210	-0.109	-0.074	-0.193	0.176	0.232	-0.120	0.162	0.669	0.556	0.662	0.654	0.298	0.068	0.102
0% Suspended, 40% Bedload	0.025	-0.136	-0.314	-0.189	-0.086	-0.078	-0.219	0.129	0.276	-0.143	0.166	0.718	0.652	0.702	0.672	0.405	0.082	0.198
0% Suspended, 5% Bedload	0.025	-0.221	-0.199	0.077	0.091	-0.054	-0.020	0.111	-0.086	-0.009	-0.013	0.342	0.295	0.370	0.359	0.115	0.033	-0.059
0% Suspended, 5% Bedload	0.035	-0.171	-0.397	-0.113	-0.130	-0.078	-0.027	0.013	-0.022	-0.048	-0.083	0.352	0.348	0.371	0.374	0.179	0.143	-0.009
0% suspended, 5% Bedload	0.055	-0.292	-0.503	-0.331	-0.232	-0.085	-0.020	-0.025	0.013	-0.063	-0.097	0.298	0.412	0.273	0.316	0.246	0.209	0.126
10% suspended, 0% Bedload	0.025	-0.122	-0.106	-0.079	-0.040	-0.083	-0.052	0.192	0.005	-0.041	-0.011	0.335	0.389	0.371	0.347	0.155	0.081	-0.015
10% suspended, 10% Bedload	0.055	-0.301	-0.505	-0.315	-0.222	-0.083	0.128	0.127	0.177	0.068	0.120	0.492	0.616	0.562	0.531	0.376	0.351	0.240
10% suspended, 10% Bedload	0.065	-0.302	-0.490	-0.316	-0.222	-0.083	0.150	0.131	0.157	0.055	0.040	0.507	0.633	0.504	0.512	0.410	0.373	0.274

Table 13: Point Scale bed elevation change (continued)

Description	Manning's n value	Point Scale (Simulated - Measured) bed elevation change (m)																
		MP-199	MP-237	MP-373	MP-378	MP-843	MP-1424	MP-1425	MP-1463	MP-1464	MP-1490	MP-1859	MP-1866	MP-1868	MP-1869	MP-1871	MP-1873	MP-1883
100% suspended, 0% Bedload	0.020	-0.034	0.016	0.004	0.011	-0.090	-0.016	0.261	0.103	-0.013	0.047	0.382	0.458	0.595	0.524	0.039	0.224	0.068
100% suspended, 0% Bedload	0.025	0.029	0.041	-0.012	0.027	-0.106	-0.100	0.118	0.007	0.194	0.064	0.389	0.422	0.500	0.422	0.166	-0.095	0.067
100% suspended, 0% Bedload	0.035	-0.073	-0.141	-0.119	-0.039	-0.090	0.031	0.117	0.088	0.031	0.087	0.529	0.550	0.530	0.524	0.210	0.032	0.069
100% suspended, 0% Bedload	0.045	-0.150	-0.300	-0.189	-0.062	-0.059	0.145	0.181	0.249	0.102	0.179	0.498	0.557	0.521	0.507	0.286	0.160	0.186
100% suspended, 0% Bedload	0.055	-0.100	-0.280	-0.189	-0.095	-0.050	0.128	0.129	0.159	0.066	0.128	0.651	0.594	0.798	0.709	0.313	0.057	0.086
20% suspended, 0% Bedload	0.025	0.422	0.485	0.486	0.443	0.195	0.705	0.838	0.772	0.768	0.882	1.053	1.148	1.172	1.176	1.006	0.932	0.945
25% Suspended, 5% Bedload	0.050	-0.155	-0.342	-0.204	-0.111	-0.066	0.085	0.099	0.130	0.032	0.097	0.436	0.478	0.582	0.493	0.205	0.169	0.112
30% suspended, 0% bedload	0.025	-0.051	0.007	-0.009	-0.018	-0.120	-0.002	0.143	-0.126	-0.203	0.027	0.349	0.294	0.399	0.385	0.006	0.058	-0.040
40% suspended, 0% bedload	0.025	-0.065	-0.058	-0.065	-0.026	-0.098	-0.030	0.165	0.070	-0.015	0.067	0.390	0.320	0.458	0.405	0.184	-0.097	0.027
5% suspended, 5% Bedload	0.025	-0.197	-0.136	-0.090	-0.041	-0.069	-0.038	0.137	-0.041	-0.041	-0.013	0.276	0.320	0.380	0.349	0.148	0.117	-0.008
5% suspended, 5% Bedload	0.035	-0.200	-0.268	-0.210	-0.118	-0.082	-0.001	0.059	-0.014	-0.014	-0.031	0.357	0.402	0.412	0.394	0.181	0.138	0.018
5% suspended, 5% Bedload	0.045	-0.196	-0.300	-0.219	-0.110	-0.073	0.096	0.091	0.138	0.044	0.026	0.411	0.501	0.406	0.423	0.262	0.203	0.073
50% suspended, 50% Bedload	0.010	-0.088	0.058	0.208	0.072	-0.052	0.145	0.347	0.560	0.286	0.550	0.662	0.763	0.775	0.731	0.517	0.407	0.492
50% suspended, 50% Bedload	0.025	-0.124	0.033	0.018	0.006	-0.070	-0.078	0.129	0.363	-0.149	0.283	0.687	0.524	0.788	0.760	0.287	0.143	0.218
50% suspended, 50% Bedload	0.050	-0.279	-0.510	-0.313	-0.218	-0.080	0.260	0.220	0.329	0.255	0.279	0.703	0.761	0.787	0.769	0.561	0.509	0.493
50% suspended, 50% Bedload	0.055	-0.286	-0.505	-0.323	-0.228	-0.081	0.154	0.126	0.188	0.082	0.039	0.688	0.782	0.673	0.723	0.620	0.557	0.525

Table 14: CCHE2D mesh evaluation

Min and Max Cell Length	
Description	Length (m)
Minimum Cell Length in I Direction	0.851
Maximum Cell Length in I Direction	1.072
Minimum Cell Length in J Direction	1.551
Maximum Cell Length in J Direction	2.849

Table 15: CCHE2D sediment size classes

Size Class	Description	Minimum Dia. Of Size Class (mm)	Maximum Dia. Of Size Class (mm)	Δ	Mean Dia. (mm)	Mean Dia. (m)
1	Suspended Sediment	0.0	4.0	4	2.00	0.00200
2		4.0	12.5	8.5	8.25	0.00825
3		12.5	22.0	9.5	17.25	0.01725
4		22.0	35.0	13	28.50	0.02850
5		35.0	48.0	13	41.50	0.04150
6		48.0	60.0	12	54.00	0.05400
7		60.0	75.0	15	67.50	0.06750
8		75.0	90.5	15.5	82.75	0.08275
9		90.5	128.0	37.5	109.25	0.10925
10		128.0	181.0	53	154.50	0.15450

Table 16: Bed gradation defined within CCHE2D

Size Class	Description	Mean Dia. (m)	Pebble Count Summary (%)
1	Suspended Sediment	0.002	0.02
2		0.00825	0.03
3		0.01725	0.06
4		0.0285	0.13
5		0.0415	0.07
6		0.054	0.1
7		0.0675	0.19
8		0.08275	0.1
9		0.10925	0.23
10		0.1545	0.07

3.2.3 CCHE2D GUI –Sediment and hydraulic boundary conditions

The suspended sediment and bedload rating curve files (.sbc and .bbc) are illustrated in Appendix J, as are the upstream discharge hydrograph and downstream stage hydrograph (.dhg and .shg).

3.3 Model performance and evaluation

3.3.1 Monitoring survey

On March 6th, 2008 a second topographic survey was performed to define the actual bed change, resulting from the storm event which produced measured bedload, at multiple monitoring points. The differences in plan form distance between the original survey points and the measured monitoring points are illustrated in Table 17. Measured bed change elevation is illustrated in Table 18. The elevation of each monitoring point was recorded within a plan view distance of 3.7 cm from the original point's location. Monitoring points 237, 373, 378, 1424, 1463, and 1859 showed less than 3.7 cm (approximately 0.12 ft) of elevation change. The measured overall reach average bed elevation change was calculated as 4.2 cm. Table 19 summarizes the measured bed change at each group, the number of monitoring points included in each group, and the standard deviation with respect to the measured bed elevation change of the monitoring points comprising each group. Groups 3 and 4 were defined by only one monitoring point so a standard deviation was not calculated. The calculated standard deviation of group 4 was less than 3 cm (0.1 ft). The calculated standard deviation of group 1 was the highest, at 11.5 cm (0.377 ft).

Table 17: Monitoring survey (Plan view distance comparison)

Original Point No.	Original		Monitoring Survey		Change in Northing (m)	Change in Easting (m)	Change in Distance (m)
	Northing (m)	Easting (m)	Northing (m)	Easting (m)			
199.000	1519.579	1533.754	1519.586	1533.769	0.007	0.015	0.017
237.000	1510.042	1529.880	1510.041	1529.847	0.000	-0.033	0.033
373.000	1510.890	1522.412	1510.879	1522.388	-0.011	-0.024	0.027
378.000	1507.437	1522.179	1507.424	1522.171	-0.012	-0.008	0.015
843.000	1497.684	1492.120	1497.669	1492.139	-0.015	0.020	0.024
1424.000	1495.124	1445.836	1495.156	1445.849	0.032	0.013	0.035
1425.000	1496.464	1445.336	1496.480	1445.354	0.016	0.018	0.024
1463.000	1491.668	1438.500	1491.639	1438.508	-0.029	0.008	0.030
1464.000	1493.241	1438.302	1493.210	1438.283	-0.032	-0.019	0.037
1490.000	1489.722	1430.971	1489.721	1430.961	-0.001	-0.010	0.010
1859.000	1475.441	1391.783	1475.461	1391.796	0.020	0.013	0.024
1866.000	1477.902	1393.059	1477.876	1393.060	-0.026	0.001	0.026
1868.000	1472.315	1387.079	1472.329	1387.092	0.014	0.013	0.019
1869.000	1473.512	1386.888	1473.498	1386.914	-0.014	0.026	0.030
1871.000	1476.052	1386.090	1476.052	1386.067	0.000	-0.023	0.023
1873.000	1478.444	1385.446	1478.463	1385.420	0.019	-0.026	0.033
1883.000	1477.125	1380.177	1477.152	1380.174	0.027	-0.004	0.028

Table 18: Monitoring survey (Measured bed elevation change)

Point Number	Original Elevation (m)	Surveyed Elevation (m)	Change in Elevation (m)
199	28.596	28.695	0.099
237	28.432	28.436	0.004
373	28.530	28.515	-0.016
378	28.493	28.522	0.030
843	28.768	28.815	0.047
1424	28.837	28.872	0.035
1425	28.833	28.874	0.041
1463	28.929	28.920	-0.009
1464	28.895	28.961	0.066
1490	28.840	28.938	0.098
1859	29.281	29.246	-0.034
1866	29.372	29.215	-0.157
1868	29.257	29.405	0.149
1869	29.435	29.486	0.051
1871	29.517	29.565	0.048
1873	29.544	29.615	0.071
1883	29.474	29.661	0.187

Table 19: Local scale, measured bed elevation change

	Average measured bed elevation change (m)	Number of points in group	Standard deviation (m)
Group 1	0.045	7	0.115
Group 2	0.046	5	0.04
Group 3	0.047	1	n/a
Group 4	0.006	3	0.023
Group 5	0.099	1	n/a

3.3.2 CCHE2D evaluation

Table 20 illustrates the nodes that define each monitoring point. Two monitoring points, MP 1490 and 1859, were located directly on J lines and were identified by six surrounding nodes; the remaining monitoring points were only defined by four surrounding nodes. To quantitatively compare simulations, the percentage difference from an equilibrium condition was also calculated. The equilibrium condition was defined numerically as the simulation that mostly closely resembled measured overall average reach bed change (i.e., the difference between simulated and measured reach-scale bed elevation change that was closest to zero). The equilibrium condition was defined by 0% sediment input at the upstream boundary condition and a Manning's n value of 0.041. The reach-scale results are presented with the data sorted by sediment rating curve in Table 21, and with the data sorted by Manning's n value in Table 22. Figure 7 illustrates the influence of the Manning's n variable on simulated reach-scale bed elevation change with respect to a fixed sediment rating curve (i.e., 0% suspended load, 0% bedload). An increase in the Manning's n value up to a value of 0.041

Table 20: Monitoring points and corresponding surrounding nodes

	Point #	G_1	G_2	G_3	G_4	G_5	G_6
	MP-199	1040	1140	1141	1041	--	--
	MP-237	1332	1432	1433	1333	--	--
	MP-373	1636	1736	1737	1637	--	--
	MP-378	1733	1833	1834	1734	--	--
	MP-843	3340	3341	3241	3240	--	--
	MP-1424	5556	5656	5657	5557	--	--
	MP-1425	5558	5658	5657	5557	--	--
	MP-1463	5954	5953	6053	6054	--	--
	MP-1464	5955	6055	6056	5956	--	--
*	MP-1490	6352	6353	6453	6452	6252	6253
**	MP-1859	8244	8245	8345	8344	8144	8145
	MP-1866	8146	8246	8247	8147	--	--
	MP-1868	8542	8442	8541	8441	--	--
	MP-1869	8443	8442	8542	8543	--	--
	MP-1871	8445	8545	8546	8446	--	--
	MP-1873	8547	8447	8448	8548	--	--
	MP-1883	8746	8745	8845	8846	--	--
	*	MP-1490	Located directly on J-64				
	**	MP-1859	Located directly on J-83				

Table 21: Reach scale bed elevation change (Sorted by sediment rating curve)

Description	Manning's n value	(Simulated - Measured) bed elevation change (m)	% difference
0% suspended, 0% Bedload	0.01	0.153	211.7
0% suspended, 0% Bedload	0.015	0.074	101.4
0% suspended, 0% Bedload	0.02	0.013	16.8
0% suspended, 0% Bedload	0.025	0.049	67.4
0% suspended, 0% Bedload	0.03	0.031	42.6
0% suspended, 0% Bedload	0.035	0.020	27.1
0% suspended, 0% Bedload	0.040	0.006	7.2
0% suspended, 0% Bedload	0.041	0.001	0.0
0% suspended, 0% Bedload	0.042	-0.021	-29.6
0% suspended, 0% Bedload	0.043	-0.023	-32.7
0% suspended, 0% Bedload	0.044	-0.032	-45.4
0% suspended, 0% Bedload	0.045	-0.037	-52.8
0% suspended, 0% Bedload	0.050	-0.054	-76.4
0% suspended, 0% Bedload	0.055	-0.077	-107.3
0% Suspended, 1% Bedload	0.025	0.034	45.7
0% Suspended, 1% Bedload	0.035	0.076	104.6
0% Suspended, 5% Bedload	0.025	0.067	91.4
0% Suspended, 5% Bedload	0.035	0.041	56.5
0% suspended, 5% Bedload	0.055	0.014	19.1
0% Suspended, 10% Bedload	0.025	0.031	42.6
0% Suspended, 20% Bedload	0.025	0.182	251.6
0% Suspended, 30% Bedload	0.025	0.140	192.9
0% Suspended, 40% Bedload	0.025	0.167	230.2

Description	Manning's n value	(Simulated - Measured) bed elevation change (m)	% difference
5% suspended, 5% Bedload	0.025	0.062	84.8
5% suspended, 5% Bedload	0.035	0.060	82.5
5% suspended, 5% Bedload	0.045	0.105	143.9
10% suspended, 0% Bedload	0.025	0.078	107.1
10% suspended, 10% Bedload	0.055	0.139	191.7
10% suspended, 10% Bedload	0.065	0.137	189.1
20% suspended, 0% Bedload	0.025	0.790	1094.1
25% Suspended, 5% Bedload	0.050	0.120	165.4
30% suspended, 0% bedload	0.025	0.065	88.7
40% suspended, 0% bedload	0.025	0.096	132.0
50% suspended, 50% Bedload	0.010	0.378	523.6
50% suspended, 50% Bedload	0.025	0.224	310.2
50% suspended, 50% Bedload	0.050	0.266	368.0
50% suspended, 50% Bedload	0.055	0.220	303.5
100% suspended, 0% Bedload	0.020	0.152	209.4
100% suspended, 0% Bedload	0.025	0.125	173.0
100% suspended, 0% Bedload	0.035	0.137	189.5
100% suspended, 0% Bedload	0.045	0.165	228.2
100% suspended, 0% Bedload	0.055	0.183	252.1

Table 22: Reach scale bed elevation change (Sorted by Manning's n value)

Description	Manning's n value	(Simulated - Measured) bed elevation change (m)	% difference
0% suspended, 0% Bedload	0.01	0.153	211.7
50% suspended, 50% Bedload	0.01	0.378	523.6
0% suspended, 0% Bedload	0.015	0.074	101.4
0% suspended, 0% Bedload	0.02	0.013	16.8
100% suspended, 0% Bedload	0.02	0.152	209.4
0% suspended, 0% Bedload	0.025	0.049	67.4
0% Suspended, 1% Bedload	0.025	0.034	45.7
0% Suspended, 10% Bedload	0.025	0.031	42.6
0% Suspended, 20% Bedload	0.025	0.182	251.6
0% Suspended, 30% Bedload	0.025	0.140	192.9
0% Suspended, 40% Bedload	0.025	0.167	230.2
0% Suspended, 5% Bedload	0.025	0.067	91.4
10% suspended, 0% Bedload	0.025	0.078	107.1
100% suspended, 0% Bedload	0.025	0.125	173.0
20% suspended, 0% Bedload	0.025	0.790	1094.1
30% suspended, 0% bedload	0.025	0.065	88.7
40% suspended, 0% bedload	0.025	0.096	132.0
5% suspended, 5% Bedload	0.025	0.062	84.8
50% suspended, 50% Bedload	0.025	0.224	310.2
0% suspended, 0% Bedload	0.03	0.031	42.6
0% suspended, 0% Bedload	0.035	0.020	27.1
0% Suspended, 1% Bedload	0.035	0.076	104.6
0% Suspended, 5% Bedload	0.035	0.041	56.5
100% suspended, 0% Bedload	0.035	0.137	189.5
5% suspended, 5% Bedload	0.035	0.060	82.5

Description	Manning's n value	(Simulated - Measured) bed elevation change (m)	% difference
0% suspended, 0% Bedload	0.04	0.006	7.2
0% suspended, 0% Bedload	0.041	0.001	0.0
0% suspended, 0% Bedload	0.042	-0.021	-29.6
0% suspended, 0% Bedload	0.043	-0.023	-32.7
0% suspended, 0% Bedload	0.044	-0.032	-45.4
0% suspended, 0% Bedload	0.045	-0.037	-52.8
100% suspended, 0% Bedload	0.045	0.165	228.2
5% suspended, 5% Bedload	0.045	0.105	143.9
0% suspended, 0% Bedload	0.05	-0.054	-76.4
25% Suspended, 5% Bedload	0.05	0.120	165.4
50% suspended, 50% Bedload	0.05	0.266	368.0
0% suspended, 0% Bedload	0.055	-0.077	-107.3
0% suspended, 5% Bedload	0.055	0.014	19.1
10% suspended, 10% Bedload	0.055	0.139	191.7
100% suspended, 0% Bedload	0.055	0.183	252.1
50% suspended, 50% Bedload	0.055	0.220	303.5
10% suspended, 10% Bedload	0.065	0.137	189.1

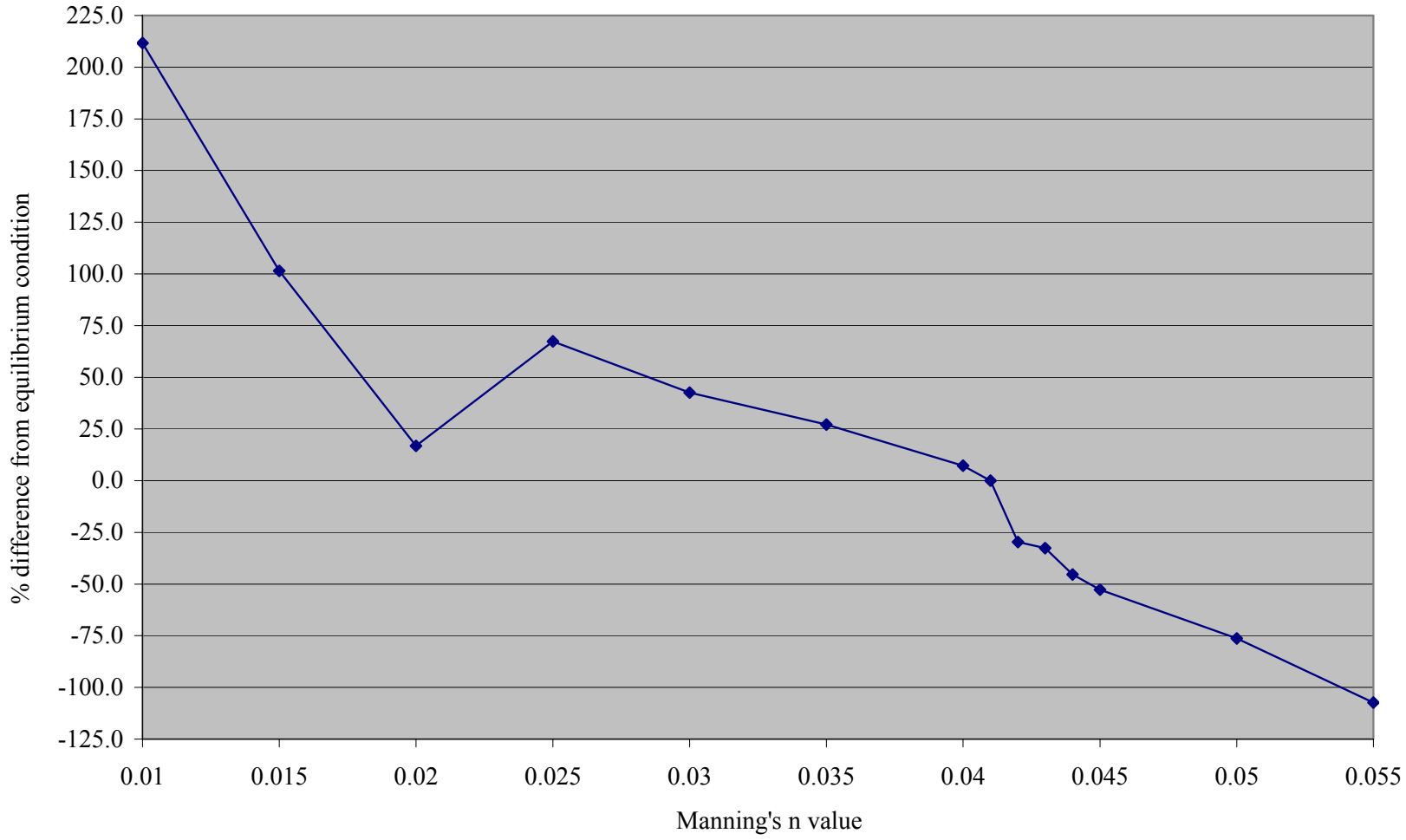

Figure 7: Manning's n influence on simulated bed elevation (0% suspended load, 0% bedload)

decreases the difference between measured and simulated results. However, Manning's n values larger than 0.041 increase the discrepancy between measured and simulated results.

Figure 8 illustrates the reach-scale bed elevation change trend for a fixed Manning's n value of 0.025, and for varying sediment rating curves, both suspended and bedload. Note that the model simulation that utilized a 20% suspended load and 0% bedload rating curves at the upstream model boundary produced a strong deviation from the equilibrium condition, but the surrounding values deviate by less than 108%. The slope of the bedload rating curve's influence on corresponding bed elevation change is greater than the slope with respect to the suspended load rating curve and corresponding bed elevation change. The simulated reach-scale bed elevation change has a greater sensitivity to the bedload rating curve. Point scale and local scale trends were examined solely by statistical analysis, discussed in the following section.

3.3.3 Statistical analysis

Table 23 illustrates the results from the first statistical analysis. The table includes the number of significant correlations (p value < 0.05) between simulated bed elevation change at each node surrounding the 17 monitoring points, and the independent variables bedload, suspended load, and Manning' n value associated with each successful simulation. Simulated bed elevation change at the nodes showed the strongest correlation with the bedload rating curve (i.e., 42.7%), followed by the suspended load rating curve (i.e., 37.5%), and the Manning's n value (i.e., 19.8%).

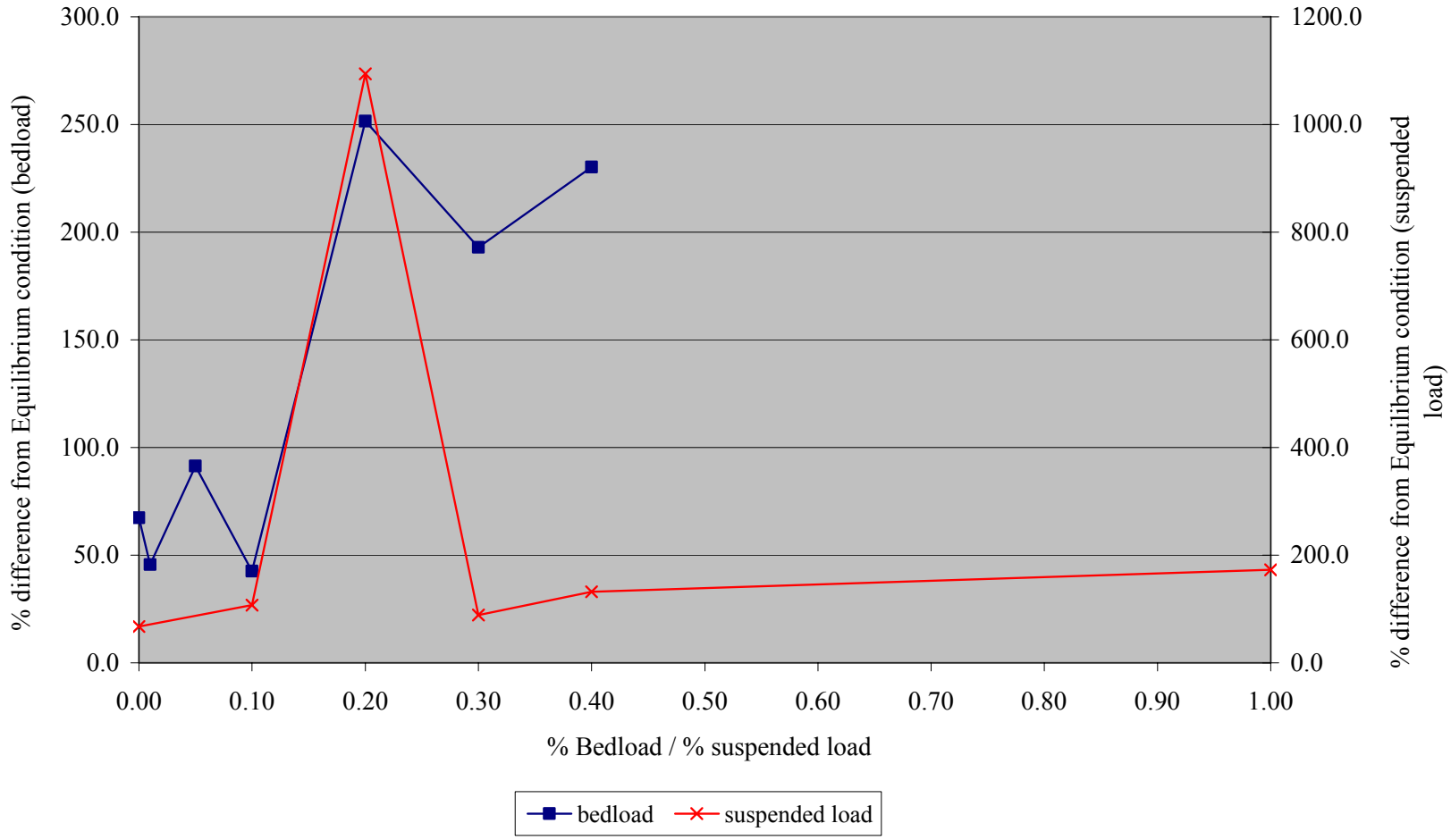

Figure 8: Sediment rating curve influence on simulated bed elevation (0.025 Manning's n value)

Table 23: Multivariate statistics results (72 nodes)

Independent Variable	Count	%
Bedload	41	42.7
Suspended	36	37.5
n value	19	19.8
Sum	96	100.0
With p value < 0.05		

Table 24 illustrates the correlation and level of significance results produced at the reach scale. The results show a strong correlation ($p = 0.008$) with the simulated reach scale bed elevation change and the bedload rating curve. The suspended load rating curve's influence on simulated bed elevation change at the reach scale is weaker ($p = 0.0191$). The Manning's n value has the smallest effect on simulated reach scale bed elevation change, with $p = 0.1635$.

The bed elevation change for each of the five groups was examined to determine if results observed at the reach scale, which showed a strong correlation between the bedload rating curve and simulated bed elevation change, was applicable at the local scale. The results, illustrated in Table 25, show that each group has a strong correlation with either the bedload rating curve or the Manning's n value. The suspended load rating curve was not observed to have a strong correlation with any of the five groups. Groups 1 and 2 showed a strong correlation with the bedload rating curve, with $p = <0.0001$ and $p = 0.0424$ respectively. Groups 3, 4 and 5 show a strong correlation with the Manning's n value, with $p = 0.2153$, $p = <0.0001$, and $p = 0.0009$, respectively. It should be noted that group 3 did not show a strong level of significance with any of the independent variables. Due to the lack of correlation, the standard deviation or the measure of how

Table 24: Multivariate statistics results (reach scale bed elevation change)

Pairwise Correlations			
Variable	by Variable	Correlation	Signif Prob
Bed elevation change metric	Suspended	0.3603	0.0191
Bed elevation change metric	bedload	0.4035	0.008
Bed elevation change metric	Manning's n value	-0.219	0.1635

Table 25: Multivariate statistics results (local scale bed elevation change)

Pairwise Correlations			
Variable	by Variable	Correlation	Signif Prob
Group 1	Suspended	0.3428	0.0263
Group 1	Bedload	0.58	<.0001
Group 1	Manning's n value	0.0031	0.9847
Group 2	Suspended	0.3006	0.0531
Group 2	Bedload	0.3147	0.0424
Group 2	Manning's n value	-0.1858	0.2387
Group 3	Suspended	-0.0729	0.6465
Group 3	Bedload	-0.0636	0.6892
Group 3	Manning's n value	-0.1952	0.2153
Group 4	Suspended	0.3209	0.0382
Group 4	Bedload	-0.0047	0.9765
Group 4	Manning's n value	-0.6618	<.0001
Group 5	Suspended	0.3536	0.0216
Group 5	Bedload	-0.1007	0.5259
Group 5	Manning's n value	-0.4934	0.0009

widely a set of values is dispersed from the mean was calculated and examined based on the results of bed elevation change produced by the successful simulations. The results of the standard deviation analysis are presented in Table 26. The results show that group 3 has little deviation despite the difference in sediment yields and Manning's n values utilized in multiple simulations. This explains the weak correlation with respect to the three independent variables (i.e., bedload and suspended load rating curves and the Manning's n value).

The statistical analysis results at the point scale were similar to those at the local scale, with results presented in Table 27. Monitoring points 1883, 1873, 1871, 1869, 1868, 1859, and 1866 showed a strong correlation with the bedload rating curve, with $p = 0.0001$, $p = 0.0094$, $p = 0.0003$, $p = <0.0001$, $p = 0.0002$, $p = <0.0001$, and $p = 0.0002$, respectively. The points included in group 2 showed mixed results. Two out of the five monitoring points, points 1490 and 1463, showed a strong correlation with the bedload rating curve, with $p = 0.0022$ and $p = 0.0001$, respectively. Two other monitoring points, point numbers 1464 and 1424, showed a correlation with suspended sediment. However, the p values were relatively high, at 0.0971 and 0.2579. One of the monitoring points, number 1425, showed a strong correlation with the Manning's n value. The remainder of

Table 26: Standard deviation analysis, Local scale simulated bed elevation change

	Standard deviation
Group 1	1.30
Group 2	0.77
Group 3	0.04
Group 4	0.49
Group 5	0.12

Table 27: Multivariate statistics results (point scale bed elevation change)

Pairwise Correlations			
Variable	by Variable	Correlation	Signif Prob
MP-199	suspended	0.3536	0.0216
MP-199	Bedload	-0.1007	0.5259
MP-199	Manning's n value	-0.4934	0.0009
MP-237	suspended	0.3916	0.0103
MP-237	Bedload	-0.005	0.9752
MP-237	Manning's n value	-0.6594	<.0001
MP-373	suspended	0.2388	0.1278
MP-373	Bedload	0.0145	0.9274
MP-373	Manning's n value	-0.6489	<.0001
MP-378	suspended	0.2809	0.0716
MP-378	Bedload	-0.0291	0.855
MP-378	Manning's n value	-0.6256	<.0001
MP-843	suspended	-0.0729	0.6465
MP-843	Bedload	-0.0636	0.6892
MP-843	Manning's n value	-0.1952	0.2153
MP-1424	suspended	0.1786	0.2579
MP-1424	Bedload	0.0522	0.7426
MP-1424	Manning's n value	0.0942	0.5531
MP-1425	suspended	0.2382	0.1287
MP-1425	Bedload	0.1837	0.2441
MP-1425	Manning's n value	-0.4672	0.0018
MP-1463	suspended	0.3112	0.0449
MP-1463	Bedload	0.5524	0.0001
MP-1463	Manning's n value	-0.0764	0.6306
MP-1464	suspended	0.2594	0.0971
MP-1464	Bedload	0.1015	0.5225
MP-1464	Manning's n value	-0.1321	0.4043

Pairwise Correlations			
Variable	by Variable	Correlation	Signif Prob
MP-1490	suspended	0.3558	0.0207
MP-1490	Bedload	0.4591	0.0022
MP-1490	Manning's n value	-0.2604	0.0958
MP-1859	suspended	0.3862	0.0115
MP-1859	Bedload	0.6094	<.0001
MP-1859	Manning's n value	-0.1412	0.3724
MP-1866	suspended	0.3687	0.0163
MP-1866	Bedload	0.5423	0.0002
MP-1866	Manning's n value	0.1063	0.5029
MP-1868	suspended	0.4842	0.0012
MP-1868	Bedload	0.5445	0.0002
MP-1868	Manning's n value	-0.2096	0.1828
MP-1869	suspended	0.4303	0.0044
MP-1869	Bedload	0.5827	<.0001
MP-1869	Manning's n value	-0.149	0.3463
MP-1871	suspended	0.1702	0.2813
MP-1871	Bedload	0.5333	0.0003
MP-1871	Manning's n value	0.1396	0.378
MP-1873	suspended	0.0442	0.7809
MP-1873	Bedload	0.3963	0.0094
MP-1873	Manning's n value	0.2003	0.2034
MP-1883	suspended	0.277	0.0758
MP-1883	Bedload	0.5585	0.0001
MP-1883	Manning's n value	0.1394	0.3787

the points in groups 3, 4 and 5 showed a correlation with the Manning's n value. All of these correlations were relatively strong, with $p < 0.05$, except for monitoring point 843. Table 28 summarizes the independent variable with the strongest correlation to each monitoring point at the point and local scales.

Table 28: Multivariate statistics results (point and local scale)

Group 1	Independent Variable	Group 2	Independent Variable	Group 3	Independent Variable	Group 4	Independent Variable	Group 5	Independent Variable
MP-1883	Bedload	MP-1490	Bedload	MP-843	Manning's n value	MP-378	Manning's n value	MP-199	Manning's n value
MP-1873	Bedload	MP-1463	Bedload			MP-373	Manning's n value		
MP-1871	Bedload	MP-1464	suspended			MP-237	Manning's n value		
MP-1869	Bedload	MP-1424	suspended						
MP-1868	Bedload	MP-1425	Manning's n value						
MP-1859	Bedload								
MP-1866	Bedload								

Chapter 4: Discussion and Conclusion

Sediment transport is one of the most difficult processes encountered by the hydraulic engineer; it is highly variable and innately difficult to quantify and predict (Bunte et al., 2004; Papanicolaou et al., 2008). It has challenged such great minds such as Vito Vanoni, Hans Alber Einstein, John Kennedy, Hunter Rouse, and Daryl Simons, and undoubtedly will continue to challenge those that take on the endeavor in the future (Barkdoll & Duan, 2008). Several authors suggest that a computational model can be a powerful tool for investigating sediment transport and in-stream hydrodynamic processes (Chen et al., 2007; Duan et al., 2007; Jia & Wang, 1999; Jia et al., 2006; Langendoen, 2001; Papanicolaou et al., 2008; Scott & Jia, 2005; White, 2008; Wu, 2008). However, caution should be applied, as a model is only an approximation of the real world physical processes, even for very simple physical problems, so the accuracy of the simulated quantities and processes are limited (Zhang, 2006). One should understand and expect errors due to mathematical approximations (i.e., Reynolds averaging, depth-averaging, and truncation errors) and physical approximations (i.e., assuming vertical flow acceleration is negligible and turbulent closure schemes) involved in formulating a numerical model for sediment transport. When a model is applied to a field study it must be calibrated with field data if reasonable results are to be expected. Calibration requires extensive field measurements of suspended sediment concentration, bedload transport, and hydraulic properties (i.e., stage measurements and discharge measurements) at sufficient temporal and spatial resolution to account for variability within a natural

system. Due to time, budget, and resource constraints practitioners are often estimating critical input parameters and performing computational simulations without the proper calibration data (Formann et al., 2007; Jia et al., 2006; Jiang et al., 2004; Scott & Jia, 2005; Wu, 2004). For this reason, there exists a demand to understand the sensitivity of sediment transport simulations to model input parameters (i.e., Manning's n value and sediment rating curves), especially when input parameters must be estimated and results can not be easily verified.

An analysis of model results showed that the correlation between simulated bed elevation change and the independent variables (i.e., bedload, suspended load, and the Manning's n value) was a function of the spatial distribution of the points and associated point groups. Groups 1 and 2, spatially located at the upstream portion of the reach, showed a strong correlation with the bedload rating curves, in contrast to groups 3, 4, and 5. Groups 3, 4, and 5, spatially located at the downstream portion of the reach, showed a strong correlation with the Manning's n value. Thus, the accurate simulation of bed elevation change at the upstream groups, 1 and 2, appears to be dependent upon the accurate definition of an upstream bedload rating curve. However, the bed elevation change at the downstream groups appears to be dependent on the successful simulation of the hydraulic relationships that dictate shear stress at the bed, including the accurate description of the Manning' n variable. For this reason, practitioners limited by time and resources should focus their efforts on accurate measurements of both the sediment rating curves and variables required to calculate the Manning's n value (i.e., upstream and downstream stage measurements, average hydraulic radius, average cross sectional area, and discharge measurements). The estimation of these variables based on best

professional judgment can lead to inaccurate results of bed elevation change along a reach.

The application of a simplified model to a complex system, the definition of complex bed topography, and the lack of model calibration prevented an accurate comparison of simulated and measured bed elevation change at the reach, local, and point scales in this study. Various other case studies and authors have noted similar problems with the application of computational models (Lane, 1998; Lane et al., 1999; Papanicolaou et al., 2008; Wu, 2008). Deviations between measured and simulated results can occur when a simplified conceptual model is applied to simulate complicated real systems and corresponding chaotic behavior. In general, the model may not accurately mathematically describe the complex hydrodynamic and sediment transport processes that occur within a natural channel (Lane et al., 1999; Wu, 2008). Within the Ligias Creek study site, complex hydraulic processes occurred due to the influence of woody vegetation and channel bifurcation. A 2D model may not be capable of accurately simulating the complex hydraulics that occur along the reach, but further study investigations were required to confirm this hypothesis.

Deviations between measured and simulated results can also occur when the complex bed topography is not adequately described by the computational mesh (Lane et al., 1994; Wu, 2008). Computational capacity and corresponding mesh definition appeared to prevent an accurate comparison of simulated and measured bed elevation change for the Ligias Creek simulations. The mesh consisted of modeling nodes which were spaced approximately 1 m parallel to the flow direction and 1.5 m perpendicular to

the flow direction. The node spacing prevented an accurate evaluation of monitoring points below a 1 m spatial resolution.

In addition, the complex bed topography exhibited along Ligias Creek may not be adequately described by traditional surveying techniques. Papanicolaou et al. (2008) states that traditional measurement protocols of bed morphology using point or cross-section measurements are applicable to a limited spatial and temporal resolution and may hinder adequate model calibration and verification. Future case studies should consider pre- and post-volumetric changes in the bed topography as opposed to evaluating the bed elevation change at a limited number of isolated points; this process would require a high level of precision to accurately compare volumes at reasonable spatial scales. High resolution photogramatry may provide better topographic resolution, with current methods achieving approximately 0.03 m resolution with airborn imagery over kilometer reaches (Lane et al., 1994; Lane and Chandler, 2003). Lane et al. (1994) incorporated photogramatry and a tacheometric survey to obtain accurate and dense digital terrain models in their study. Comparison of consecutive DTMs allowed for visualization of channel morphology, and quantification of net and distributed volumes of channel change. However, resolution is limited in streams with coarse substrate due to problems associated with the definition of volume and surface elevations between large particles in close proximity. For this reason, the spatial resolution of measured topographic data and simulated results is limited by the size of the substrate contained within the channel bed.

Papanicolaou et al. (2008) states that inherent model limitations do not allow for the accurate simulation of processes independent of data input and model calibration (i.e., site specific sediment rating curves and Manning's n value). The problem is

compounded for sediment transport models, which rely heavily on experimental and field information and whose formulations involve a high degree of empiricism. This confirms the observation that additional field measurements are required to simulate bed elevation change with a 2D model. The development of an extensive field measurement database is needed to validate computational models and existing empirically derived sediment transport formulas. Future case studies should include sufficient bedload and suspended load measurements, with sufficient spatial and temporal resolution to account for the inherent variability in sediment transport and measurement error. This data could then be used to develop site specific sediment rating curves and sufficient flow and stage measurements at the upstream and downstream project extent to support the calculation of a site specific Manning's n value.

In summary, the choice of a numerical model depends on the complexity and nature of the problem, the time and spatial scale of interest, availability of data for model calibration and verification, and time, budget, and resource constraints. Extensive field measurements are required to collect the necessary data to accurately calibrate and simulate a computational model. These field measurements should include detailed topographic data, with sufficient resolution to accurately describe the spatial scale of interest, extending upstream and downstream of the modeling boundary, sufficient data to calculate a site specific Manning's n value, and sufficient sediment samples to calculate sediment rating curves at the upstream modeling boundary. The field data needed to calculate a site specific Manning's n value include water surface elevations at the upstream and downstream extents of the modeling reach, discharge measurements, and hydraulic geometry (i.e., hydraulic radius and area). Water surface elevation data and

discharge measurements should include sufficient resolution above and below the discharge of interest. If spatial variation in the Manning's n value is considered, additional measurements are required to accurately calibrate the roughness value along different portions of the reach. If sediment transport is simulated, sufficient sediment samples, both suspended load and bedload, are required to calculate upstream sediment rating curves. A higher priority should be placed on bedload sampling if bedload transport is the dominant transport mode and morphological change is predominately caused by the transport of bedload (Wu, 2004).

The ability of CCHE2D to simulate hydraulic (Jia et al., 2002; Jin & Steffler, 1993; Wu, 2004; Wu & Wang, 2006) and sediment transport (Duan et al., 2001; Wu, 2002; Wu et al., 2004) processes has been validated in multiple flume studies (Appendix B). However, the validation of a computational model based solely on empirical flume data, does not define a model's limits with respect to successful performance as a function of channel morphological complexity (Lane, 1998; Lane et al., 1999; Papanicolaou et al., 2008; Wu, 2008). The model has yet to be validated in a reach (<500 m) contain coarse substrate ($d_{50} \geq 66$ mm) and simulated over short temporal scales (one storm event). The results of this study suggest the model may have limited application to the combination of short spatial and temporal scales and reaches with coarse substrate. However several authors suggest, once calibrated a computational model can be a powerful tool for investigating and increasing our understanding of in-stream hydrodynamic and sediment transport processes (Jia et al., 2002; Jin & Steffler, 1993; Langendoen, 2001; White, 2005; Wu, 2008; Wu & Wang, 2004). This may be true at

large temporal and spatial scales, but additional case studies are requires to validate and determine the applicable limits of CCHE2D to short time and spatial scales.

List of References

List of References

Abad, J.D., Buscaglia, G.C., Garcia, M.H. (2008). 2D stream hydrodynamic, sediment transport and bed morphology model for engineering applications. *Hydrological Processes*, 22(10), 1443-1459.

Bagnold, R.A. (1977). Bed load transport by natural rivers. *Water Resources Research*, 13(2), 303-312.

Barkdoll, B.D., Duan, J.G., Fan, S.S., Klumpp, C.C., McAnnally, B., Papanicolaou, T., Scott, S., Wang, S.S.Y., Wu, W.M., Ying, X.Y. (2004). Computational modeling of sediment transport processes. *Journal of Hydraulic Engineering*, 130(7), 597-598.

Barkdoll, B.D., Duan, J.G. (2008). Sediment modeling: issues and future directions. *Journal of Hydraulic Engineering*, 134(3), 285.

Bathurst, J.C., Thorne, C.R., Hey, R.D. (1979). Secondary flow and shear stress at river bends. *Journal of the Hydraulics Division*, 105(10), 1277– 1295.

Bennett, J.P. (1974). Concepts of mathematical modeling of sediment yield. *Water Resources Research*, 10(3), 485-492.

Biron, P.M., Lane, S.N., Roy, A.G., Bradebrook, K.F., Richards, K.S. (1998). Sensitivity of bed shear stress estimated from vertical velocity profiles: The problem of sampling resolution. *Earth Surface Processes and Landforms*, 23, 133-139.

Buchanon, T.J. & Somers, W.P. (1960). Discharge measurements at gaging stations. *U.S. Geological Survey Techniques of Water-resources Investigations Book 3*, A8, 65.

Bunte, K., & MacDonald, L.H. (1995). Detecting change in sediment loads: where and how is it possible? Effects of scale on interpretation of sediment and water quality. *International Association of Hydrological Sciences*, 226, 253-261.

Bunte, K., Abt, S.R., Potyondy, J.P., Ryan, S.E. (2004). Measurement of coarse gravel and cobble transport using portable bedload traps. *Journal of Hydraulic Engineering*, 130(9), 879-893.

Carbonneau, P.E., Lane, S.N., Bergeron, N.E. (2003). Cost-effective non-metric close-range digital photogrammetry and its application to a study of coarse gravel river beds. *International Journal of Remote Sensing*, 24(14), 2837-2854.

Chen, D., Zhang, Y., Duan, J.G., Stone, M., Acharya K. (2007). Two-dimensional simulation of hydrodynamic and sediment transport in a gravel bed channel: The Salt River. *Proc., 2007 World Environmental and Water Resources Congress*, Tampa, Florida, May 15-19, 2007. American Society of Civil Engineers, Reston, Va.

Chow, V.T. (1959). *Open Channel Flow*. McGraw-Hill Book Company, New York, NY.

Cowan, W.L. (1956). Estimating hydraulic roughness coefficients. *Agricultural Engineering*, 37(7), 473-475.

Crawford, C.G. (1991). Estimation of suspended-sediment rating curves and mean suspended-sediment loads. *Journal of Hydrology*, 129, 331-348.

Dietrich, W.E., & Smith, J.D. (1983). Influence of the point bar on flow through curved channels. *Water Resources Research*, 19(5), 1173–1192.

Dietrich, W.E. (1987). Mechanics of flow and sediment transport in river bends. In: Richards, K. (Ed.), *River Channel Environment and Process*., 179– 227.

Ding, Y., Jia Y., Wang, S.S.Y. (2004). Identification of manning's roughness coefficients in shallow water flows. *Journal of Hydraulic Engineering*, 130(6), 501-510.

Duan, J.G., Wang, S.S.Y., Jia, Y. (2001). The application of enhanced CCHE2D model to study the alluvial channel migration processes. *Journal of Hydraulic Research*, 39(5), 469-480.

Duan, J.G., Chen, D., Weller, J., Benoit, T. (2007). Two-dimensional simulation of flow hydraulics and bed-load transport in a mountain gravel-bed stream: the Upper Spanish Creek. *Proc., 2007 World Environmental and Water Resources Congress*, Tampa, Florida, May 15-19, 2007. American Society of Civil Engineers, Reston, Va.

Dworak, F.J. (2005). Characterizing turbulence structure along woody vegetated banks in incised channels: implications for stream restoration. MS thesis, Dept. of Environmental Engineering, University of Tennessee, Knoxville, TN.

Dysart, B.C. III, & Langdon, C.H. III (1976). Sediment transport in a South Carolina mountain stream. *Proc., 1976 Irrigation and Drainage Specialty Conference on Environmental Aspects of Irrigation and Drainage*, Ottawa, Ontario, Canada. American Society of Civil Engineers, Reston, Va.

Einstein, H.A. (1950). The bed-load function for sediment transportation in open channel flows. *Technical Bulletin Number 1026.* U.S. Dept. Agric. Soil Conservation Service, Washington, DC.

Formann, E., Habersack, H.M., Schober, S.T. (2007). Morphodynamic river processes and techniques for assessment of channel evolution in Alpine gravel bed rivers. *Geomorphology*, 90, 340-355.

Galay, V.J. (1983) Causes of river bed degradation. *Water Resources Research*, 19, 1057-1090.

Garbrecht, J., Kuhnle, R.A., Alonso C.V. (1996). A sediment transport capacity formulation for application to large channel networks. *Journal of Soil and Water Conservation*, 50(5), 527-529.

Garbrecht, J., Kuhnle, R.A., Alonso C.V. (1996). A transport algorithm for variable sediment sizes: Fundamental concepts and equations. *Proc., 1996 Sixth Federal Interagency Sedimentation Conference*, Las Vegas, Nevada, March 25-29, 1996. U.S. Department of the Interior, U.S. Geological Survey, Reston, Va.

Haan, C.T., Barfield, B.J., Hayes, J.C. (1994) *Design Hydrology and Sedimentology for Small Catchments*. Academic Press, San Diego, California.

Habersack, H.M., & Laronne, J.B. (2002). Evaluation and improvement of bed load discharge formulas based on Helley-Smith sampling in an Alpine gravel bed river. *Journal of Hydraulic Engineering*, 128(5), 484-499.

He, Z., Wu, W., Wang, S.S.Y. (2006). A depth-averaged 2-D analysis of fish habitat suitability impacted by vegetation and sediment. *Proc., 2006 World Environmental and Water Resources Congress*, Omaha, Nebraska, May 21-25, 2006. American Society of Civil Engineers, Reston, Va.

Jia, Y., & Alonso, C.V. (1994). One- and two-dimensional analysis of flow in Hotophia Creek, MS. *Proc. 1994 Hydraulic Engineering Conference*, Buffalo, New York, August 1-5, 1994. American Society of Civil Engineers, Reston, Va.

Jia, Y., & Wang, S.S.Y. (1999). Numerical model for channel flow and morphological change studies. *Journal of Hydraulic Engineering*, 125(9), 924-933.

Jia, Y., & Wang, S.S.Y. (2001a). CCHE2D: Two-dimensional hydrodynamic and sediment transport model for unsteady open channel flows over loose bed. *Technical Report No. NCCHE-TR-2001-1*. National Center for Computational Hydroscience and Engineering, Oxford, M.S.

Jia, Y. & Wang S.S.Y. (2001b). CCHE2D Verification and validation test documentation. *Technical Report No. NCCHE-TR-2001-2*. National Center for Computational Hydroscience and Engineering, Oxford, M.S.

Jia, Y., Wang, S.S.Y., Xu, Y. (2002). Validation and application of a 2D model to channels with complex geometry. *International Journal of Computational Engineering Science*, 3(1), 57-71.

Jia, Y., Zhang, Y., Wang, S.S.Y, Raible, G.A. (2006). Numerical simulations of channel response to riverine structures in Arkansas River. *Proc., 2006 7th International Conference on HydroScience and Engineering*, Philadelphia, P.A., September 10-13, 2006. International Association of Hydraulic Engineering and Research, Madrid, Spain.

Jia, Y., & Wu, W. (2007). Numerical and empirical modeling tools development for studying bank erosion and evolution of headcut and tailcut due to sand and gravel mining pits in alluvial rivers. *Technical Report No. NCCHE-TR-2007-2.* National Center for Computational Hydroscience and Engineering, Oxford, M.S.

Jiang, E, Wu, W., Wang, S.S.Y. (2004). Calculation of flow and sediment transport in the Lower Yellow River using CCHE2Dfvm model. *Proc., 2004 World Environmental and Water Resources Congress*, Salt Lake City, Utah, June 27-July 1, 2004. American Society of Civil Engineers, Reston, Va.

Jin, Y.C., & Steffler, P.M. (1993). Predicting flow in curved open channels by depth-averaged method. *Journal of Hydraulic Engineering*, 119(1), 109-124.

Julien, P.Y. (1995). *Erosion and Sedimentation*. Cambridge University Press, New York, NY.

Khan, A.A., Cadavid, R., Wang, S.S.Y. (2000). Simulation of channel confluence and bifurcation using the CCHE2D model. *Institution of Civil Engineers Proceedings, Water and Maritime engineering*, 142(2), 97-102.

Khan, A.A., & Koshino, K. (2000). Application of three two-dimensional depth-averaged models to flow in river bends. *Proc., 2000 4th International Conference on Hydroscience and Engineering*, Seoul, Korea, September 26-29, 2000. Korea Water Resource Association, Seoul, Korea.

Khan, A.A. (2003). CCHE2D-GUI – Graphical user interface for the CCHE2D model user's manual – Version 2.0, *Technical Report*, National Center for Computational Hydroscience and Engineering, Oxford, M.S.

Lane, S.N., Chandler, J.H., Richards, K.S. (1994). Developments in monitoring and modelling small-scale river bed topography. *Earth Surface Processes Landforms*, 19, 349–368.

Lane, S.N., Richards, K.S., Chandler, J.H. (1995). Within reach spatial pattern of process and channel adjustment, In: Hickin, E.J. (Ed.) *River Geomorphology,* 105-130.

Lane, S.N., Richards, K.S., Chandler, J.H. (1996). Discharge and sediment supply controls on erosion and deposition in a dynamic alluvial channel. *Geomorphology*. 15, 1-15.

Lane, S.N., & Richards, K.S. (1997). Linking river channel form and process: time, space and causality revisited. *Earth Surface Processes and Landforms*, 22, 249-260.

Lane, S.N. (1998). Hydraulic modelling in hydrology and geomorphology: A review of high resolution approaches. *Hydrological Processes*, 12, 1131-1150.

Lane, S.N., Bradbrook, K.F., Richards, K.S., Biron, P.A., Roy, A.G. (1999). The application of computational fluid dynamics to natural river channels: Three-dimensional versus two-dimensional approaches. *Geomorphology*, 20(1), 1-20.

Lane, S.N. & Chandler, J.H. (2003). The generation of high quality topographic data for hydrology and geomorphology: New data sources, new applications and new problems. *Earth Surface Processes and Landforms*, 28, 229-230.

Lane, S.N., Westaway, R.M., Hicks, D.M. (2003). Estimation of erosion and deposition volumes in a large, gravel-bed, braided river using synoptic remote sensing. *Earth Surface Processes and Landforms*, 28, 249-271.

Lane, S.N. (2005). Roughness – time for a re-evaluation? *Earth Surface Processes and Landforms*, 30, 251-253.

Langendoen, E.J. (2000). CONCEPTS – Conservational Channel Evolution and Pollutant Transport System, *Research Report 16*, U.S. Department of Agriculture, Agriculture Research Service, USDA-ARS National Sedimentation Laboratory, Oxford, MS.

Langendoen, E.J. (2001). Evaluation of the effectiveness of selected computer models of depth-averaged free surface flow and sediment transport to predict the effects of hydraulic structures on river morphology. *Project Report*, USDA-ARS National Sedimentation Laboratory, Oxford M.S.

Langendoen, E.J., Simon, A., Thomas, R.E. (2001). CONCEPTS-a process-based modeling tool to evaluate stream-corridor restoration designs. *Proc., 2001 Wetlands Engineering and River Restoration Conference*, Reno, NV, August 27-31, 2001. American Society of Civil Engineers, Reston, VA.

Langendoen, E.J., & Alonso, C.V. (2008). Modeling the evolution of incised streams: I. Model formulation and validation of flow and streambed evolution components. *Journal of Hydraulic Engineering*, 134(6), 749-762.

Laursen, E.M. (1958). The total sediment load of streams. *Journal of the Hydraulic Division*, ASCE, 84, 1-36.

Martin, Y. (2003). Evaluation of bed load transport formulae using field evidence from the Vedder River, British Columbia. *Geomorphology*, 531(2), 75–95.

Massey, M.P. (2008). Use of the AnnAGNPS pollutant loading model for prediction of sediment yields in a mountainous Cumberland Plateau region: correlations with the stream bed sediment characteristics. MS thesis, Dept. of Civil and Environmental Engineering, The University of Tennessee, Knoxville, TN.

Meyer-Peter, E., & Muller, R. (1948). Formulas for bed-load transport. *Proc., 1948 Second Meeting of International Association for Hydraulic Research,* Stockholm, Sweden, 1948. International Association of Hydraulic Engineering and Research, Madrid, Spain.

Nakato, T. (1990). Tests of selected sediment - transport formulas. *Journal of Hydraulic Engineering*, 116(3), 362-379.

Papanicolaou, A.N., Elhakeem, M., Krallis, G., Prakash, S., Edinger, J. (2008). Sediment transport modeling review-current and future developments. *Journal of Hydraulic Engineering*, 134(1), 1-14.

Parker, G., & Anderson, A.G. (1977). Basic principles of river hydraulics. *Journal of The Hydraulics Division*, 103(9), 1077-1087.

Phillips, B.C., & Sutherland, A.J. (1989). Spatial lag effects in bed load sediment transport. *Journal of Hydraulic Research*, 27(1) 115-133.

Reid, S.C., Lane, S.N., Berney, J.M., Holden, J. (2007). The timing and magnitude of coarse sediment transport events within an upland, temperate gravel-bed river. *Geomorphology*, 83, 152-182.

Rhoads, B.L., & Welford, M.R. (1991). Initiation of river meandering. *Progress in Physical Geography*, 15(2), 127–156.

Robinson, J.L. (2005). Assessment of in-stream processes in urban streams for development of sediment total maximum daily loads. MS thesis, Dept. of Civil Engineering, Georgia Institute of Technology, Atlanta, Ga.

Rouse, H. (1965). Critical analysis of open channel resistance. *Journal of the Hydraulic Division*, ASCE, 91(4), 1-25.

Schwartz, J.S. (2003). Use of 2D hydrodynamic model for stream restoration design of high-flow habitat in low-gradient Midwest streams. *Proc., 2003 Protection and Restoration of Urban and Rural Streams*, Philadelphia, P.A., June 23-25, 2003. American Society of Civil Engineers, Reston, VA.

Scott, S.H., & Jia Y. (2005). Simulation of sediment transport and channel morphology change in large river systems. *Proc., 2005 U.S.-China Workshop on Advanced Computational Modeling in Hydroscience and Engineering, Oxford*, MS, September 19-23, 2005. International Research and Training Center on Erosion and Sedimentation, Beijing, China.

Simon, A., Langendoen, E.J., Bingner, R.L., Wells, R., Yuan, Y., Alonso, C.V. (2004). Suspended-sediment transport and bed-material characteristics of Shades Creek, Alabama and ecoregion 67: Developing water-quality criteria for suspended and bed-material sediment. *Research Report No. 43*, USDA-ARS National Sedimentation Laboratory, Oxford, M.S.

Slate, L.O., Shields, D.F., Schwartz, J.S., Carpenter, D.D., Freeman, G.E. (2007). Engineering design standards and liability for stream channel restoration. *Journal of Hydraulic Engineering*, 133(10), 1099-1102.

Smith, D.I., & Stopp, P. (1978). *The River Basin*. Cambridge University Press, Cambridge, MA.

Sturm, T. (2001). *Open Channel Hydraulics*. McGraw-Hill, New York, NY.

Thomas, R.E., & Langendoen, E.J. (2002). Numerical simulation of post-disturbance stream channel evolution: the Yalobusha River, Mississippi, USA. *Research Report No. 29*, USDA-ARS National Sedimentation Laboratory, Oxford, M.S.

U.S. Army Corps of Engineers. (2005). River Analysis System HEC-RAS, H*ydraulic Reference Manual Version 3.1.3*. U.S. Army Corps of Engineers, Hydrologic Engineering Center, Davis, CA.

Vidal, J.P., Moisan, S., Faure, J.B., Dartus, D. (2007). River model calibration, from guidelines to operational support tools. *Environmental modelling and Software*, 22, 1628-1640.

Waddle, T., Steffler, P., Ghanem, A., Katopodis, C., Locke, A. (2000). Comparison of one- and two-dimensional open channel flow models for a small habitat stream. *Rivers*, 3, 205-220.

Weinhold, M.R. (2001). Application of a site-calibrated Parker- Klingeman bedload transport model. M.S. thesis, Dept. of Civil Engineering, Colorado State Univ., Fort Collins, Colorado.

Wells, R.R., Langendoen, E.J., Simon, A. (2007). Modeling pre- and post-dam removal sediment dynamics: The Kalamazoo River, Michigan. *Journal of the American Water Resources Association*, 43(3), 773–785.

White, S. (2005). Sediment yield prediction and modeling. *Hydrological processes*, 19, 3053-3058.

Wilcock, P.R. (2001). Toward a practical method for estimating sediment-transport rates in gravel-bed rivers. *Earth Surface Processes and Landforms*, 26, 1395-1408.

Wolman, M.G. (1954). A method of sampling coarse river-bed material. *American Geophysical Union Transactions*, 15(6), 951-956.

Wu, W., Wang, S.S.Y., Jia, Y. (2000). Nonuniform sediment transport in alluvial rivers. *Journal of Hydraulic Research*, 38(6), 427-434.

Wu, W. (2001). CCHE2D Sediment Transport Model (Version 2.1). *Technical Report No. NCCHE-TR-2001-3*, National Center for Computational Hydroscience and Engineering, Oxford, M.S.

Wu, W. (2004). Depth-averaged two-dimensional numerical modeling of unsteady flow and nonuniform sediment transport in open channels. *Journal of Hydraulic Engineering*, 130(10), 1013-1024.

Wu, W., Jiang, E., Wang, S.S.Y. (2004). Depth-averaged 2-D calculation of flow and sediment transport in the Lower Yellow River. *International Journal of River Basin Management*, IAHR, 2(1).

Wu, W., & Wang, S.S.Y. (2004). Depth-averaged 2-D calculation of flow and sediment transport in curved channels. *International Journal of Sediment Research*, 19(4), 241-257.

Wu, W., Shields, F.D. Jr., Bennett, S.J., Wang, S.S.Y. (2005). A depth-averaged 2-D model for flow, sediment transport and bed topography in curved channels with riparian vegetation. *Water Resource Research*, 41, 15.

Wu, W., & Wang, S.S.Y. (2006). Application of a depth averaged 2-D model in river restoration. *Proc., 2006 World Environmental and Water Resources Congress*, Omaha, Nebraska, May 21-25, 2006. American Society of Civil Engineers, Reston, VA.

Wu, Weiming. (2008). *Computational River Dynamics*. Taylor & Francis – Balkema, Leiden, The Netherlands.

Xu, Y., Wang, S.S.Y., Jia, Y. (2001). Application of a depth-integrated two-dimensional numerical model to the Lauffen Reservoir on the Neckar River. Proc., 2001 International Conference of IAHR, Beijing, China, Sept. 16-21, 2001. International Association of Hydraulic Engineering and Research, Madrid, Spain.

Yang, C.T. (1973). Incipient motion and sediment transport. *Journal of Hydraulics Division*, 99(10), 1679–1704.

Yen, B.C. (1999). Identification problem of open-channel friction parameters – Discussion. *Journal of Hydraulic Engineering*, 125(5), 552-553.

Zhang, Y., & Jia, Y. (2005). CCHE2D mesh generator user's manual – version 2.6. *Technical Report No. NCCHE-TR-2005-05*, National Center for Computational Hydroscience and Engineering, Oxford, M.S.

Zhang, Y. (2006). CCHE-GUI – graphical users interface for NCCHE model user's manual – version 3.0. *Technical Report No. NCCHE-TR-2006-02*, National Center for Computational Hydroscience and Engineering, Oxford, M.S.

Zhang, Y., & Jia, Y. (2007). CCHE-MESH: 2D structured mesh generator user's manual – version 3.0. *Technical Report No. NCCHE-TR-2007-01*, National Center for Computational Hydroscience and Engineering, Oxford, M.S.

Appendices

Appendix A: Description of 1D, 2D, and 3D models

One-dimensional sediment transport modeling

One-dimensional (1D) models require the least amount of data to initiate a simulation and remain popular for this reason, despite the development of multi-dimensional models (Wu, 2008; Langendoen & Alonso, 2008). These models simulate flow and sediment transport in the stream-wise longitudinal direction of a channel without solving the details over the cross-section. For this reason, these models may provide reasonable results when applied to channels with longitudinal flow fields, limited hydraulic complexity, and minimal variation in channel geometry in the stream-wise direction. The use of 1D models compared to multi-dimensional models is based on the engineering problem, project objectives, spatial and temporal scales of interest and the solution accuracy required. For example, one-dimensional models provide a reasonable prediction of water surface elevations, but may over or under predict cross-sectional average velocities by 10 to 20%. These models are most commonly applied in the study of long-term sedimentation problems at reach scales (Formann et al., 2007; USACE, 2005; Langendoen, 2000; Langendoen & Alonso, 2008). Several current one-dimensional models are listed in Table 29 (Papanicolau et al., 2008).

1D sediment transport models are formulated in a rectilinear coordinate system and solve the differential conservation equations of mass and momentum of flow, the Saint Venant equations, along with the sediment mass continuity equation, the Exner equation, by using finite-difference schemes (Papanicolaou et al., 2008; Sturm, 2001;

Table 29: Summary of selected one-dimensional sediment transport models

Model and references	Last Update	Flow	Bed sediment transport	Suspended sediment transport	Sediment mixtures	Cohesive sediment	Sediment exchange processes	Executable	Source code	Language
HEC-6: Hydraulic Engineering Center; Thomas and Prashum (1977)	V. 4.2 (2004)	Steady	Yes	Yes	Yes	No	Entrainment and deposition	PD	PD	F77
MOBED: Mobile BED; Krishnappan (1981)	--	Unsteady	Yes	Yes	Yes	No	Entrainment and deposition	C	C	F90
IALLUVIAL: Iowa ALLUVIAL; Karim and Kennedy (1982)	--	Quasi-steady	Yes	Yes	Yes	No	Entrainment and deposition	C	C	FIV
FLUVIAL 11; Chang (1984)	--	Unsteady	Yes	Yes	Yes	No	Entrainment and deposition	C	P	FIV
GSTARS: Generalized sediment transport models for alluvial River simulation (Molinas and Yang, 1986)	V. 3 (2002)	Unsteady	Yes	Yes	Yes	No	Entrainment and deposition	PD	PD	F90/95
CHARIMA: Acronym of the word CHARiage which means bedload in French Holley et al. (1990)	--	Unsteady	Yes	Yes	Yes	Yes	Entrainment and deposition	C	C	F77
SEDICOUP: SEDIment COUPled; Holly and Rahauel (1990)	--	Unsteady	Yes	Yes	Yes	No	Entrainment and deposition	C	C	F77
OTIS: One-dimensional transport with inflow and storage; Runkel and Broshears (1991)	V. OTIS-P (1998)	Unsteady	No	Yes	No	No	Advection-diffusion	PD	PD	F77
EFDC1D: Environmental fluid dynamics code; Hamrick (2001)	--	Unsteady	Yes	Yes	Yes	Yes	Entrainment and deposition	PD	PD	F77
3STD1, steep stream sediment Transport 1D model; Papanicolaou et al. (2004)	--	Unsteady	[a]Yes	[a]Yes	Yes	No	Entrainment and deposition	C	P	F90

Note: V=Version; C=copyright; LD=limitied distribution; P=proprietary; PD=public domain; and F=FORTRAN.
[a]Treated as a total load without seperation

Wu, 2008; Langendoen, 2001; USACE, 2005). The Saint Venant equations or dynamic wave model (Continuity and momentum equation), friction slope equation, and Exner equation are illustrated below.

$$B\frac{\partial y}{\partial t}+\frac{\partial Q}{\partial x}=q \tag{4}$$

where,

y = stage

Q = Discharge

B = flow top width

Q = lateral flow into the channel per unit length of channel

x = distance along the channel

t = time

$$\frac{\partial Q}{\partial t}+\frac{\partial}{\partial x}\left(\frac{Q^2}{A}\right)+gA\left(\frac{\partial y}{\partial x}+S_f\right)=0 \tag{5}$$

where,

A = flow area

g = gravitational acceleration

S_f = friction slope

$$S_f=\frac{Q^2}{K^2}=\frac{n^2Q^2}{A^2R^{4/3}} \tag{6}$$

where,

K = conveyance

R = hydraulic radius

n = Manning roughness coefficient

$$B(1-p_0)\frac{\partial z_b}{\partial t}+\frac{\partial Q_t}{\partial x}=0 \quad (7)$$

where,

B = stream width

p_0 = porosity of the sediment bed

z_b = bed elevation

x = longitudinal distance along the stream

Q_t = total volumetric sediment discharge

These models can predict the basic parameters of a particular channel, including the water surface elevation, hydraulic radius, downstream velocity, bed-elevation variation, and sediment transport load (Papanicolau et al., 2008). The initiation of a one-dimensional simulation requires definition of the channel geometry via transverse section interconnected through reach lengths, most often defined by the downstream distance between subsequent cross sections (USACE, 2005; Langendoen, 2001). At a minimum two cross sections are required before a simulation can be initiated. The defined cross section(s) and channel geometry are assumed representative for some pre-determined channel length. This assumption limits the model's application with respect to abrupt changes in hydraulic geometry or roughness. Parameters such as energy head loss and

friction slope are computed as averaged values between cross sections. Thus, the accurate computation of one-dimensional values depends on the cross section spacing, definition, and density. Boundary conditions must still be established upstream, downstream, or both upstream and downstream of the reach of interest based on the simulation regime (steady flow, unsteady, subcritical, supercritical, or mixed flow).

The basic assumption for mathematical development of a 1D model lies in the computation of the governing equations solely in the longitudinal (downstream) direction (USACE, 2005; Langendoen, 2001). Additional assumptions include a hydrostatic water surface elevation, or no variation in water stage across a cross-section, and that a constant velocity represents an entire horizontal section throughout the water column or corresponding depth, though cross sections can be divided into multiple sections to better represent the flow field. Despite these assumptions, 1D models have been successfully applied and the results have been well received by multiple federal and state government agencies for well over a decade (Langendoen, 2000). Such applications include FEMA flood mapping (i.e., the CLOMR and LOMR process), stream restoration assessment, and stream restoration, bridge, and culvert design Generally, 1D models produce accurate results when applied to channels that are relatively straight, incised, shallow, and exhibit limited hydraulic complexity (Langendoen, 2000; Langendoen, 2001; Langendoen & Alonso, 2008). One-dimensional models are limited in channels that exhibit significant lateral flow, flow producing varying velocities throughout the water column, flow depths that are large with respect to the roughness element, and varying degrees of sinuosity. Thus, the hydraulic boundary conditions and constraints of a site influence the applicability of a one-dimensional model.

The fundamental assumptions governing sediment transport limit the application and validity of the results produced by 1D sediment transport models. For instance, a majority of the available sediment transport equations are capacity limited (i.e., Meyer Peter Muller) and are only applicable to channel reaches that are not supply limited (Weinhold, 2001; Meyer-Peter & Muller, 1948; Martin, 2003). The sediment transport capacity of a stream under unlimited sediment supply is simply a function of the hydraulic variables and the shape of the stream cross section (Julien, 1995). The underlying assumption of these equations is the excess shear stress concept, which is a function of the shear velocity at the bed. It is assumed the sediment is transported when the calculated hydraulic shear stress on the streambed exceeds some critical value required to set an individual particle in motion. Thus, the averaging of the velocity in the longitudinal and vertical directions limits the accuracy of the calculated shear velocity at the bed, the sediment transport prediction, and the simulation capabilities of a 1D model. An example of transverse and vertical variations in velocity include helical flow patterns, illustrated in Figure 9 (Smith & Stopp, 1978). For this reason, these models are best utilized in predicting net aggradation or degradation at a reach scale as opposed to aggradation or degradation at specific cross section locations (i.e., proposed bridge site or civil structure) (Formann et al., 2007).

Two-dimensional sediment transport modeling

Two-dimensional (2D) models have increased application with respect to 1D models because structured grids are utilized to define topography and these models allow

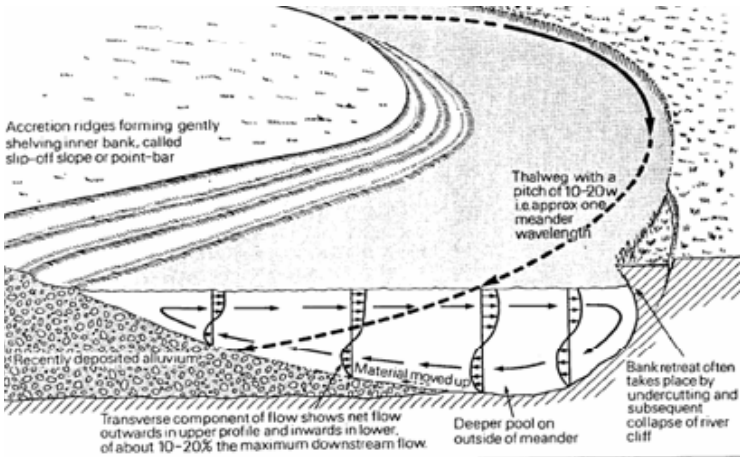

Figure 9: Helical flow patterns (Smith & Stopp, 1978)

for the simulation of the transverse flow vector, and for this reason 2D models have been the focus of research since the early 1990s (Papanicolaou et al., 2008; Langendoen, 2001; Lane et al., 1999). These models are advantageous because they are capable of simulating complex flow situations such as sinuous channels where significant transverse flow is present. Unfortunately, the increased complexity of 2D models necessitate significantly more data input compared to the one-dimensional models. However, these data allow the model to provide a spatially explicit solution of the flow field and potentially a more accurate description of the hydrodynamics (Waddle et al. 2000; Langendoen, 2001; Papanicolaou et al., 2008). If the vertical variations of flow and sediment quantities are sufficiently small, their variations in the horizontal plane or transverse direction can be approximated by a depth-averaged 2-D model (Wu, 2008). Table 30 lists several current two-dimensional models (Papanicolau et al., 2008).

The structured grid and the incorporation of turbulence through depth averaged eddy viscosity coefficients are the main advantage of the 2D model (Chen et al., 1999;

Table 30: Summary of selected two-dimensional sediment transport models

Model and references	Last Update	Flow	Bed sediment transport	Suspended sediment transport	Sediment mixtures	Cohesive sediment	Sediment exchange processes	Executable	Source code	Language
SERATRA: Sediment and Radionuclide Transport; Onishi and Wise (1982)	--	Unsteady	[a]Yes	[a]Yes	No	Yes	Advection-diffusion	C	C/LD	FIV
SUTRENCH- 2D: Suspended sediment transport in TRENCHes; van Rign and Tan (1985)	--	Quasi steady	[a]Yes	[a]Yes	No	No	Advection-diffusion	C	LD	F90
TABS-2; Thomas and McAnnally (1985)	--	Unsteady	[a]Yes	[a]Yes	No	Yes	Entrainment and deposition	C	C	F77
MOBED2: Mobile BED; Spasojevic and Holly (1990a)	--	Unsteady	Yes	Yes	Yes	No	Entrainment and deposition	C	C	F77
ADCIRC: Advanced CIRCulation; Luettich et al. (1992)	--	Unsteady	[a]Yes	[a]Yes	No	Yes	Advection-diffusion	C/LD	C/LD	F90
MIKE 21: Danish acronym of the word microcumputer; Danish Hydraulic Institute (1993)	--	Unsteady	[a]Yes	[a]Yes	No	Yes	Entrainment and deposition	C	P	F90
UNIBEST- TC: UNIform Beach Sediment Transport - Transport Cross-shore; Bosboom et al. (1997)	--	Quasi steady	[a]Yes	[a]Yes	No	No	Entrainment and deposition	C	LD	F90
USTARS: Unsteady Sediment Transport models for Alluvial Rivers Simulations; Lee et al. (1997)	--	Unsteady	Yes	Yes	Yes	No	Entrainment and deposition	PD/C	P	F90
FAST2D: Flow Analysis Simulation Tool; Minh Duc et al. (1998)	--	Unsteady	Yes	Yes	No	No	Entrainment and deposition	LD	P	F90
FLUVIAL 12; Chang (1998)	--	Unsteady	Yes	Yes	Yes	No	Entrainment and deposition	C	P	F77
Delft 2D; Walstra et al. (1998)	--	Unsteady	Yes	Yes	No	Yes	Advection-diffusion	C	LD	F90
CCHE2D: The National Center for Computational Hydroscience and Engineering; Jia and Wang (1999)	V. 2.1 (2001)	Unsteady	Yes	Yes	Yes	No	Advection-diffusion	PD/C	LD	F77/F90

Note: V=Version; C=copyright; LD=limitied distribution; P=proprietary; PD=public domain; and F=FORTRAN.
[a]Treated as a total load without seperation

Langendoen, 2001; Wu, 2008; Zhang, 2006; Jia & Wang, 2001a; Zhang & Jia, 2007). The structured grid or mesh is defined by multiple nodes and "wall" boundaries (outer and inner). The mesh allows for the simulation of transverse and longitudinal flow patterns, two-dimensional flow, and a more accurate representation of bed topography. In addition, turbulence is incorporated differently in the 2D model, than in the 1D model. In a 1D model, the energy loss due to turbulence is lumped into the Manning's n or Chezy C value. A 2D model incorporates turbulence by accounting for Reynolds stress in the momentum solution through depth averaged eddy viscosity coefficients. The two-dimensional depth-averaged mass and momentum conservation equations are illustrated in Equations 8 to 10 (Khan et al., 2000; Khan & Koshino, 2000; Zhang, 2006; Jia & Wang, 2001a; Khan, 2003; Langendoen, 2001).

$$\frac{\partial h}{\partial t}+\frac{\partial hu}{\partial x}+\frac{\partial hv}{\partial y}=0 \tag{8}$$

$$\frac{\partial u}{\partial t}+u\frac{\partial u}{\partial x}+v\frac{\partial u}{\partial y}+g\frac{\partial n}{\partial x}=\frac{1}{\rho h}\frac{\partial h\tau_{xx}}{\partial x}+\frac{1}{\rho h}\frac{\partial h\tau_{xy}}{\partial x}-\frac{\tau_{bx}}{\rho h}+f_{cor}v \tag{9}$$

$$\frac{\partial v}{\partial t}+u\frac{\partial v}{\partial x}+v\frac{\partial v}{\partial y}+g\frac{\partial n}{\partial y}=\frac{1}{\rho h}\frac{\partial h\tau_{yx}}{\partial x}+\frac{1}{ph}\frac{\partial h\tau_{yy}}{\partial x}-\frac{\tau_{by}}{\rho h}+f_{cor}u \tag{10}$$

where,

h = depth of flow

u = longitudinal velocity component

v = transverse velocity component

x = spatial coordinate in the longitudinal direction

y = spatial coordinate transverse direction

t = time

g = gravitational acceleration

n = water surface elevation

ρ = density of water

τ_{xx} = normal and turbulent stresses in the longitudinal direction

τ_{yy} = normal and turbulent stresses in the transverse direction

τ_{xy} and τ_{yx} = shear stresses in the longitudinal and transverse directions

τ_{bx} and τ_{by} = bed shear stresses in the longitudinal and transverse directions

f_{cor} = Coriolis parameter.

The variables u and v are often described as the depth-integrated velocity components in the x and y directions, and the variables τ_{xx}, τ_{xy}, τ_{yx}, and τ_{yy} as the depth-interegrated Reynolds stresses or fluid shear stresses representing turbulent diffusion and dispersion. The Reynolds stresses are approximated based on Boussineq's assumption, illustrated in Equations 11 to 13 (Zhang, 2006; Langendoen, 2001).

$$\tau_{xx} = 2\nu_t \frac{\partial u}{\partial x} \tag{11}$$

$$\tau_{xy} = \tau_{yx} = \nu_t \left(\frac{\partial u}{\partial y} + \frac{\partial v}{\partial x} \right) \tag{12}$$

$$\tau_{yy} = 2\nu_t \frac{\partial v}{\partial y} \tag{13}$$

where,

ν_t = eddy viscosity.

Various approaches exist to determine eddy viscosity, including the mixing-length model, two-equation model, and Reynolds stress model. The calculation of the depth averaged eddy viscosity is discussed in later section.

Similar to a one-dimensional unsteady flow simulation, boundary conditions are required at both the upstream and downstream extent of the 2D modeling reach. Commonly, an upstream discharge and a downstream water surface elevation are specified as boundary conditions for a steady flow simulation. An upstream discharge hydrograph and a downstream stage hydrograph are commonly specified as boundary conditions for an unsteady flow simulation. The vector flow field results produced by a 2D model are illustrated in Figure 10.

Most open-channel applications can be treated as shallow water problems, because the effect of vertical motions is usually insignificant, as see in the previously discussed assumptions of the 2D depth averaged continuity and momentum equations (Jia & Wang, 1999; Wu, 2008; Langendoen, 2001). Therefore, the depth-integrated 2D equations are generally accepted for studying open channel hydraulics with reasonable accuracy and efficiency. Most 2D models solve the depth-averaged continuity and Navier-Stokes equations along with the sediment mass balance equation by implementing finite difference, finite element, or finite volume schemes (Papanicolau et al., 2008).

Similar to a 1D model's limitations, the sediment transport capabilities of 2D models are limited by the averaging of the velocity over the water column depth (Lane et

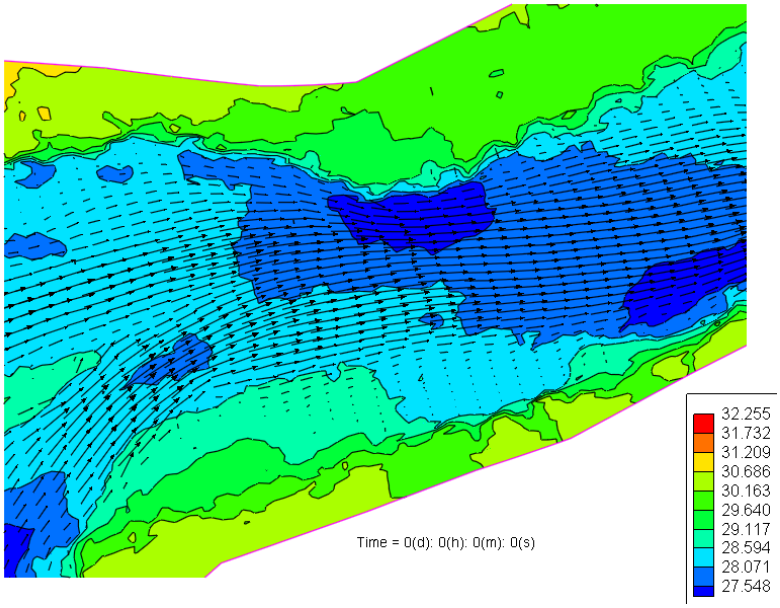

Figure 10: Vector flow field produced by a 2D model

al., 1999; Langendoen, 2001; Wu, 2001; Zhang, 2006; Jia & Wang, 2001a; Jia & Wang, 2001b). A 2D model calculates shear as a function of the depth-averaged velocity on the bed. Thus, estimates of bed shear stress are not based upon a proper assessment of the vertical variation of velocity with respect to depth and the actual shear stress exerted on the bed. This results in shear stress predictions that are strongly inversely correlated with water depth. This limitation prevents 2D models from accurately representing hydraulic phenomena and accurately predicting sediment transport in the presence of vertical variations in velocity. Recent advancements in model development now allow for the simulation of helical flow patterns and often vertical variations in velocity on bedload transport. CCHE2D, a two-dimensional model developed by the National Center for Computational Hydroscience and Engineering, accounts for the effects of helical flow in

river bends by adjusting the direction of the bed shear stress (Duan et al, 2001; Langendoen, 2001). In conclusion, 2D models are limited by the definition of the bed topography, the computational abilities of the system executing the model, and averaging of the velocity along the depth of the water column.

2D models have been applied to numerous sites and various applications. The results of these applications are not surprising. In summary, the objectives of the research or project necessitate the complexity and accuracy of predictions required of any model or process. Thus, where the flow is essentially one-dimensional, both the two-dimensional and the existing 1D models have the ability to produce accurate predictions of sediment and hydraulic variables with respect to flow in the longitudinal direction at a reach scale. If the objectives of the project involves the prediction of hydraulic and sediment variables along multiple spatially varying points or cells defining the channel or where the flow exhibits significant lateral flow, only two- and three-dimensional models can give accurate predictions (Waddle et al., 2000).

Three-dimensional sediment transport modeling

The advantages of 3D modeling include the ability to simulate the complex near-field flow phenomena that occur in natural channels, and variations in velocity in the vertical direction (Lane et al., 1999; Dworak, 2005; Wu, 2008; Formann et al., 2007). Flow in the vicinity of hydraulic structures and curved and braided channels are examples in which 2D and 1D models do not adequately represent the hydraulic processes, and 3D modeling should be implemented. However, these advantages are only important if they

coincide with the project or research objectives (i.e., the analysis of hydraulic processes in close proximity to a in-stream structure or debris). These models have the ability to provide a more reliable estimate of bed shear stress and the potential to simulate the three-dimensional flow field, but they impose high demands on data collection and computational time. For instance, a three-dimensional flow vector is required for every grid cell at the upstream boundary condition of a 3D simulation. As with 2D models, these models are limited by the definition of the bed topography and require increased computational resources when compared to a 2D simulation. In summary, these models are increasingly more complicated and require a higher level of comprehension of the fundamental assumptions behind model development. Several three-dimensional models are listed in Table 31 (Papanicolau et al., 2008).

Three-dimensional models incorporate the full three-dimensional form of the Navier-Stokes equations comprising the law of conservations of mass and momentum for an incompressible fluid. Similar to the two-dimensional equation, turbulence is incorporated via Reynolds stresses, which are approximated by the Boussineq approximation. Three-dimensional modeling is not in the scope of this project and thus these equations will not be discussed in detail.

Shear stress predictions will differ fundamentally between a 3D and a 2D model, as a 3D model computes stress directly from the shear created by the velocity of the bottom cell with respect to the bed (Lane et al., 1999; Wu, 2008). This will result in a more accurate prediction of the bed shear stress when compared to a 2D model simulation, in most applications. However, 3D models are still limited in gravel bed or coarse substrate reaches as a result of the problems associated with the specification of

Table 31: Summary of selected three-dimensional sediment transport models

Model and references	Last Update	Flow	Bed sediment transport	Suspended sediment transport	Sediment mixtures	Cohesive sediment	Sediment exchange processes	Executable	Source code	Language
ECOMSED: Estuarine, Coastal, and Ocean Model - SEDiment Transport; Blumber and Mellor (1987)	V. 1.3 (2002)	Unsteady	[a]Yes	[a]Yes	No	Yes	Entrainment and deposition	PD	PD	F77
RMA-10: Resource Management Associates; King (1988)	--	Unsteady	[a]Yes	[a]Yes	No	Yes	Entrainment and deposition	C	P	F77
GBTOXe: Green Bay TOXic enhancement; Bierman er al. (1992)	--	Unsteady	No	Yes	No	Yes	Entrainment and deposition	NA	NA	F77
EFDC3D: Environmental Fluid Dynamics code; Hamrick (1992)	--	Unsteady	Yes	Yes	Yes	Yes	Entrainment and deposition	PD	P	F77
ROMS: Regional Ocean Modeling System; Song and Haidvogel (1994)	V. 1.7.2 (2002)	Unsteady	Yes	Yes	Yes	No	Entrainment and deposition	LD	LD	F77
CH3D-SED: Computational Hydrauilcs 3D-SEDiment; Spasojevic and Holly (1994)	--	Unsteady	Yes	Yes	Yes	Yes	Entrainment and deposition	C	C	F90
SSIIM: Sediment Simulation In Intakes with Multiblock options; Olsen (1994)	V. 2.0 (2006)	Steady	Yes	Yes	Yes	No	Advection-diffusion	PD	P	C-Langua.
MIKE 3: Danish acronym of the word Microcomputer; Jacobsen and Rasmussen (1997)	--	Unsteady	[a]Yes	[a]Yes	No	Yes	Entrainment and deposition	C	P	F90
FAST3D: Flow Analysis Simulation Tool; Landsberg et al. (1998)	V. Beta-1.1 (1998)	Unsteady	Yes	Yes	No	No	Entrainment and deposition	LD	P	F90
Delft 3D; Delft Hydraulics (1999)	V.3.25.00 (2005)	Unsteady	Yes	Yes	No	Yes	Entrainment and deposition	C	LD	F77
TELEMAC; Hervouet and Bates (2000)	--	Unsteady	[a]Yes	[a]Yes	No	Yes	Entrainment and deposition	C	P	F90
Zeng et al. (2005)	--	Unsteady	Yes	Yes	No	No	Entrainment and deposition	P	P	F90

Note: V=Version; C=copyright; LD=limitied distribution; P=proprietary; PD=public domain; and F=FORTRAN.
[a]Treated as a total load without seperation

the complex variation in bed topography.

Appendix B: Validation and applications of the CCHE2D model

The following paragraphs discuss various case studies involving the application and validation of the two-dimensional model CCHE2D in natural channels and based on historical flume studies.

CCHE2D was applied to two flume studies to determine the capability of the model to simulate flow and sediment transport around vegetation bars with various wavelengths (Wu & Wang, 2006). Bennett et al. (2002) simulated a fixed bed with alternating vegetative bars along both banks. A CCHE2D model was constructed based on the data supplied by Bennett et al. (2002) and extended to simulate the flow field around the vegetated bars with various wavelengths. The authors concluded that CCHE2D successfully simulated flow patterns influenced by the vegetated bars. Bennett et al. (2003) simulated two vegetation bars on opposite banks with a movable bed. Simulated bed changes induced by the vegetation bars agreed well with measured data provided by Bennett et al. (2003).

Duan et al. (2001) implemented CCHE2D to study the model's ability to simulate bank migration of alluvial channels. In addition, a new module of CCHE2D was introduced, incorporating mass conservation of sediment in a control volume of each cell adjacent to the bank. This included sediment input from bank erosion and failure, sediment storage due to deposition in the element, and sediment transported into and out of the element. The bank advance or retreat depends on the net sediment accumulated in the control volume adjacent to the bank (sediment balance) in addition to bank friction

erosion. The model was applied to laboratory experiments on the widening of a sine-generated channel following Nagata et al. (1997). Unfortunately, the flow field and bed elevation measurements were not available, so only measured bank line displacement was available for comparison. However, good agreement existed between simulated and measured bank lines. Both simulated and field observations show the increase and decrease of the wavelength and amplitude of a meandering channel during its evolution, as well as the locations and movements of the bars and pools. In addition, the authors further explored the accurate simulation of bed load transport. The effects of secondary flow and the transversal component of the gravitational force were considered in addition to that of the primary shear force on bed load transport. The authors concluded that the model is capable of predicting realistic phenomena with reasonable approximation while remaining computationally cost-effective.

CCCHE2D was implemented on a sinuous reach of the Mississippi river to test the model's ability to simulate complex hydraulics and in-stream structures in a natural channel (Jia et al., 2002). The Victoria bendway, located between Arkansas and Mississippi, is a highly curved reach of the meandering Mississippi river with a complex bend. The river changes heading in this location and cuts back 108 degrees with a radius of curvature of approximately 1,280 m. Three spur dikes and six submerged weirs has been placed in the main channel to realign the flow for improved channel navigation. CCHE2D model results were compared to measured three-dimensional velocity data. The authors agree that the model results compared favorably despite the complex geometry, uncertainties of bed roughness, and highly three-dimensional flow patterns.

Another study compared the relative accuracy of one- and two-dimensional hydraulic models with respect to simulating flow in a sinuous channel (Jia & Alonso, 1994). Both models were applied to a sinuous section of the Hotophia Creek in Panola County, Mississippi. The project reach was limited to 350 meters and the channel was described as approximately 50-m wide with an average grade of 0.00077. Results of stream velocity and water edge distributions produced by HEC-2 and CCHE2D were compared. The authors concluded that the two-dimensional model produced a more realistic description of flow under and over the point bar, particularly near the area of maximum constriction. In addition, the authors noted the limitations of the one-dimensional model in areas that experience transverse flows and lateral sediment transport.

CCHE2D was implemented to study the effect of large wood structures on fish habitat along a reach of the Mississippi River (He et al., 2006). In this article the CCHE2D habitat model is introduced, which weighs each cell using habitat suitability curves that assign a relative value between 0 and 1 for the target species. Incorporating this module, the stream reach can be assessed based on the weighted useable area, a summation of the area, and the combined suitability index of each grid cell divided by the total area of the reach. CCHE2D was utilized to determine water depth, velocity, and turbidity along the study reach. These values were then used to define the combined suitability index. The paper concluded that vegetation and sediment transport have important impacts on fish habitat. No validation of the model was provided.

CCHE2D was implemented on 9.5 miles of the Salt River or Rio Salado to simulate the sediment transport and hydraulic processes responsible for the change in bed

elevation (Chen et al., 2007). The bed material gradation was determined to be 90% very coarse sand and gravels, with a median particle diameter range of 20 mm to 40 mm, 2% fine sand, and 0.6% wash load containing clays and silts. The computational mesh was constructed based on channel topography data extracted from a digital contour map, thus the topographic data and corresponding mesh lacked the resolution provided by a topographic survey. When compared to a one-dimensional hydraulic model (HEC-RAS), results showed that CCHE2D more accurately predicted water surface elevations based on a comparison with an actual five year recurrence interval (R.I.) flood event. The HEC-RAS model did not produce floodplain inundation during the five year R.I. event, while actual inundation of the floodplain was observed during the event. No field measurements of suspended or bedload were used for comparison in this study. Thus, this paper provided no validation of the sediment transport module within CCHE2D.

CCHE2D was implemented on a 100 km reach of the lower Yellow River in China to calculate the flood routing and sediment transport between the Huayuankow and Jiahetan gauging stations (Jiang et al., 2004). The lower Yellow River has a mean annual runoff of 58 billion m^3 and a mean annual sediment amount of 4.24 billion tons. The sediment is non-uniform, with sizes ranging from 0.002 mm to 0.5 mm. Two floods (in 1982 and 1986) were simulated with the model. The simulated flow fields, discharge, water levels, and sediment concentrations were compared to measured values. The simulated results agreed well with measured data. The authors concluded that the model is capable of handling the complex topography and abrupt wetting and drying processes that occur in the lower Yellow River.

The response of the Arkansas River navigation channel to riverine structure modification was also simulated using CCHE2D (Jia et al., 2006). The computed flow field was validated by comparisons with measured velocity profiles across several sections that included numerous spur dikes. The simulated and measured results showed excellent agreement in the main channel, but flow around the spur dikes was not defined as well by the model. Suspended sediment simulations were compared with dredging locations and showed good qualitative agreement. Neither suspended sediment nor bedload was actually measured for comparison to simulated results. Thus this case study did not validate the sediment transport module within CCHE2D.

CCHE2D was implemented to predict water surface elevations under unsteady states and suspended sediment transport for the Lauffen Reservoir on the Neckar River, Germany (Jia & Wang, 2001b; Xu et al., 2001). Model calibration was performed to identify the roughness coefficients. The data used for the calibration included the water surface elevation measured along the channel during a flood event in 1990, with a peak discharge of 1644 m^3/s. Bed material in the study reach is non-uniform and varies from coarse gravel to sand and fine clay from upstream to downstream. The calibrated Manning's coefficient varied from 0.017 to 0.031 in the main channel and 0.04 to 0.06 on the floodplains, from downstream to upstream respectively. The average difference between observed and predicted water surface elevations was less than 0.17 m. Once calibrated, the model was utilized to simulate the hydrographs of three floods with different characteristics (i.e., different flood duration, total volumes, peak discharges, and discharge varying rates). The maximum difference between simulated and measured water surface elevations was 0.27 m at a discharge of approximately 958 m^3/s.

Suspended sediment concentrations were compared at multiple cross sections along the reach. The concentration distribution in both the lateral and longitudinal direction were predicted well. This case study did not simulate bedload transport and thus did not provide validation for the bedload transport module within CCHE2D.

Khan et al. (2000) utilized CCHE2D to simulate both diverging and converging channels. Due to the lack of field data, experimental observations of the depth-averaged velocity and water surface elevations were used to verify the simulated results. For a right-angled channel divergence the simulated water surface profiles in both the main and branch channels showed satisfactory agreement with observed data. In addition, the velocity profiles in the main channel, at the junction, and downstream of the junction are accurately predicted by the model. The peak velocity in the branch channel is under-predicted. The model also predicted the recirculation zones, represented by negative velocity, in the main and branch channels. The simulated water surface profile for the converging channel, where the angle between the branch and main channel was equal to 30 degrees, compared well with the observed data. The authors conclude that CCHE2D is capable of simulating channel bifurcation and confluence applications.

Khan & Koshino (2000) compared simulated and measured water surface elevations and velocity profiles computed by three different two-dimensional models (CCHE2D, RMA-2, and FESWMS-2DH). The simulated site consisted of two consecutive bends with long straight reaches upstream and downstream of the two bends. A constant Manning's n value of 0.03, the same number of quadrilateral elements, and the same upstream, flow, and downstream, water surface elevation, boundary conditions were used for all three models. The calculated volumetric discharge data at various

sections of the river showed that the RMA-2 model under-predicted the discharge along the reach, while FESWMS-2DH over-predicted the volumetric discharge near the upstream extent of the project reach and oscillated around the prescribed value in the remained of the reach. At sections where mass loss was significant, the velocity profile computed by the RMA-2 model showed significant deviation from the measured profile in both shape and magnitudie. The velocity profiles predicted by the FESWMS-2DH model were lower than the measured profiles in the center of the measured sections. The author concluded that CCHE2D showed excellent mass conservation characteristics and the computed velocity profiles agreed well with measured results.

Wu & Wang (2004) compared simulated and measured water surface elevations and velocity profiles along two bends of the Fall River, located in the Rocky Mountain National Park. The simulated reach was 100 m long and consisted of two opposing bends with radius of curvatures of 11.0 m and 13.5 m. The channel bankfull width was approximately 9 m. The reach is dominated by coarse sand. The flow discharge was 4 m^3/s at bankfull stage, with a corresponding water surface elevation of 2.61 m. The general trends of helical flow patterns are represented well in the simulation, but adequate data were not available to quantitatively compare simulated and measured results throughout the reach. However, depth average velocity was compared at six cross sections and agreed well with simulated results.

Wu & Wang (2004) implemented CCHE2D to simulate water surface profiles and bed-material discharge along a 3.3 km reach of the East Fork River. This study was unique because bed load traps were implemented to develop a bedload rating curve. The bed material was composed predominantly of sand with gravel bars spaced at regular

intervals, median grain size of 1.28 mm. The main mode of sediment transport is bedload. The simulation period was 17 days and consisted of a time step of 60 minutes. The author concluded that the model was capable of handling the drying and wetting process very well, that measured and simulated water surface profiles agreed at two different discharges, and that measured and simulated bed-material discharges agreed well at the outlet.

Appendix C: Site aerial images and photos

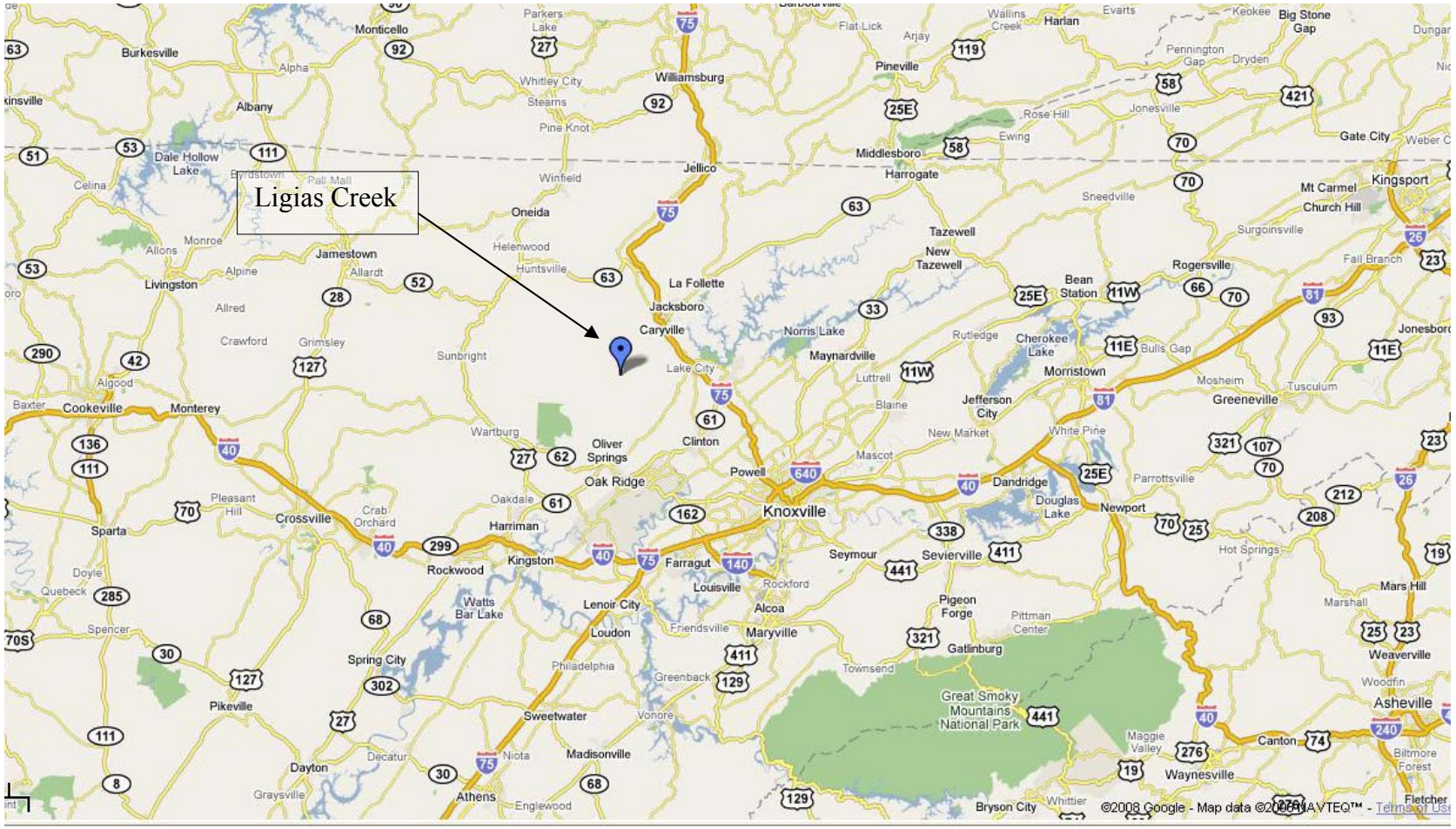

Figure 11: Google Earth map

Figure 12: Google Earth map

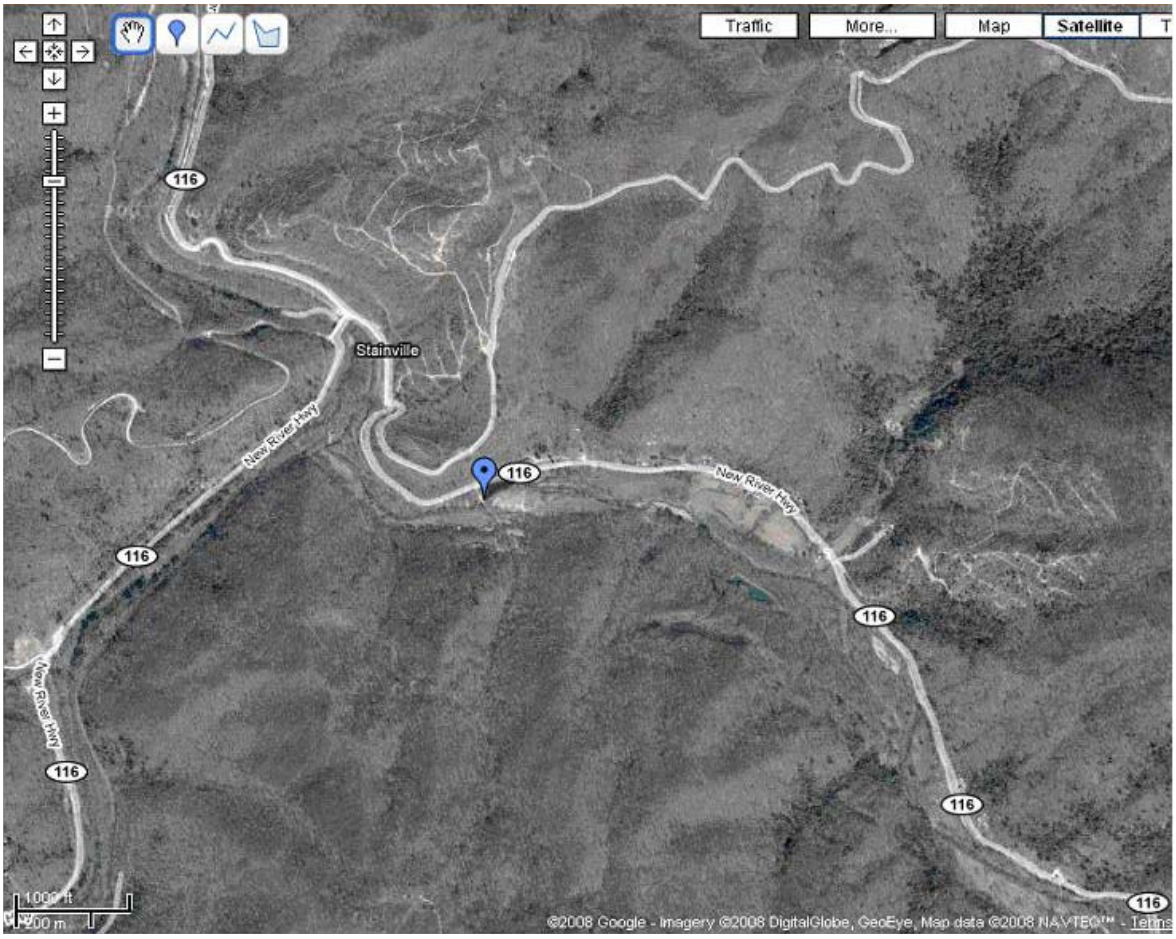

Figure 13: Google Earth site aerial image

Figure 14: Google Earth site aerial image (2)

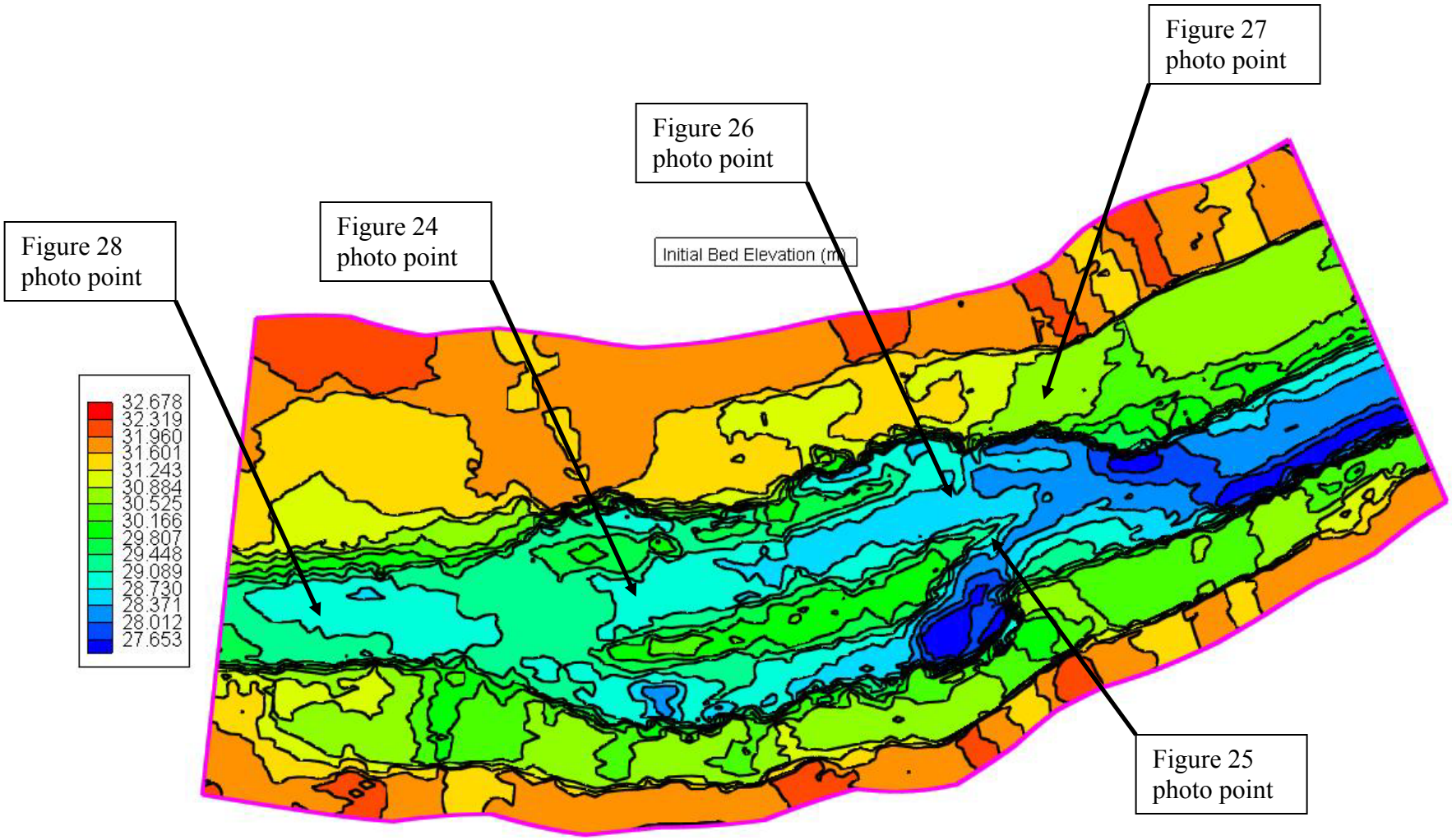

Figure 15: CCHE2D digital elevation map

Figure 16: Ligias Creek looking downstream (left side of mid-channel island)

Figure 17: Ligias Creek looking downstream (downstream extent of mid-channel island)

Figure 18: Ligias Creek looking upstream (left side of mid-channel island)

Figure 19: Ligias Creek looking upstream

Figure 20: Ligias Creek, looking downstream (near upstream modeling boundary)

Appendix D: CCHE2D sediment transport model

CCHE2D Mesh Generator

Due to significant transverse flow patterns exhibited on the site, the two-dimensional model, CCH2D was implemented in this study. The CCHE modeling system includes a Graphical Users Interface (CCHE-GUI), a separate hydrodynamic numerical model (CCHE2D model), and a structured mesh generator (CCHE2D Mesh Generator) (Jia & Wang, 2001a; Jia & Wu, 2007; Khan, 2003; Zhang, 2006).

The exported ASCII file can be viewed with Microsoft™ Notepad or equivalent software. The ASCII file was modified using Microsoft™ Excel and saved as a tab delimited text file. The tab delimited text file can be opened using Microsoft™ Notepad and saved as a topographic database file (.mesh_xyz). Figure 21 illustrates the format of the file. The first line contains the number of data points included in the topographical database; sequential lines contain the coordinates and elevation associated with each data point defining the bed topography in the following format (easting, northing, elevation).

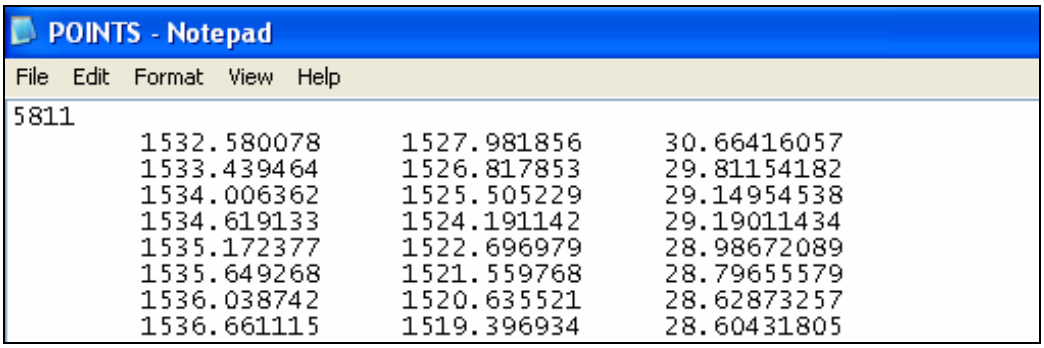

Figure 21: Example of CCHE2D topography database (.mesh_xyz)

Coordinates and elevations are reported in the SI system of units.

Internal and external boundaries must be defined before an algebraic mesh can be generated. A domain is established by the external or outer boundary, while internal boundaries define areas inside the external boundary that are outside of the domain. Several steps are involved with the boundary definition. These steps include: defining the outer boundaries and the inner boundaries with boundary control points, distributing an equal number of boundary points along the top and the bottom boundaries whereby each pair of the boundary points forms a control line, and distributing the internal mesh nodes along the control lines (Zhang & Jia, 2007). All steps are automated within CCHE2D except the definition of the outer boundary and inner boundary control points. Once these steps are complete the boundary file is saved as a (.mesh_mb) file.

The following seven steps must be executed before a simulation can be performed: 1) define the flow initial conditions, 2) define the bed material properties, 3) define the flow parameters, 4) define the sediment parameters, 5) define the sediment discharge boundary conditions (bedload and suspended load), 6) define the inlet and outlet boundary conditions, and 7) define the bed gradation or bed material samples (Zhang, 2006).

CCHE2D Flow initial conditions

Defining the flow initial conditions includes the definition of the initial water surface and bed elevations. Both the flow initial conditions and bed material properties, discussed in the subsequent section, can be defined by four different methods. The four

methods include: 1) assigning a value to a defined rectangular region, 2) assigning a value to a defined polygonal region, 3) assigning a value to the whole domain, or 4) assigning a value to multiple defined rectangular regions and interpolating in the I or J direction.

CCHE2D GUI - Bed material properties

Defining the bed material properties includes the definition of the bed roughness, bed erodibility, maximum deposition thickness, maximum erosion thickness, and the bed layer gradation and thickness (Zhang, 2006). The bed material sample establishes the initial bed material composition in both the horizontal and vertical directions for the entire domain (Zhang, 2006). The porosity of the bed gradation is automatically calculated in CCHE2D.

CCHE2D GUI – Flow Parameters

The flow parameters include the definition of several constants and coefficients, the turbulence closure scheme, and the time component involved with the simulation and output. The Coriolis force coefficient, acceleration due to gravity (m/s^2), von Karman constant, and the fluid kinematic viscosity (m^2/s) can all be modified to more accurately simulate site conditions, but were not modified for this project. The time step, simulation time, and time steps necessary to generate an output or history file are also defined in this step. In addition, the turbulence closure is defined in the flow parameter menu. Three

turbulence closure schemes are available in CCHE2D, including the parabolic eddy viscosity model, mixing length model, and k-Epsilon model.

Unsteady flow sediment transport simulations require a great deal of time due to the interpolation of discharge, suspended sediment concentration (kg/m^3) and bed load (kg/m/s) between time steps. To increase the computational efficiency unsteady flow can be computed as quasi-steady flow (Zhang, 2006). During a quasi-steady flow simulation the discharge during each step is considered a constant and the flow and sediment simulations are performed as a steady flow simulation. To compute as quasi-steady flow the discharge hydrograph must be formatted to be a step function and the option must be selected within CCHE2D. The following example is illustrated in Zhang (2006). For example, suppose (Q_i, T_i) and (Q_{i+1}, T_{i+1}) represent two consecutive hydrograph ordinates. During a quasi-steady computation the discharge Q_i is assumed to be valid for the duration between T_i and T_{i+1}. The time steps to reach steady state must be defined in the flow parameters options and "Compute as quasi steady flow" must be selected on the screen. It is important to note that the time series in the hydrograph files at the inlet and outlet boundary conditions must be the same. In addition, the quasi-steady simulation cannot start from rest and must run from a prior simulation. The flow parameter screen is shown in Figure 22.

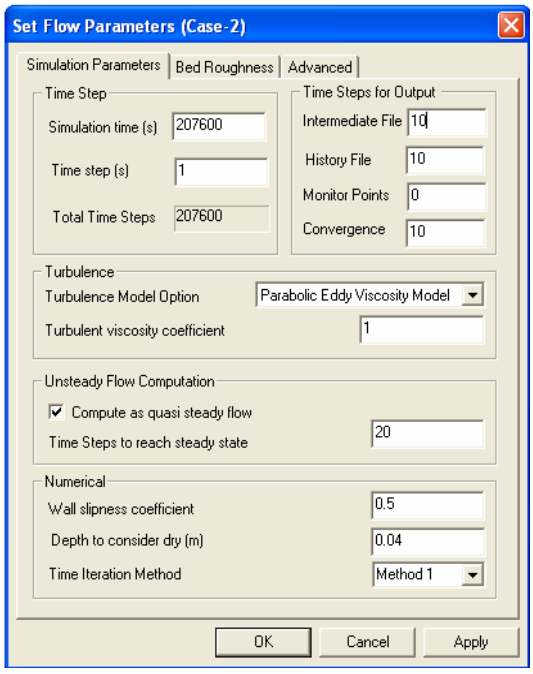

Figure 22: CCHE2D flow parameters screen

CCHE2D GUI - Sediment parameters

The sediment parameters menu in CCHE2D contains 5 tabs which include sediment, bed roughness, bank erosion, sediments size classes, and sediment transport. The sediment size classes tab includes the definition of the number of bed layers, minimum mixing layer thickness, and sediment size classes.

The transport mode, sediment simulation mode, adaptation length for bedload, and addition factor for suspended load are defined in the sediment transport tab. The sediment tab contains information concerning the sediment specific gravity, which remained unchanged at a value of 2.65 g/cm^3, curvature effects, and steady flow computation. This tab was not modified for this project. The bed roughness tab includes

information related to the bed roughness. As stated in the literature review, the user has the choice of defining a Manning's n value, roughness height (ks), or a roughness formula.

CCHE2D GUI - Sediment boundary conditions

The sediment boundary conditions include a suspended sediment boundary condition file (.sbc) and a bedload boundary condition file (.bbc). Sediment is defined as a function of time for each predefined size class for both conditions. Suspended sediment discharge has the units of (kg/m^3) and bedload has the units of (kg/m/s).

CCHE2D GUI – inlet and outlet boundary conditions

Two steps are involved with defining the inlet and outlet boundary conditions: defining the boundary node string and associating boundary conditions to the node string (Zhang, 2006). The inlet boundary condition consists of the flow and sediment discharges. The upstream flow boundary condition can be defined by a discharge hydrograph (.dhg) file for unsteady flow simulations, or a total constant discharge (m^3/s) for steady flow simulations. In addition, the flow angle (in degrees) can be specified for flow entering the channel at a specific angle towards either bank. The sediment entering the upstream extent of the project is specified by the bedload (.bbc) and suspended load (.sbc) files discussed earlier.

The outlet boundary condition can be defined by an open boundary condition, water surface elevation, rating curve or a stage hydrograph. The water surface level is

utilized for steady flow simulations only. The open boundary condition allows CCHE2D to estimate the water surface level at the outlet boundary based on the kinematic wave condition. The Rating curve (.rcv file) contains a stage versus discharge relationship. The stage hydrograph option allows the user to specify a stage hydrograph file (.sgh) which contains a time versus stage relationship.

General description of CCHE2D sediment transport model

CCHE2D is a two-dimensional, depth averaged, unsteady flow, water quality model with sediment transport capabilities (Zhang, 2006; Jia & Wang, 2001a; Jia & Wu, 2007; Khan, 2003). The model was developed at the National Center for Computational Hydroscience and Engineering (NCCHE), at the University of Mississippi School of Engineering. The CCHE modeling system includes a Graphical Users Interface (CCHE-GUI), a separate hydrodynamic numerical model (CCHE2D model), and a structured mesh generator (CCHE2D Mesh Generator).

A simulation within CCHE2D requires a structured mesh, sediment and flow initial conditions, and discharge and sediment boundary conditions at the upstream and downstream extent of the project reach (Zhang, 2006; Jia & Wang, 2001a; Jia & Wu, 2007; Khan, 2003). Zhang (2006) describes the general procedure of a numerical simulation as follows: generate the mesh, specify the boundary conditions, assign the flow and sediment parameters, perform the simulation, and visualize the results.

The two-dimensional continuity and momentum equations are solved in CCHE2D. The two-dimensional, depth-averaged mass and momentum conservation

equations used in the current model are illustrated in Equations 8 to 10 (Jia & Wang, 2001; Jia & Wu, 2007; Khan, 2003; Zhang, 2006).

Three methods are available in CCHE2D for calculating the depth averaged eddy viscosity (Zhang, 2006). The first method consists of calculating the eddy viscosity by assuming a parabolic distribution of the turbulent viscosity. The second method uses the depth-averaged mixing-length formulation. The third method is the k-epsilon model. The parabolic eddy viscosity model is selected by default. The mixing length model and the k-epsilon model are more suitable to reaches containing recirculation flow structures (Khan & Koshino, 2000). Each method is described in detail in Zhang (2006).

Total discharge (m^3/s) or a discharge hydrograph is required at the upstream boundary condition (Khan & Koshino, 2000; Zhang, 2006). One of the following four boundary conditions can be applied at an outlet: 1) the stage; 2) stage hydrograph (the stage as function of time); 3) rating curve (the stage-discharge relationship); and 4) open boundary conditions or a kinematic wave condition, useful when the stage at the outlet cannot be ascertained.

Bed roughness can be defined by a Manning's n value, roughness height (ks), or a roughness formula (Zhang, 2006). The bed roughness formulas include Wu and Wang (1999) and Van Rign (1986). The formula parameters include: D_{16}, D_{50}, D_{90}, and the calibration factor. The default value for the calibration factor is 1.0. To perform a sediment transport simulation the user has the choice of several methods to calculate the bed roughness. Values in the geometry file can be utilized (Manning's n value or roughness height) or the bed roughness can be calculated according to the sediment diameter size of D_{90} or D_{50}. The Wu and Wang (1999) and Van Rijn (1986) formulas can

also be utilized for the bed roughness calculation. The Van Rign (1986) formula is illustrated in Equations 14 to 16.The Wu and Wang (1999) formula is illustrated in Equation 17.

$$\frac{\Delta}{h} = 0.11\left(\frac{d_{50}}{h}\right)^{0.3}\left(1-e^{-0.5T}\right)(25-T) \tag{14}$$

where,

Δ = bed roughness height

h = flow depth

T = non-dimensional excess bed shear stress

d_{50} = median particle diameter of the bed material

$$T = \left(U_*^{'}\right)^2 / \left(U_{*cr}\right)^2 - 1 \tag{15}$$

where,

$U_*^{'}$ = effective bed shear velocity relating to grain roughness

U_{*cr} = critical bed shear velocity for sediment motion given by Shields diagram

$$U_*^{'} = Ug^{0.5} / [18\log(4h / d_{90})] \tag{16}$$

where,

d_{90} = maximum size particle for the smallest 90% of the bed material sample

$$n = \frac{d^{1/6}}{A} \tag{17}$$

where,

d = diameter of the bed material

A = empirical roughness parameter relation to the gradation, shape and distribution of bed material, bed forms, and flow conditions

CCHE2D MESH Generator

CCHE2D solves a set of non-linear partial differential equations on a physical domain, which is discretized and represented by a computational structured mesh (Jia & Wang, 2001a; Khan & Koshino, 2000; Zhang & Jia, 2007). The scheme requires a quadrilateral mesh system in which a working element is formed around each node. The two-dimensional elements consist of a central node (the node at which the variables are calculated) and eight surround nodes, illustrated in Figure 23 (Jia & Wang, 2001a, Khan & Koshino, 2000). The solution utilizes quadratic interpolation functions to approximate the variables and their derivatives and progresses element by element. Zhang & Jia (2007) states "Despite the numerical method used, the success of solving the set of highly non-linear partial differential equations depends largely on the mesh quality." They describe the characteristics of a high quality mesh as follows: contains sufficient resolution in the zones of interest, transitions smoothly between areas of different densities, and contains sufficient length so that the inlet and outlet are adequately far away from the zones of interest.

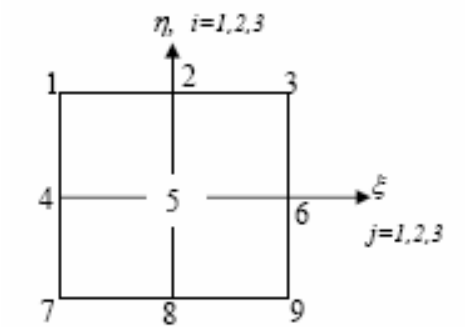

Figure 23: Nodal element (Jia & Wang, 2001a)

CCHE2D and sediment transport

Three modes or approaches are implemented in CCHE2D to simulate non-uniform sediment transport (Wu, 2001). One approach simulates bedload only without the consideration of the diffusion of suspended load. The second approach simulates suspended load only or treats bed-material load as suspended load. The third and final approach is to compute bed load and suspended load separately. If total load as bedload mode or total load as suspended load mode is selected the user must specify the appropriate sediment transport capacity formula. Four sediment transport formulas are included in CCHE2D. The formulas included in the model are: 1) Wu. et al. (2001), 2) the modified Ackers and White, 3) the modified Engelund and Hansen formula, and 4) the SEDTRA module which includes the Yang, Laursen, and Meyer-Peter and Muller equations. Each sediment transport formula is discussed in detail in the following paragraphs.

A data set composed of a wide range of flow and sediment conditions was utilized to calibrate the fractional bed and suspended load transport capacity formulas utilized in

the Wu. et al. (2001) formula (Wu, 2001). The data set included laboratory data of non-uniform bed and suspended load measurements as well as bedload measurements and suspended load measurements from natural rivers. The fractional bed material load transport capacity is calculated by summing the calculated fractional bedload and suspended load transport capacities. The fractional bedload transport capacity is defined by Equations 18 to 23. The parameters for bedload data used in Wu et al.'s formula are illustrated in Figure 24. The fractional suspended load transport capacity is defined by Equations 24 and 25.

$$\phi_{bk} = 0.0053\left[\left(\frac{n'}{n}\right)^{3/2}\frac{\tau_b}{\tau_{ck}} - 1\right]^{2.2} \tag{18}$$

$$n' = \frac{d_{50}^{1/6}}{20} \tag{19}$$

$$\tau_{ck} = 0.03(\gamma_s - \gamma)d_k\left(\frac{p_{hk}}{p_{ek}}\right)^{0.6} \tag{20}$$

$$\phi_{bk} = \frac{q_{b*k}}{p_{bk}\sqrt{\left(\frac{\gamma_s}{\gamma} - 1\right)gd_k^3}} \tag{21}$$

$$p_{hk} = \sum_{j=1}^{N}\frac{p_{bj}d_j}{(d_k + d_j)} \tag{22}$$

$$p_{ek} = \sum_{j=1}^{N}\frac{p_{bj}d_k}{(d_k + d_j)} \tag{23}$$

where,

ϕ_{bk} = non-dimensional bed load transport capacity

Data Source	Q	U	H	S	D_I	q_b
	(m^3/s)	(m/s)	(m)	(10^{-3})	(mm)	($10^{-3}m^2/s$)
Samaga (1986a)	0.006-0.015	0.49-0.78	0.06-0.11	4.49-6.93	0.073-2.366	0.04-0.22
Kuhnle (1993)	0.01-0.03	0.28-0.81	0.101-0.107	0.47-2.22	0.2-10	1.5e-6-0.064
Wilcock (1993)	0.017-0.057	0.26-1.08	0.088-0.12	0.59-16.2	0.21-64	8.7e-7-0.22
Liu (1986)	0.0035-0.023	0.14-0.67	0.03-0.083	1.5-4	0.31-30	4.9e-5-6.4e-4
Susitna River	799-2800	1.8-2.1	2.4-4.4	1.4-2.4	0.062-128	0.028-0.11
Chulitna River	261-348	1.5-1.8	1.7-1.9	0.64-0.74	0.062-128	0.11-0.23
Black River	20-256	0.44-1.0	0.55-1.9	0.11-0.29	0.062-16	0.0048-0.016
Toutle River	9.3-248	1.3-2.8	0.39-1.5	1.9-5.5	0.062-32	0.11-0.95
Yampa River	26.3-447	0.59-1.3	0.65-3.9	0.40-0.87	0.062-32	0.003-0.054

Figure 24: Parameters of bedload data used in Wu et al.'s formula (Wu, 2001)

n = Manning's roughness coefficient for the channel bed

n' = Manning's coefficient corresponding to the grain roughness

τ_b = bed shear stress

τ_{ck} = critical shear stress

q_{b*k} = equilibrium transport rate [k-th size class of bed load per unit width (m^2/s)]

p_{bk} = bed material gradation

p_{hk} = hiding probabilities [k-th size class of bed material]

p_{ek} = exposure probabilities[k-th size class of bed material]

$$\phi_{sk} = 0.0000262\left[\left(\frac{\tau}{\tau_{ck}} - 1\right)\frac{U}{\omega_{sk}}\right]^{1.74} \tag{24}$$

$$\phi_{sk} = \frac{q_{s*k}}{p_{bk}\sqrt{\left(\frac{\gamma_s}{\gamma} - 1\right)gd_k^3}} \tag{25}$$

where,

q_{s*k} = equilibrium transport rate [k-th size class of suspended load per unit with (m^2/s)]

τ = shear stress of entire cross-section

ω_{sk} = settling velocity of sediment particles

A modified version of the Ackers and White's (1973) formula is included in CCHE2D. The developers chose to include the formula because the original Ackers and White formula has been widely adopted and can provide reliable results for single-size (uniform or quasi-uniform) sediment transport. The Ackers and White bedload formula is implemented with an exposure correction factor developed by Proffit and Sutherland in 1983. According to Proffit and Sutherland's test, their method can provide good prediction for experimental cases, but it is not successful for field cases. Wu (2001) cautions the modified Ackers and White's formula should not be used to predict the transport capacity of very fine sediment. For the k-th size class of sediment, the modified Ackers and White's formulas is illustrates in Equations 26 to 29; coefficients are listed in Figure 25 (Wu, 2001).

$$G_{gr,k} = C\left(\frac{F_{gr,k}}{A} - 1\right)^m \tag{26}$$

$$F_{gr,k} = \varepsilon_k \frac{U_*^n}{\left[(\gamma_s/\gamma - 1)gd_k\right]^{1/2}}\left[\frac{V}{\sqrt{32}\log(\alpha h/d_k)}\right]^{1-n} \tag{27}$$

	1973 version	1990 version
$d_{gr} \geq 60$	$n = 0.0$ $A = 0.17$ $m = 1.50$ $C = 0.025$	$n = 0.0$ $A = 0.17$ $m = 1.78$ $C = 0.025$
$1 < d_{gr} < 60$	$n = 1.00 - 0.56 \log d_{gr}$ $A = 0.23 d_{gr}^{-1/2} + 0.14$ $m = 9.66 d_{gr}^{-1} + 1.34$ $\log C = -3.53 + 2.86 \log d_{gr}$ $- (\log d_{gr})^2$	$n = 1.00 - 0.56 \log d_{gr}$ $A = 0.23 d_{gr}^{-1/2} + 0.14$ $m = 6.83 d_{gr}^{-1} + 1.67$ $\log C = -3.46 + 2.79 \log d_{gr}$ $- 0.98 (\log d_{gr})^2$

Figure 25: Coefficient of Ackers and White formula (Wu, 2001)

$$G_{gr,k} = \frac{C_{*k} h}{d_k \gamma_s / \gamma} \left(\frac{U_*}{V} \right)^n \tag{28}$$

$$\varepsilon_k = \begin{cases} 1.30, & d_k / d_u > 3.7 \\ 0.53 \log(\frac{d_k}{d_u}) + 1.0, & 0.075 < d_k / d_u \leq 3.7 \\ 0.40, & d_k / d_u \leq 0.075 \end{cases} \tag{29}$$

where,

d_k = mean diameter of the k-th size fraction

d_u = reference diameter used by Proffit and Sutherland

A modified version of the Engelund and Hansen's formula is also included in CCHE2D. Engelund and Hansen (1967) used Bagnold's stream power concept and the similarity principle to obtain their sediment transport equation. Their formula was modified to calculate the fractional transport capacity of non-uniform bed-material load (Wu and Vieira, 2000). Wu et al. (2001) determined that this formula is not as successful in predicting fractional transport rate of nonuniform sediment mixtures as Wu et al.'s

(2000) formula or the SEDTRA module. Despite its inefficiencies, the modified formula was included in the model because the original Engelund and Hansen's formula has been widely adopted throughout the industry. The modified formula is illustrated in Equations 30 to 36.

$$f'\phi_k = 0.1\left(\varepsilon_k \tau_{*k}\right)^{5/2} \tag{30}$$

$$\varepsilon_k = \left(\frac{p_{ek}}{p_{hk}}\right)^m \tag{31}$$

$$p_{hk} = \sum_{j=1}^{N} \frac{p_{bj} d_j}{\left(d_k + d_j\right)} \tag{32}$$

$$p_{ek} = \sum_{j=1}^{N} \frac{p_{bj} d_k}{\left(d_k + d_j\right)} \tag{33}$$

$$\phi_k = \frac{q_{t*k}}{p_{bk}\sqrt{\left(\frac{\gamma_s}{\gamma} - 1\right) g d_k^3}} \tag{34}$$

$$\tau_{*k} = \frac{\tau_0}{\left(\frac{\gamma_s}{\gamma} - 1\right) d_k} \tag{35}$$

$$f' = \frac{2gRS}{U^2} \tag{36}$$

where,

ε_k = correction factor, accounts for hiding and exposure mechanism of nonuniform sediment transport

m = power index = 0.45

p_{hk} = hiding probabilities [k-th size class of bed material]

p_{ek} = exposure probabilities[k-th size class of bed material]

f' = friction factor

U = average flow velocity

R = hydraulic radius of the cross section

S = energy slope

ϕ_k = dimensionless sediment transport rate

q_{t*k} = bed-material load transport rate (m^2/s)

τ_{*k} = dimensionless bed shear stress

d_k = diameter of the k-th size class of bed material

The SEDTRA module uses three different established transport relations to calculate the transport rate for different size classes (Garbrecht et al., 1995 and 1996; Langendoen, 2000; Wu, 2001). SEDTRA has been found to be applicable to channels with widely graded sediment distributions and to channel networks with variable sediment characteristics. The Laursen (1985) formula is implemented for silt size classes from 0.01 mm to 0.25 mm, Yang's (1973) formula for sand size classes from 0.25 mm to 2.0 mm, and Meyer-Peter and Muller (1948) formula for gravel and larger size classes from 2.0 mm to 50.0 mm. Total sediment discharge is calculated as,

$$C_{*t} = \sum_k p_k C_{*k} \tag{37}$$

where,

C_{*t} = total sediment capacity in parts per million by weight (ppmw)

C_{*k} = sediment transport capacity for the k-th size class (ppmw)

p_k = percentage of k-th size class of sediment, defined by the bed material gradation

Non-uniform sediment mixtures are accounted for by using the following equations (Wu, 2001). When B is less than 1.7, x is equal to 1, and for high values of B, x approaches zero. The value of x is specified in the model based on Figure 26.

$$d_{ek} = d_k \left(\frac{d_k}{d_m} \right)^{-x} \tag{38}$$

$$x = \frac{1.7}{B} \tag{39}$$

$$B = \left(\frac{d_c}{d_f} \right)^{1/2} \sum p_m \tag{40}$$

where,

d_k = mean size of k-th size class

d_{ek} = sediment size used to calculate the critical flow strength for the k-th size class

d_m = mean diameter of bed material

x = empirical parameter

B = bimodality parameter

dc = diameters of coarse modes

Mixture Name	Reference	d_m (mm)	Mixture Type	B	x
SG10 (lab.)	Kuhnle (1993)	0.616	Bimodal	2.49	0.7
SG25 (lab.)	Kuhnle (1993)	0.927	Bimodal	2.60	0.7
SG45 (lab.)	Kuhnle (1993)	1.454	Bimodal	2.73	0.6
1/2 ψ (lab.)	Wilcock & S.(1988)	1.82	Unimodal	0.67	1.0
ψ (lab.)	Wilcock & S.(1988)	1.85	Unimodal	0.37	1.0
Goodwin Creek	Kuhnle (1993)	1.189	Bimodal	3.10	0.5

Note: The mixture names for the laboratory data (Kuhnle, 1993) refer to the percentage of gravel in the bed material: SG10 - 10% gravel, 90% sand; SG25 - 25% gravel, 75% sand; SG45 - 45% gravel, 55% sand; The mixture names of Wilcock and Southard (1988) refer to the standard deviation of the bed material.

Figure 26: Values of x recommended by Kuhnle et al. (1996)

df = diameters of fine modes

pm = portion of the sediment mixture contained in the coarse and fine modes.

The Meyer-Peter & Muller (MPM) formula was explored with further detail because it is frequently used to estimate rates of bedload transport in alluvial channels dominated by coarse substrate (Langendoen, 2000; Martin, 2003; Meyer-Peter & Muller, 1948; Weinhold, 2001). Equations 41 to 44 illustrate the MPM equation's application within the SEDTRA module.

$$c = \frac{8\times10^{6}\gamma_s u_* d_c}{\rho q}\left(r^{3/2}\theta - 0.047\right) \tag{41}$$

$$\theta = \frac{\gamma R S_f}{(\gamma_s - \gamma)d_c} \tag{42}$$

$$r^{3/2} = \left(\frac{n'}{n_e} \right)^2 \tag{43}$$

$$n' = \frac{d_{90}^{1/6}}{26} \tag{44}$$

where,

ρ = water density

q = unit discharge

r = ratio of bed roughness and grain roughness (Strickler coefficient)

θ = Shields parameter

n' = grain roughness

Appendix E: Stage discharge curve, HEC-RAS, and Energy slope

The Marsh-McBirney™ Flo-Mate model 2000 flowmeter, a top-setting wading rod marked in tenths of a foot, and a 100 meter fiberglass measuring tape were utilized to measure in-stream velocities. Velocity measurements were performed at cross sections with stable geometries, i.e., not actively changing during the duration of this project, and were located in close proximity to the installed downstream stage recorder. In addition, the cross section location was chosen to supported laminar flow conditions, to be free of obstructions, and to be flat bottomed. The width of the cross section or water surface elevation was determined by stringing a measuring tape between both banks at a right angle to the direction of flow. If the water depth was less than or equal to 0.76 m, one velocity measurement was taken at 60% of the flow depth at each increment. If the water depth exceeded 0.76 m, velocity measurements were also taken at 20% and 80% of the flow depth. Three velocity measurements and the corresponding water depth were recorded at a minimum of ten points along the transect. The average velocity at each point along the transect, incremental width, incremental depth, and distance from initial point were used to calculate the velocity at each section along the transect. The resulting incremental discharges were summed to determine the cumulative discharge at the transect. Finally, the starting and ending time of the velocity measurements were recorded in the field notes during the sampling procedure. The time was utilized to extrapolate the stream stage height from the downstream stage recorder data. The

discharge thorough the partial section was calculated according to Equation 45. The discharge at the cross section extents is calculated via Equation 46 and 47.

$$q_x = v_x\left[\left(b_{(x+1)} - b_{(x-1)}\right)/2\right]d_x \quad (45)$$

where,

q_x = discharge through the partial section x

v_x = measured mean velocity at vertical x

$b_{(x+1)}$ = the distance from initial point to the next location

$b_{(x-1)}$ = the distance from the initial point to the preceding location

d_x = the depth of flow at vertical x

$$q_1 = v_1\left[\left(b_2 - b_1\right)/2\right]d_1 \quad (46)$$

$$q_2 = v_n\left[\left(b_n - b_{(n-1)}\right)/2\right]d_n \quad (47)$$

A stage versus discharge curve was created by associating measured and simulated discharge values with measured and assumed stage readings. A power function fit to the data was utilized to develop the discharge hydrograph at the upstream boundary.

Application of HEC-RAS

The lack of measured in-stream velocities and stage data during large discharge events resulted in applying the one-dimensional hydraulic model HEC-RAS to

supplement the stage versus discharge curve and measured energy slope data. The same topography data used to establish the mesh for the 2D model was utilized to develop the HEC-RAS model, with downstream reach lengths measured in AutoDesk™ Land Desktop 2007. The first one-dimensional model simulation involved simulating a measured discharge through the defined reach. The produced water surface elevation at the downstream stage recorder geometry was compared with measured stage data associated with the simulated discharge. Manning's n values were adjusted until general agreement occurred between the computed and measured water surface elevations. The simulated water surface elevation matched measured results when the channel Manning's n value was set equal to a value of 0.09.

Chow (1959) recommends a range of Manning's n values for mountain streams which is dependent on the amount and size of large substrate in the bed. Chow specifies a minimum value of 0.03 for beds composed of gravels and cobbles up to a value of 0.07 for beds composed of cobbles and large boulders. (Sturm, 2001) Thus, a Manning's n value of 0.09 seemed large for this reach. This can be explain by considering the roughness element and its impact on discharge at different stages. At low discharges the roughness element is large with respect to the discharge value. Thus, the Manning's n value has more influence on the water surface elevation at the lower discharges; higher discharges are less influenced by the roughness element. Unfortunately, access to the stream at high discharges was limited, and for this reason flow measurements were only measured up to a discharge of 3.25 m^3/s, which produced a stage of only 0.87 m. Thus the measured discharges did not provide adequate data to calibrate the HEC-RAS model. For this reason, the data collected from both stage recorders and the corresponding

calculated energy slope were utilized to calibrate the one-dimensional hydraulic model, HEC-RAS. A Manning's n value of 0.025 was assumed for the entire channel geometry, and produced results that compared well with measured values.

Once calibrated, the energy slope was simulated in HEC-RAS by assigning an observed water surface elevation at the downstream stage recorder in half-foot increments above the maximum downstream recorded stage while both stage recorders were installed along the reach. The value for discharge was iterated until the simulated downstream stage matched that of the observed water surface elevation assigned at the downstream stage recorder. Once the observed and simulated water surface elevations matched, the water surface elevation at the upstream stage recorder cross section was recorded. The energy slope was calculated as the difference between the upstream and downstream water surface elevations at the stage recorders divided by the distance along the thalweg between the two stage recorders (209 m). In addition, the model was utilized to supplement the stage discharge relationship for discharges in excess of the maximum measured discharge value.

Energy Slope

The average difference between the upstream and downstream water surface elevations are presented in Table 32. Values were measured at water surface elevations less then 29.27 m and simulated for the remaining water surface elevation up to 30.34 m. The energy slope and duration at each specific stage is illustrated in Table 33. The 28.674 m value reflects the minimum simulated downstream water surface elevation, and

Table 32: Summary of energy slope data

DS WSEL (m)		Average
Upper Limit	Lower Limit	Δ WSEL (m)
28.51	28.35	1.28
28.66	28.51	1.23
28.81	28.66	1.14
28.96	28.81	1.05
29.12	28.96	1.03
29.27	29.12	0.90
29.42	29.27	0.93
29.57	29.42	0.88
29.73	29.57	0.84
29.88	29.73	0.81
30.03	29.88	0.76
30.18	30.03	0.71
30.26	30.18	0.67
30.34	30.26	0.65
Note: Grayed cells illustrate measured data		
DS - Downstream		
WSEL - Water surface elevation		

Table 33: Energy slope summary

Upstrem WSEL (m)		DS WSEL (m)	Energy Slope (m/m)	Duration at stage, time (seconds)
Lower Limit	Upper Limit			
29.360	29.390	--	--	--
29.390	29.421	--	--	--
29.421	29.451	--	--	--
29.451	29.482	--	--	--
29.482	29.512	--	--	--
29.512	29.543	--	--	--
29.543	29.573	--	--	--
29.573	29.604	--	--	--
29.604	29.634	--	--	--
29.634	29.665	--	--	--
29.665	29.695	--	--	--
29.695	29.726	--	--	--
29.726	29.756	--	--	--
29.756	29.787	--	--	--
29.787	29.817	28.674	0.00547	210120
29.817	29.848	28.704	0.00547	199320
29.848	29.878	28.801	0.00515	188520
29.878	29.909	28.854	0.00504	182520
29.909	29.939	28.884	0.00504	178920
29.939	29.970	28.915	0.00504	176520
29.970	30.000	28.945	0.00504	175320
30.000	30.030	29.104	0.00443	164520
30.030	30.061	29.062	0.00478	144120
30.061	30.091	29.105	0.00471	123720
30.091	30.122	29.173	0.00453	92520
30.122	30.152	29.181	0.00464	70920

Table 33: Energy slope summary (continued)

Upstrem WSEL (m)		DS WSEL		Duration at stage,
Lower Limit	Upper Limit	(m)	Energy Slope (m/m)	time (seconds)
30.152	30.183	29.286	0.00429	66120
30.183	30.213	29.280	0.00446	64920
30.213	30.244	29.311	0.00446	57720
30.244	30.274	29.341	0.00446	52920
30.274	30.305	29.372	0.00446	46920
30.305	30.335	29.423	0.00436	40920
30.335	30.366	29.467	0.00429	34920
30.366	30.396	29.515	0.00421	32520
30.396	30.427	29.546	0.00421	30120
30.427	30.457	29.601	0.00410	25320
30.457	30.488	29.643	0.00404	22920
30.488	30.518	29.674	0.00404	21720
30.518	30.549	29.723	0.00395	19320
30.549	30.579	29.753	0.00395	16920
30.579	30.610	29.793	0.00391	16920
30.610	30.640	29.832	0.00386	15720
30.640	30.671	29.878	0.00379	12120
30.671	30.701	29.924	0.00372	12120
30.701	30.732	29.970	0.00364	10920
30.732	30.762	30.027	0.00351	8520
30.762	30.793	30.085	0.00338	8520
30.793	30.823	30.116	0.00338	6120
30.823	30.854	30.166	0.00329	4920
30.854	30.884	30.207	0.00324	3720
30.884	30.915	30.247	0.00319	120
Water surface elevation is abbreviated WSEL				
Downstream is abbreviated DS				

the values show that energy slope decreased as stage increased.

Stage vs. Discharge Curve

The resulting stage and discharge values are shown in Table 34 and Figure 27. The recorded downstream stage data throughout the simulated storm event is included in Appendix F.

HEC-RAS Validation

HEC-RAS validation results are presented in Table 35.

Table 34: Stage discharge data

Sample Number	Sample Date (M/D/Y)	Sample Time (H:M)	Measured Stream Discharge (ft^3/sec)	Stream Stage Reading (ft)	WSEL (ft)	Measured Stream Discharge (m^3/sec)	Stream Stage Reading (m)
1	18-Jul-2007	5:30 PM	2.23	0.97	91.86	0.06	0.30
2	18-Oct-2007	3:00 PM	0.92	1.40	92.29	0.03	0.43
3	11-Dec-2007	10:15 AM	7.43	1.80	92.69	0.21	0.55
4	7-Jan-2008	9:00 AM	14.14	2.12	93.01	0.40	0.65
5	30-Nov-2007		21.21	2.13	93.02	0.60	0.65
6	24-Jan-2008	11:15 AM	25.83	2.55	93.44	0.73	0.78
7	21-Jan-2008	2:00 PM	23.32	2.57	93.46	0.66	0.78
8	30-Jan-2008	12:00 PM	37.23	2.59	93.48	1.05	0.79
9	10-Jan-2008	11:00 AM	114.77	2.84	93.73	3.25	0.87
10	HEC-RAS SIMULATION		137.00	3.00	93.89	3.88	0.91
11	HEC-RAS SIMULATION		188.00	3.50	94.39	5.32	1.07
12	HEC-RAS SIMULATION		315.00	4.00	94.89	8.92	1.22
13	HEC-RAS SIMULATION		465.00	4.50	95.39	13.17	1.37
14	HEC-RAS SIMULATION		640.00	5.00	95.89	18.12	1.52
15	HEC-RAS SIMULATION		850.00	5.50	96.39	24.07	1.68
16	HEC-RAS SIMULATION		1125.00	6.00	96.89	31.86	1.83
17	HEC-RAS SIMULATION		1425.00	6.50	97.39	40.35	1.98
18	HEC-RAS SIMULATION		1750.00	7.00	97.89	49.55	2.13
19	HEC-RAS SIMULATION		2115.00	7.50	98.39	59.89	2.29
20	HEC-RAS SIMULATION		2500.00	8.00	98.89	70.79	2.44
21	HEC-RAS SIMULATION		2935.00	8.50	99.39	83.11	2.59

Note: Grayed cells are measured values

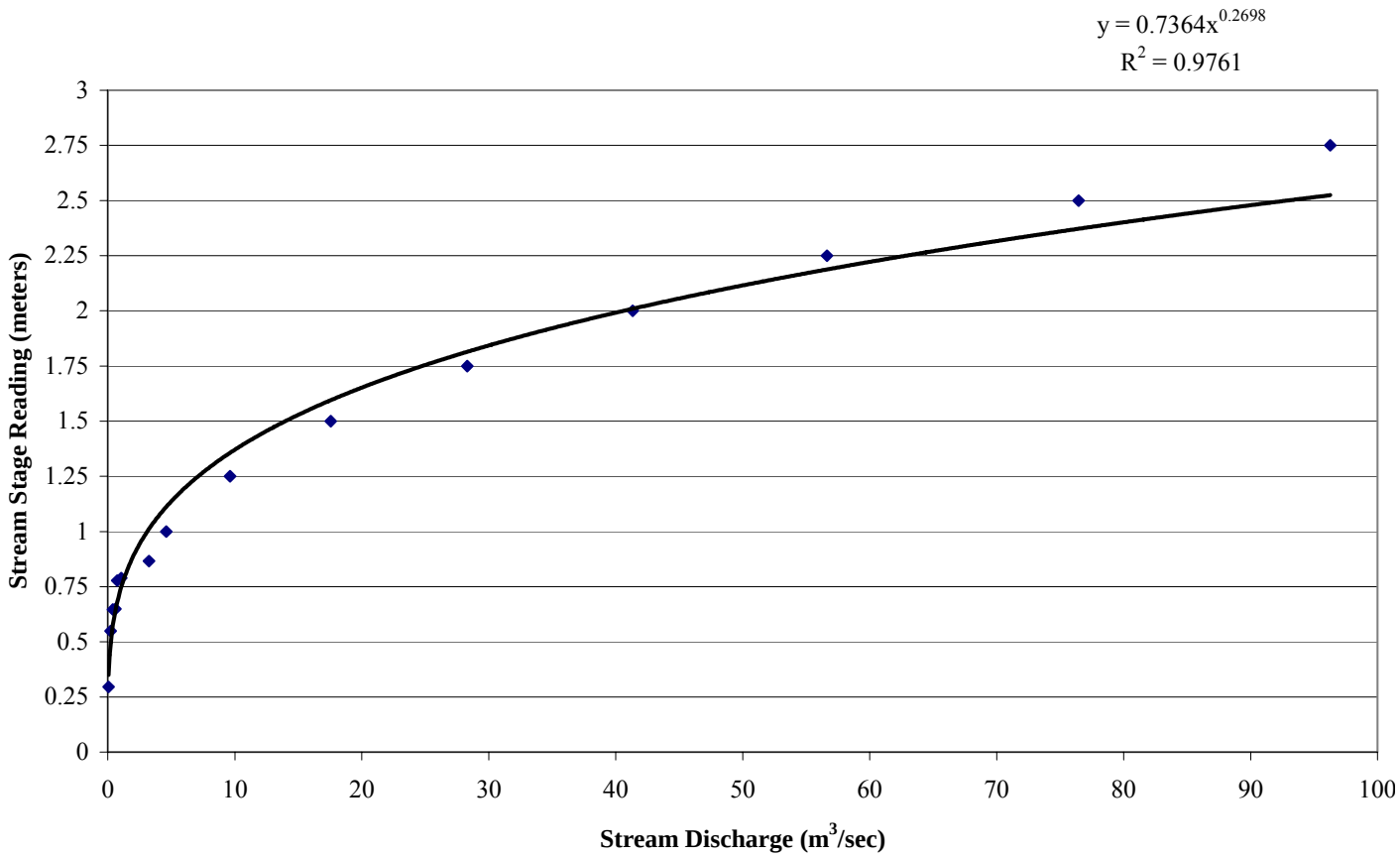

Figure 27: Stage discharge graph

Table 35: HEC-RAS validation

Date	Time	Recorded				Simulated				Difference (Simulated - Measured)				% Difference			
		Downstream WSEL		Upstream WSEL		Downstream WSEL		Upstream WSEL		Downstream WSEL		Upstream WSEL		Downstream WSEL		Upstream WSEL	
		(ft)	(m)	(ft)	(m)	(ft)	(m)	(ft)	(m)	(ft)	(m)	(ft)	(m)	(ft)	(m)	(ft)	(m)
04/03/2008	20:18:38	96.03	29.28	99.03	30.19	96.03	29.28	99.07	30.20	0.00	0.00	0.04	0.01	0.00	0.00	0.04	0.01
04/03/2008	11:20:03	94.44	28.79	98.07	29.90	94.44	28.79	98.02	29.88	0.00	0.00	-0.05	-0.01	0.00	0.00	-0.05	-0.01
05/27/2008	11:28:00	93.00	28.35	97.69	29.78	93.00	28.35	97.48	29.72	0.00	0.00	-0.21	-0.06	0.00	0.00	-0.22	-0.07
04/11/2008	19:30:03	94.00	28.66	97.79	29.81	93.99	28.66	97.89	29.84	-0.01	0.00	0.10	0.03	-0.01	0.00	0.10	0.03
04/03/2008	12:10:03	95.03	28.97	98.43	30.01	95.03	28.97	98.41	30.00	0.00	0.00	-0.02	-0.01	0.00	0.00	-0.02	-0.01
Water surface elevation is abbreviated as WSEL																	

Appendix F: Pebble count data and recorded downstream stage data

Table 36: Recorded downstream stage data, simulated storm event

Time & Date	Stage (m)	Elevation (m)	Time & Date	Stage (m)	Elevation (m)	Time & Date	Stage (m)	Elevation (m)	Time & Date	Stage (m)	Elevation (m)
03/04/2008 03:08	0.954	28.657	03/04/2008 18:02	2.426	30.129	03/05/2008 09:02	1.551	29.255	03/06/2008 00:02	1.347	29.050
03/04/2008 03:28	0.957	28.660	03/04/2008 18:22	2.374	30.078	03/05/2008 09:22	1.545	29.249	03/06/2008 00:22	1.347	29.050
03/04/2008 03:48	0.966	28.669	03/04/2008 18:42	2.323	30.026	03/05/2008 09:42	1.536	29.239	03/06/2008 00:42	1.344	29.047
03/04/2008 04:08	0.969	28.673	03/04/2008 19:02	2.277	29.980	03/05/2008 10:02	1.530	29.233	03/06/2008 01:02	1.344	29.047
03/04/2008 04:28	0.969	28.673	03/04/2008 19:22	2.234	29.937	03/05/2008 10:22	1.524	29.227	03/06/2008 01:22	1.338	29.041
03/04/2008 04:48	0.972	28.676	03/04/2008 19:42	2.179	29.883	03/05/2008 10:42	1.518	29.221	03/06/2008 01:42	1.332	29.035
03/04/2008 05:08	0.972	28.676	03/04/2008 20:02	2.146	29.849	03/05/2008 11:02	1.509	29.212	03/06/2008 02:02	1.332	29.035
03/04/2008 05:28	0.972	28.676	03/04/2008 20:22	2.109	29.812	03/05/2008 11:22	1.503	29.206	03/06/2008 02:22	1.329	29.032
03/04/2008 05:48	0.972	28.676	03/04/2008 20:42	2.051	29.755	03/05/2008 11:42	1.503	29.206	03/06/2008 02:42	1.329	29.032
03/04/2008 06:08	0.978	28.682	03/04/2008 21:02	2.024	29.727	03/05/2008 12:02	1.497	29.200	03/06/2008 03:02	1.329	29.032
03/04/2008 06:28	0.985	28.688	03/04/2008 21:22	1.996	29.700	03/05/2008 12:22	1.487	29.191	03/06/2008 03:22	1.326	29.029
03/04/2008 06:48	0.994	28.697	03/04/2008 21:42	1.978	29.681	03/05/2008 12:42	1.481	29.185	03/06/2008 03:42	1.326	29.029
03/04/2008 07:08	1.003	28.706	03/04/2008 22:02	1.951	29.654	03/05/2008 13:02	1.472	29.175	03/06/2008 04:02	1.317	29.020
03/04/2008 07:28	1.018	28.721	03/04/2008 22:22	1.929	29.633	03/05/2008 13:22	1.466	29.169	03/06/2008 04:22	1.317	29.020
03/04/2008 07:48	1.106	28.810	03/04/2008 22:42	1.905	29.608	03/05/2008 13:42	1.460	29.163	03/06/2008 04:42	1.317	29.020
03/04/2008 08:08	1.487	29.191	03/04/2008 23:02	1.890	29.593	03/05/2008 14:02	1.448	29.151	03/06/2008 05:02	1.317	29.020
03/04/2008 08:22	1.506	29.209	03/04/2008 23:22	1.875	29.578	03/05/2008 14:22	1.445	29.148	03/06/2008 05:22	1.317	29.020
03/04/2008 08:42	1.512	29.215	03/04/2008 23:42	1.856	29.560	03/05/2008 14:42	1.448	29.151	03/06/2008 05:42	1.317	29.020
03/04/2008 09:02	1.518	29.221	03/05/2008 00:02	1.835	29.538	03/05/2008 15:02	1.442	29.145	03/06/2008 06:02	1.320	29.023
03/04/2008 09:22	1.521	29.224	03/05/2008 00:22	1.823	29.526	03/05/2008 15:22	1.414	29.118	03/06/2008 06:22	1.320	29.023
03/04/2008 09:42	1.521	29.224	03/05/2008 00:42	1.807	29.511	03/05/2008 15:42	1.417	29.121	03/06/2008 06:42	1.317	29.020
03/04/2008 10:02	1.515	29.218	03/05/2008 01:02	1.789	29.492	03/05/2008 16:02	1.411	29.114	03/06/2008 07:02	1.320	29.023
03/04/2008 10:22	1.506	29.209	03/05/2008 01:22	1.774	29.477	03/05/2008 16:22	1.396	29.099	03/06/2008 07:22	1.317	29.020
03/04/2008 10:42	1.512	29.215	03/05/2008 01:42	1.762	29.465	03/05/2008 16:42	1.384	29.087	03/06/2008 07:42	1.317	29.020
03/04/2008 11:02	1.512	29.215	03/05/2008 02:02	1.747	29.450	03/05/2008 17:02	1.393	29.096	03/06/2008 08:02	1.308	29.011
03/04/2008 11:22	1.512	29.215	03/05/2008 02:22	1.734	29.438	03/05/2008 17:22	1.420	29.124	03/06/2008 08:22	1.286	28.990
03/04/2008 11:42	1.509	29.212	03/05/2008 02:42	1.722	29.425	03/05/2008 17:42	1.417	29.121	03/06/2008 08:42	1.268	28.971
03/04/2008 12:02	1.506	29.209	03/05/2008 03:02	1.710	29.413	03/05/2008 18:02	1.411	29.114	03/06/2008 09:02	1.225	28.929
03/04/2008 12:22	1.484	29.188	03/05/2008 03:22	1.698	29.401	03/05/2008 18:22	1.405	29.108	03/06/2008 09:22	1.198	28.901
03/04/2008 12:42	1.478	29.182	03/05/2008 03:42	1.689	29.392	03/05/2008 18:42	1.402	29.105	03/06/2008 09:42	1.170	28.874
03/04/2008 13:02	1.417	29.121	03/05/2008 04:02	1.676	29.380	03/05/2008 19:02	1.399	29.102	03/06/2008 10:02	1.180	28.883
03/04/2008 13:22	1.503	29.206	03/05/2008 04:22	1.667	29.371	03/05/2008 19:22	1.393	29.096	03/06/2008 10:22	1.155	28.858
03/04/2008 13:42	1.554	29.258	03/05/2008 04:42	1.658	29.361	03/05/2008 19:42	1.390	29.093	03/06/2008 10:42	1.167	28.871
03/04/2008 14:02	1.573	29.276	03/05/2008 05:02	1.649	29.352	03/05/2008 20:02	1.387	29.090	03/06/2008 11:02	1.106	28.810
03/04/2008 14:22	1.576	29.279	03/05/2008 05:22	1.637	29.340	03/05/2008 20:22	1.387	29.090	03/06/2008 11:22	1.103	28.807
03/04/2008 14:42	1.609	29.313	03/05/2008 05:42	1.631	29.334	03/05/2008 20:42	1.381	29.084	03/06/2008 11:42	1.103	28.807
03/04/2008 15:02	1.631	29.334	03/05/2008 06:02	1.622	29.325	03/05/2008 21:02	1.381	29.084	03/06/2008 12:02	1.116	28.819
03/04/2008 15:22	1.753	29.456	03/05/2008 06:22	1.618	29.322	03/05/2008 21:22	1.372	29.075	03/06/2008 12:22	1.125	28.828
03/04/2008 15:42	2.146	29.849	03/05/2008 06:42	1.603	29.307	03/05/2008 21:42	1.372	29.075	03/06/2008 12:42	1.116	28.819
03/04/2008 16:02	2.396	30.099	03/05/2008 07:02	1.597	29.300	03/05/2008 22:02	1.369	29.072	03/06/2008 12:50	1.119	28.822
03/04/2008 16:22	2.509	30.212	03/05/2008 07:22	1.588	29.291	03/05/2008 22:22	1.369	29.072	03/06/2008 13:10	1.116	28.819
03/04/2008 16:42	2.536	30.239	03/05/2008 07:42	1.582	29.285	03/05/2008 22:42	1.359	29.063	03/06/2008 13:30	1.113	28.816
03/04/2008 17:02	2.533	30.236	03/05/2008 08:02	1.576	29.279	03/05/2008 23:02	1.359	29.063	03/06/2008 13:50	1.113	28.816
03/04/2008 17:22	2.527	30.230	03/05/2008 08:22	1.567	29.270	03/05/2008 23:22	1.359	29.063			
03/04/2008 17:42	2.475	30.178	03/05/2008 08:42	1.558	29.261	03/05/2008 23:42	1.359	29.063			

Table 37: Pebble count data

	Dia. (mm)	Dia (mm)	Dia (mm)	Dia (mm)
1	75	108	35	12
2	45	144	62	180
3	40	45	66	55
4	62	52	4	22
5	69	64	54	25
6	129	84	59	107
7	78	100	77	137
8	100	72	70	16
9	72	82	85	115
10	80	12	66	20
11	74	22	80	15
12	110	35	94	30
13	45	98	32	28
14	70	64	28	18
15	28	60	60	2
16	26	92	70	100
17	32	104	120	28
18	155	98	94	144
19	114	60	130	84
20	112	65	97	52
21	71	80	80	66
22	35	105	115	95
23	40	12	48	92
24	52	63	92	72
25	35	52	118	36

Appendix G: Sediment transport functions

Sediment transport functions

The simulation of sediment transport involves the numerical solution of one or more of the governing differential equations of continuity, momentum, and energy of fluid, along with the differential equation for sediment continuity (Langendoen, 2001; Papanicolaou et al., 2008; Wu, 2001). Non-cohesive bed particles begin moving when the driving forces initiating motion exceed forces that resist motion, or when the shear stress applied to the particle exceeds the critical shear stress, and move as either bedload or suspended load (Strum, 2001; Langendoen, 2001; Julien, 1995; Haan et al., 1994). Bedload can be defined as the individual sediment particles that are transported downstream by rolling, sliding, and saltation within a thin layer near the bed, referred to as the bed layer. Bedload is often presented as a volumetric transport rate of sediment per unit of stream width (ft^2/s or m^2/s) or a flux of sediment per unit width per unit time that is in motion in the area defined by the bed layer. The bed layer thickness can be defined as approximately twice the diameter of the largest particle in movement. The bed load transport rate can also be expressed in terms of dry weight of sediment transported per unit of width and time in the English system. Bed load transport rate is often expressed as mass transport rate per unit of channel width (kg/s/m) in the SI system.

Suspended sediment consists of fine sands, clays, and silts that are lifted into the flow by turbulence (Julien, 1995; Robinson, 2005;Strum, 2001). Suspended sediment transport is primarily a function of turbulent diffusion forcing the grains upward and the

fall velocity of the individual particles due to gravity. A more detailed discussion of suspended sediment transport can be found in Robinson (2005). Figure 28 illustrates the interaction and transport of suspended and bedload material (Langendoen, 2000).

Wash load is yet another component of sediment transport (Sturm, 2001; Julien, 1995; Robinson, 2005; Langendoen & Alonso, 2008). Wash load can be defined as the fine sediment resulting from erosion in the watershed. This component of sediment transport is often lumped with suspended sediment, or is simulated as passing through the system uninhibited. This method is sufficient if bedload is the main mode of sediment transport. However, the interactions between the transport modes (i.e., suspended load, bedload, and wash load) and the interaction of each transport mode on the bed gradation must be accounted for if suspended sediment or wash load is the main mode of sediment transport.

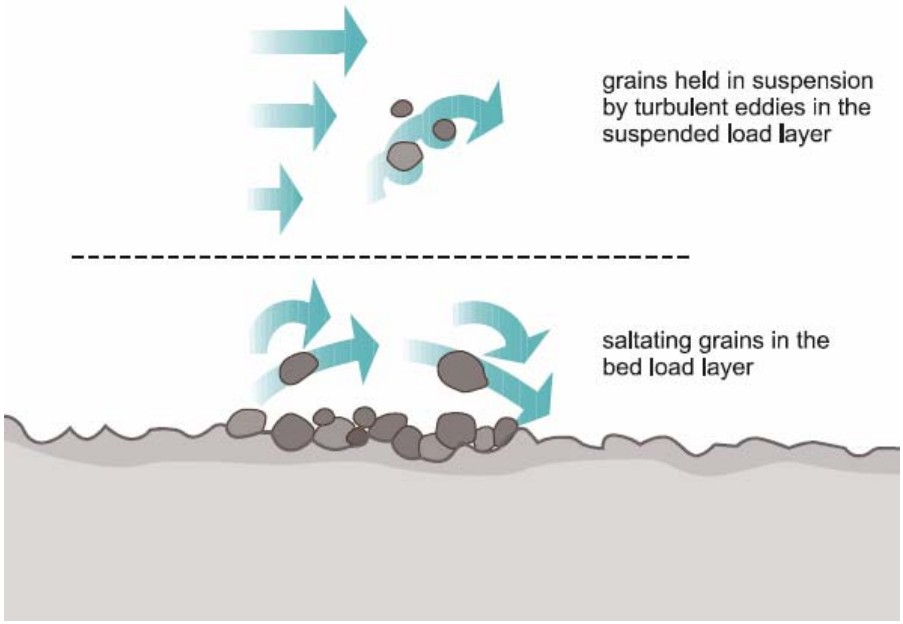

Figure 28: Illustration of suspended and bedload transport (Langendoen, 2000)

Bedload transport

The collected bedload sample did not provide adequate data to develop a bedload rating curve, so a bedload curve was developed based on the Meyer-Peter and Muller (MPM) empirical formula and a calculated critical diameter for each size class defined within CCHE2D. The MPM formula is used frequently to estimate rates of bedload transport in alluvial channels dominated by large substrate (Foremann et al., 2007; Gabrecht et al., 1996; Langendoen, 2000; Meyer-Peter & Muller, 1948). This equation is empirically derived and based on incipient motion of sediment sized between 5mm and 28.6mm (Sturm, 2001). The MPM formula defines sediment discharge as a function of sediment size or calculated critical diameter for each size class, specific gravity of the sediment, and the shields parameter. The shields parameter is a function of the water depth, specific gravity, and the energy slope. Sturm (2001) presents the MPM equation in dimensionless form, illustrated in Equation 48, and the shields parameter, illustrated in Equation 49.

$$\phi_b = \frac{q_b}{\sqrt{(SG-1)gd_s^3}} = 8.0(\tau_* - 0.047)^{\frac{3}{2}} \tag{48}$$

$$\tau_* = \frac{y_0 S}{(SG-1)d_s} \tag{49}$$

where,

d_s = sediment size

y_0 = water depth

S = energy slope

SG = specific gravity of the sediment

τ_* = shields parameter (a value of 0.047 is assumed equal to the critical value of the Shields parameter)

Suspended sediment transport

Suspended sediment transport relations were derived from measured values. For this reason, suspended sediment formulas are not discussed in this literature review.

Appendix H: Portable bedload trap construction

Multiple bedload samples are required to develop a bedload rating curve, and the corresponding upstream boundary condition required to initiate a two-dimensional simulation. Literature pertaining to pit traps, Helley-Smith sampling, and bedload traps was reviewed before a method was selected to measure bedload transport. After reviewing the literature the decision was made to install pit traps according to Wilcock (2001). Despite several attempts, the coarse substrate prevented adequate excavation to install a five gallon plastic bucket in the bed. Additional literature revealed that bedload traps could provide a greater efficiency in sampling bedload than deploying a Helley-Smith sampler (Bunte et al., 2004). For this reason, bedload traps were chosen as a viable method and constructed.

Traps were constructed of 6.35 mm (1/4") aluminum flat bar, cut to produce 0.3048 m (12") and 0.1524 m (6") pieces, which were tig welded into rectangular shapes. The final product was approximately 0.3175 m (12.5") wide and 0.1651 m (6.5") high. A 4.76 mm (3/16") aluminum plate (0.406 m by 0.305 m) was used as a base plate for the trap. The base plate was bent at a 5 degree angle 4" from the upstream end. This angled front edge was driven into the bed of the stream to provide a smooth transition between the bedload trap device and the particles in the bed. Two 0.610 m pieces of #4 rebar with (3.18 mm) flat washer welded to the top were used to secure the base plate and attached bedload trap to the stream bed. Nets were installed on the downstream end of the bedload traps to capture sediment moving through the inlet of the trap. The nets were

constructed of 3.75 mm (1/8”) nylon mesh secured inside a 12.7 mm (½”) outer nylon mesh. The smaller mesh provided the resolution of capturing bed load material greater than or equal to 4mm. The outside mesh supported the weight of the material captured inside the smaller nylon mesh. Figures 29 and 30 illustrate the bedload traps.

Figure 29: Bedload trap frame

Figure 30: Bedload trap in use

Appendix I: Bedload rating curve data

Table 38: Bedload discharge per unit width (8.25 mm)

Energy slope (ft/ft)	Y_o (ft)	WSEL	d_s (mm)	d_s (ft)	Calculated Shields parameter	Gravity (ft/s^2)	Shields - Critical	Bedload discharge per unit width (ft^2/s)	Top width (ft)	Volumetric discharge (ft^3/s)	Duration at stage or greater stage (time, seconds)	Total volume transported (ft^3)	Total weight transported (lbs)
0.0055	1.56	97.80	36	0.118	0.044	32.2	-0.003	0.00000	67.1	0.00000	210120	0	0
0.0055	1.66	97.90	36	0.118	0.047	32.2	0.000	0.00000	67.1	0.00000	199320	0	0
0.0051	1.75	97.99	36	0.118	0.046	32.2	-0.001	0.00000	67.1	0.00000	188520	0	0
0.0050	1.85	98.09	36	0.118	0.048	32.2	0.001	0.00006	67.1	0.00410	182520	748	123387
0.0050	1.94	98.18	36	0.118	0.050	32.2	0.003	0.00043	67.1	0.02877	178920	5147	849231
0.0050	2.04	98.28	36	0.118	0.053	32.2	0.006	0.00104	67.1	0.06994	176520	12345	2036984
0.0050	2.15	98.39	36	0.118	0.056	32.2	0.009	0.00190	67.1	0.12741	175320	22337	3685638
0.0044	2.25	98.49	36	0.118	0.051	32.2	0.004	0.00064	67.1	0.04285	164520	7049	1163062
0.0048	2.35	98.59	36	0.118	0.058	32.2	0.011	0.00259	67.1	0.17358	144120	25016	4127672
0.0047	2.45	98.69	36	0.118	0.059	32.2	0.012	0.00322	67.1	0.21605	123720	26729	4410314
0.0045	2.55	98.79	36	0.118	0.059	32.2	0.012	0.00325	67.1	0.21792	92520	20162	3326761
0.0046	2.65	98.89	36	0.118	0.063	32.2	0.016	0.00486	67.1	0.32607	70920	23125	3815556
0.0043	2.75	98.99	36	0.118	0.061	32.2	0.014	0.00373	67.1	0.25047	66120	16561	2732598
0.0045	2.85	99.09	36	0.118	0.065	32.2	0.018	0.00583	67.1	0.39103	64920	25386	4188637
0.0045	2.95	99.19	36	0.118	0.068	32.2	0.021	0.00696	67.1	0.46691	57720	26950	4446719
0.0045	3.05	99.29	36	0.118	0.070	32.2	0.023	0.00816	67.1	0.54714	52920	28955	4777509
0.0045	3.15	99.39	36	0.118	0.072	32.2	0.025	0.00941	67.1	0.63150	46920	29630	4888984
0.0044	3.26	99.50	36	0.118	0.073	32.2	0.026	0.00990	67.1	0.66422	40920	27180	4484652
0.0043	3.36	99.60	36	0.118	0.074	32.2	0.027	0.01054	67.1	0.70682	34920	24682	4072543
0.0042	3.45	99.69	36	0.118	0.075	32.2	0.028	0.01084	67.1	0.72734	32520	23653	3902765
0.0042	3.56	99.80	36	0.118	0.077	32.2	0.030	0.01227	67.1	0.82339	30120	24801	4092084
0.0041	3.66	99.90	36	0.118	0.077	32.2	0.030	0.01226	67.1	0.82222	25320	20819	3435065
0.0040	3.76	100.00	36	0.118	0.078	32.2	0.031	0.01286	67.1	0.86280	22920	19775	3262919
0.0040	3.86	100.10	36	0.118	0.080	32.2	0.033	0.01417	67.1	0.95098	21720	20655	3408137
0.0039	3.96	100.20	36	0.118	0.080	32.2	0.033	0.01437	67.1	0.96376	19320	18620	3072270
0.0039	4.05	100.29	36	0.118	0.082	32.2	0.035	0.01556	67.1	1.04409	16920	17666	2914891
0.0039	4.15	100.39	36	0.118	0.083	32.2	0.036	0.01630	67.1	1.09336	16920	18500	3052449
0.0039	4.26	100.50	36	0.118	0.084	32.2	0.037	0.01715	67.1	1.15045	15720	18085	2984025
0.0038	4.36	100.60	36	0.118	0.085	32.2	0.038	0.01739	67.1	1.16668	12120	14140	2333135
0.0037	4.46	100.70	36	0.118	0.085	32.2	0.038	0.01758	67.1	1.17952	12120	14296	2358807
0.0036	4.56	100.80	36	0.118	0.085	32.2	0.038	0.01772	67.1	1.18892	10920	12983	2142194
0.0035	4.66	100.90	36	0.118	0.084	32.2	0.037	0.01685	67.1	1.13037	8520	9631	1589079
0.0034	4.76	101.00	36	0.118	0.083	32.2	0.036	0.01590	67.1	1.06677	8520	9089	1499659
0.0034	4.86	101.10	36	0.118	0.084	32.2	0.037	0.01708	67.1	1.14569	6120	7012	1156919
0.0033	4.96	101.20	36	0.118	0.084	32.2	0.037	0.01662	67.1	1.11471	4920	5484	904925
0.0032	5.06	101.30	36	0.118	0.084	32.2	0.037	0.01693	67.1	1.13560	3720	4224	697033
0.0032	5.16	101.40	36	0.118	0.085	32.2	0.038	0.01721	67.1	1.15438	120	139	22857

sum = 95,959,462 lbs

Table 39: Bedload mass transport per unit of channel width (8.25 mm)

W.S. Elev.	Upstream Yo	Downstream WSEL	Stage	Discharge Q	Volumetric transport rate of sediment per unit stream width q_b	Specific weight of Sediment	Dry weight of sediment transported per unit width and time g_b	Gravitational acceleration g	Mass transport rate per unit of channel width	Mass transport rate per unit of channel width
(ft)	(ft)	(ft)	(ft)	(m^3/s)	(ft^2/s)	(lbs/ft^3)	(lbs/s/ft)	(ft/s^2)	($Slugs*s^{-1}*ft^{-1}$)	($kg*m^{-1}*s^{-1}$)
97.80	1.56	94.05	3.16	2.5	0.00000	165	0.00000	32.2	0.00000	0.00000
97.90	1.66	94.15	3.26	2.8	0.00000	165	0.00000	32.2	0.00000	0.00000
97.99	1.75	94.47	3.58	4.0	0.00000	165	0.00000	32.2	0.00000	0.00000
98.09	1.85	94.64	3.75	4.8	0.00006	165	0.01008	32.2	0.00031	0.01498
98.18	1.94	94.74	3.85	5.3	0.00043	165	0.07075	32.2	0.00220	0.10520
98.28	2.04	94.84	3.95	5.9	0.00104	165	0.17200	32.2	0.00534	0.25576
98.39	2.15	94.94	4.05	6.5	0.00190	165	0.31335	32.2	0.00973	0.46593
98.49	2.25	95.46	4.57	10.4	0.00064	165	0.10537	32.2	0.00327	0.15668
98.59	2.35	95.32	4.43	9.2	0.00259	165	0.42690	32.2	0.01326	0.63478
98.69	2.45	95.47	4.58	10.4	0.00322	165	0.53134	32.2	0.01650	0.79008
98.79	2.55	95.69	4.80	12.5	0.00325	165	0.53595	32.2	0.01664	0.79694
98.89	2.65	95.71	4.82	12.8	0.00486	165	0.80192	32.2	0.02490	1.19243
98.99	2.75	96.06	5.17	16.7	0.00373	165	0.61601	32.2	0.01913	0.91598
99.09	2.85	96.04	5.15	16.5	0.00583	165	0.96169	32.2	0.02987	1.43000
99.19	2.95	96.14	5.25	17.8	0.00696	165	1.14830	32.2	0.03566	1.70748
99.29	3.05	96.24	5.35	19.1	0.00816	165	1.34562	32.2	0.04179	2.00089
99.39	3.15	96.34	5.45	20.6	0.00941	165	1.55311	32.2	0.04823	2.30942
99.50	3.26	96.51	5.62	23.1	0.00990	165	1.63356	32.2	0.05073	2.42904
99.60	3.36	96.65	5.76	25.5	0.01054	165	1.73834	32.2	0.05399	2.58484
99.69	3.45	96.81	5.92	28.4	0.01084	165	1.78881	32.2	0.05555	2.65989
99.80	3.56	96.91	6.02	30.3	0.01227	165	2.02503	32.2	0.06289	3.01115
99.90	3.66	97.09	6.20	33.9	0.01226	165	2.02215	32.2	0.06280	3.00686
100.00	3.76	97.23	6.34	37.0	0.01286	165	2.12194	32.2	0.06590	3.15525
100.10	3.86	97.33	6.44	39.3	0.01417	165	2.33883	32.2	0.07263	3.47776
100.20	3.96	97.49	6.60	43.3	0.01437	165	2.37025	32.2	0.07361	3.52448
100.29	4.05	97.59	6.70	45.9	0.01556	165	2.56782	32.2	0.07975	3.81825
100.39	4.15	97.72	6.83	49.4	0.01630	165	2.68900	32.2	0.08351	3.99844
100.50	4.26	97.85	6.96	53.2	0.01715	165	2.82939	32.2	0.08787	4.20719
100.60	4.36	98.00	7.11	57.8	0.01739	165	2.86932	32.2	0.08911	4.26658
100.70	4.46	98.15	7.26	62.6	0.01758	165	2.90090	32.2	0.09009	4.31352
100.80	4.56	98.30	7.41	67.8	0.01772	165	2.92401	32.2	0.09081	4.34789
100.90	4.66	98.49	7.60	74.8	0.01685	165	2.78002	32.2	0.08634	4.13379
101.00	4.76	98.68	7.79	82.4	0.01590	165	2.62358	32.2	0.08148	3.90117
101.10	4.86	98.78	7.89	86.6	0.01708	165	2.81769	32.2	0.08751	4.18981
101.20	4.96	98.94	8.05	93.8	0.01662	165	2.74151	32.2	0.08514	4.07652
101.30	5.06	99.08	8.19	99.9	0.01693	165	2.79288	32.2	0.08674	4.15291
101.40	5.16	99.21	8.32	106.4	0.01721	165	2.83906	32.2	0.08817	4.22157

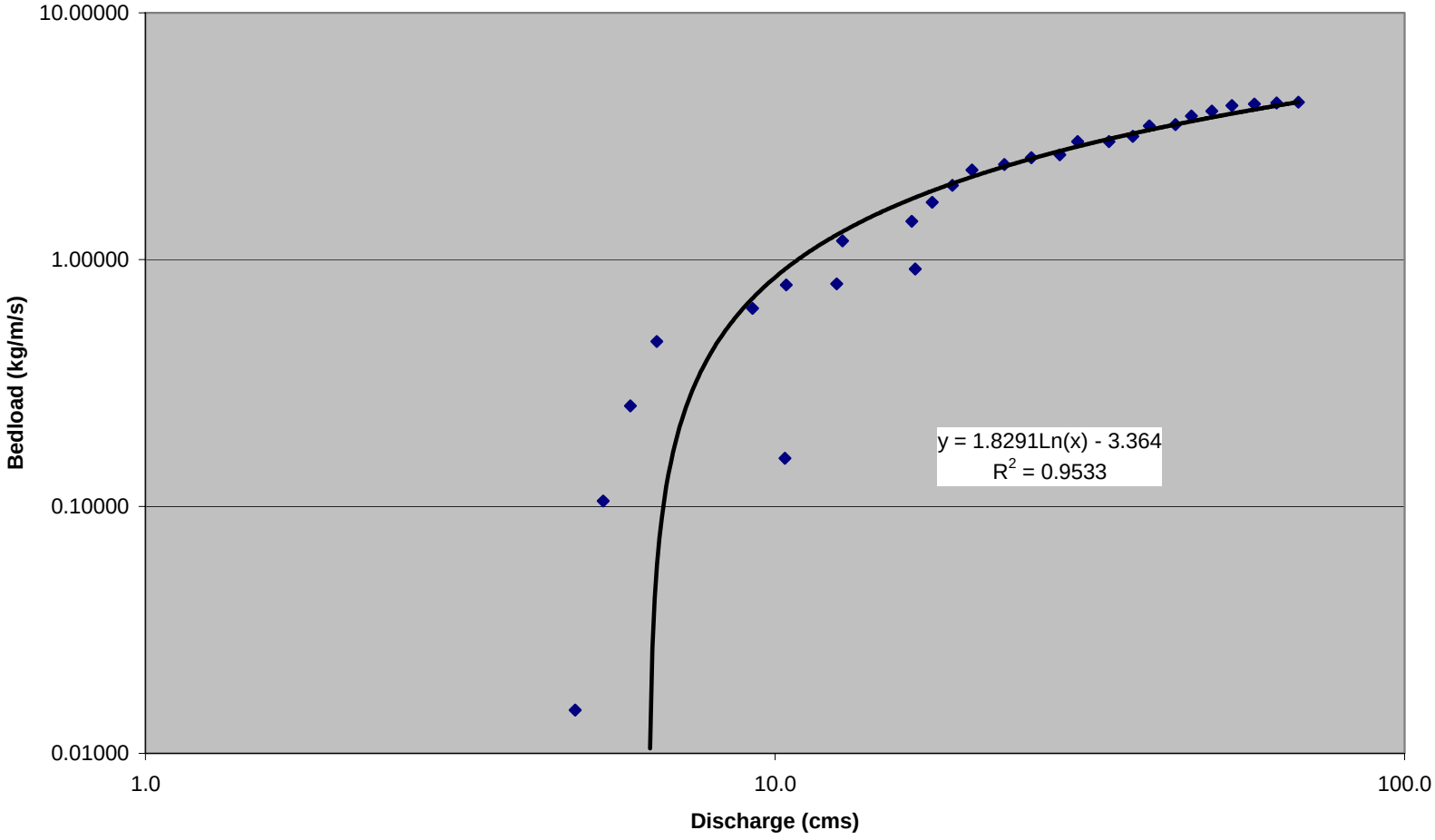

Figure 31: Bedload rating curve (8.25 mm)

Table 40: Bedload discharge per unit width (17.25 mm)

Energy slope (ft/ft)	Y_o (ft)	WSEL	d_s (mm)	d_s (ft)	Calculated Shields parameter	Gravity (ft/s^2)	Shields - Critical	Bedload discharge per unit width (ft^2/s)	Top width (ft)	Volumetric discharge (ft^3/s)	Duration at stage or greater stage (time, seconds)	Total volume transported (ft^3)	Total weight transported (lbs)
0.0055	1.56	97.80	46	0.151	0.034	32.2	-0.013	0.00000	67.1	0.00000	210120	0	0
0.0055	1.66	97.90	46	0.151	0.036	32.2	-0.011	0.00000	67.1	0.00000	199320	0	0
0.0051	1.75	97.99	46	0.151	0.036	32.2	-0.011	0.00000	67.1	0.00000	188520	0	0
0.0050	1.85	98.09	46	0.151	0.037	32.2	-0.010	0.00000	67.1	0.00000	182520	0	0
0.0050	1.94	98.18	46	0.151	0.039	32.2	-0.008	0.00000	67.1	0.00000	178920	0	0
0.0050	2.04	98.28	46	0.151	0.041	32.2	-0.006	0.00000	67.1	0.00000	176520	0	0
0.0050	2.15	98.39	46	0.151	0.044	32.2	-0.003	0.00000	67.1	0.00000	175320	0	0
0.0044	2.25	98.49	46	0.151	0.040	32.2	-0.007	0.00000	67.1	0.00000	164520	0	0
0.0048	2.35	98.59	46	0.151	0.045	32.2	-0.002	0.00000	67.1	0.00000	144120	0	0
0.0047	2.45	98.69	46	0.151	0.046	32.2	-0.001	0.00000	67.1	0.00000	123720	0	0
0.0045	2.55	98.79	46	0.151	0.046	32.2	-0.001	0.00000	67.1	0.00000	92520	0	0
0.0046	2.65	98.89	46	0.151	0.049	32.2	0.002	0.00041	67.1	0.02744	70920	1946	321150
0.0043	2.75	98.99	46	0.151	0.047	32.2	0.000	0.00003	67.1	0.00176	66120	117	19242
0.0045	2.85	99.09	46	0.151	0.051	32.2	0.004	0.00088	67.1	0.05925	64920	3847	634696
0.0045	2.95	99.19	46	0.151	0.053	32.2	0.006	0.00153	67.1	0.10255	57720	5919	976700
0.0045	3.05	99.29	46	0.151	0.055	32.2	0.008	0.00228	67.1	0.15312	52920	8103	1336971
0.0045	3.15	99.39	46	0.151	0.056	32.2	0.009	0.00313	67.1	0.21001	46920	9854	1625876
0.0044	3.26	99.50	46	0.151	0.057	32.2	0.010	0.00347	67.1	0.23288	40920	9529	1572362
0.0043	3.36	99.60	46	0.151	0.058	32.2	0.011	0.00392	67.1	0.26323	34920	9192	1516692
0.0042	3.45	99.69	46	0.151	0.058	32.2	0.011	0.00414	67.1	0.27806	32520	9043	1492032
0.0042	3.56	99.80	46	0.151	0.060	32.2	0.013	0.00520	67.1	0.34904	30120	10513	1734677
0.0041	3.66	99.90	46	0.151	0.060	32.2	0.013	0.00519	67.1	0.34816	25320	8816	1454559
0.0040	3.76	100.00	46	0.151	0.061	32.2	0.014	0.00565	67.1	0.37882	22920	8683	1432629
0.0040	3.86	100.10	46	0.151	0.063	32.2	0.016	0.00666	67.1	0.44663	21720	9701	1600648
0.0039	3.96	100.20	46	0.151	0.063	32.2	0.016	0.00681	67.1	0.45658	19320	8821	1455481
0.0039	4.05	100.29	46	0.151	0.064	32.2	0.017	0.00775	67.1	0.51974	16920	8794	1450998
0.0039	4.15	100.39	46	0.151	0.065	32.2	0.018	0.00833	67.1	0.55896	16920	9458	1560510
0.0039	4.26	100.50	46	0.151	0.066	32.2	0.019	0.00902	67.1	0.60482	15720	9508	1568788
0.0038	4.36	100.60	46	0.151	0.066	32.2	0.019	0.00921	67.1	0.61795	12120	7489	1235767
0.0037	4.46	100.70	46	0.151	0.067	32.2	0.020	0.00937	67.1	0.62834	12120	7616	1256558
0.0036	4.56	100.80	46	0.151	0.067	32.2	0.020	0.00948	67.1	0.63596	10920	6945	1145881
0.0035	4.66	100.90	46	0.151	0.066	32.2	0.019	0.00877	67.1	0.58865	8520	5015	827521
0.0034	4.76	101.00	46	0.151	0.065	32.2	0.018	0.00802	67.1	0.53774	8520	4582	755961
0.0034	4.86	101.10	46	0.151	0.066	32.2	0.019	0.00896	67.1	0.60099	6120	3678	606877
0.0033	4.96	101.20	46	0.151	0.065	32.2	0.018	0.00859	67.1	0.57607	4920	2834	467650
0.0032	5.06	101.30	46	0.151	0.066	32.2	0.019	0.00884	67.1	0.59286	3720	2205	363896
0.0032	5.16	101.40	46	0.151	0.066	32.2	0.019	0.00906	67.1	0.60800	120	73	12038
												sum =	28,426,160 lbs

Table 41: Bedload mass transport per unit of channel width (17.25 mm)

W.S. Elev.	Upstream Yo	Downstream WSEL	Stage	Discharge Q	Volumetric transport rate of sediment per unit stream width q_b	Specific weight of Sediment	Dry weight of sediment transported per unit width and time g_b	Gravitational acceleration g	Mass transport rate per unit of channel width	Mass transport rate per unit of channel width
(ft)	(ft)	(ft)	(ft)	(m^3/s)	(ft^2/s)	(lbs/ft^3)	(lbs/s/ft)	(ft/s^2)	($Slugs*s^{-1}*ft^{-1}$)	($kg*m^{-1}*s^{-1}$)
97.80	1.56	94.05	3.16	2.5	0.00000	165	0.00000	32.2	0.00000	0.00000
97.90	1.66	94.15	3.26	2.8	0.00000	165	0.00000	32.2	0.00000	0.00000
97.99	1.75	94.47	3.58	4.0	0.00000	165	0.00000	32.2	0.00000	0.00000
98.09	1.85	94.64	3.75	4.8	0.00000	165	0.00000	32.2	0.00000	0.00000
98.18	1.94	94.74	3.85	5.3	0.00000	165	0.00000	32.2	0.00000	0.00000
98.28	2.04	94.84	3.95	5.9	0.00000	165	0.00000	32.2	0.00000	0.00000
98.39	2.15	94.94	4.05	6.5	0.00000	165	0.00000	32.2	0.00000	0.00000
98.49	2.25	95.46	4.57	10.4	0.00000	165	0.00000	32.2	0.00000	0.00000
98.59	2.35	95.32	4.43	9.2	0.00000	165	0.00000	32.2	0.00000	0.00000
98.69	2.45	95.47	4.58	10.4	0.00000	165	0.00000	32.2	0.00000	0.00000
98.79	2.55	95.69	4.80	12.5	0.00000	165	0.00000	32.2	0.00000	0.00000
98.89	2.65	95.71	4.82	12.8	0.00041	165	0.06750	32.2	0.00210	0.10036
98.99	2.75	96.06	5.17	16.7	0.00003	165	0.00434	32.2	0.00013	0.00645
99.09	2.85	96.04	5.15	16.5	0.00088	165	0.14572	32.2	0.00453	0.21669
99.19	2.95	96.14	5.25	17.8	0.00153	165	0.25222	32.2	0.00783	0.37504
99.29	3.05	96.24	5.35	19.1	0.00228	165	0.37657	32.2	0.01169	0.55994
99.39	3.15	96.34	5.45	20.6	0.00313	165	0.51650	32.2	0.01604	0.76802
99.50	3.26	96.51	5.62	23.1	0.00347	165	0.57274	32.2	0.01779	0.85165
99.60	3.36	96.65	5.76	25.5	0.00392	165	0.64739	32.2	0.02011	0.96264
99.69	3.45	96.81	5.92	28.4	0.00414	165	0.68386	32.2	0.02124	1.01688
99.80	3.56	96.91	6.02	30.3	0.00520	165	0.85843	32.2	0.02666	1.27646
99.90	3.66	97.09	6.20	33.9	0.00519	165	0.85627	32.2	0.02659	1.27324
100.00	3.76	97.23	6.34	37.0	0.00565	165	0.93167	32.2	0.02893	1.38536
100.10	3.86	97.33	6.44	39.3	0.00666	165	1.09844	32.2	0.03411	1.63335
100.20	3.96	97.49	6.60	43.3	0.00681	165	1.12290	32.2	0.03487	1.66971
100.29	4.05	97.59	6.70	45.9	0.00775	165	1.27823	32.2	0.03970	1.90068
100.39	4.15	97.72	6.83	49.4	0.00833	165	1.37470	32.2	0.04269	2.04413
100.50	4.26	97.85	6.96	53.2	0.00902	165	1.48749	32.2	0.04620	2.21184
100.60	4.36	98.00	7.11	57.8	0.00921	165	1.51976	32.2	0.04720	2.25983
100.70	4.46	98.15	7.26	62.6	0.00937	165	1.54533	32.2	0.04799	2.29785
100.80	4.56	98.30	7.41	67.8	0.00948	165	1.56408	32.2	0.04857	2.32573
100.90	4.66	98.49	7.60	74.8	0.00877	165	1.44771	32.2	0.04496	2.15269
101.00	4.76	98.68	7.79	82.4	0.00802	165	1.32252	32.2	0.04107	1.96654
101.10	4.86	98.78	7.89	86.6	0.00896	165	1.47806	32.2	0.04590	2.19782
101.20	4.96	98.94	8.05	93.8	0.00859	165	1.41677	32.2	0.04400	2.10668
101.30	5.06	99.08	8.19	99.9	0.00884	165	1.45806	32.2	0.04528	2.16809
101.40	5.16	99.21	8.32	106.4	0.00906	165	1.49530	32.2	0.04644	2.22345

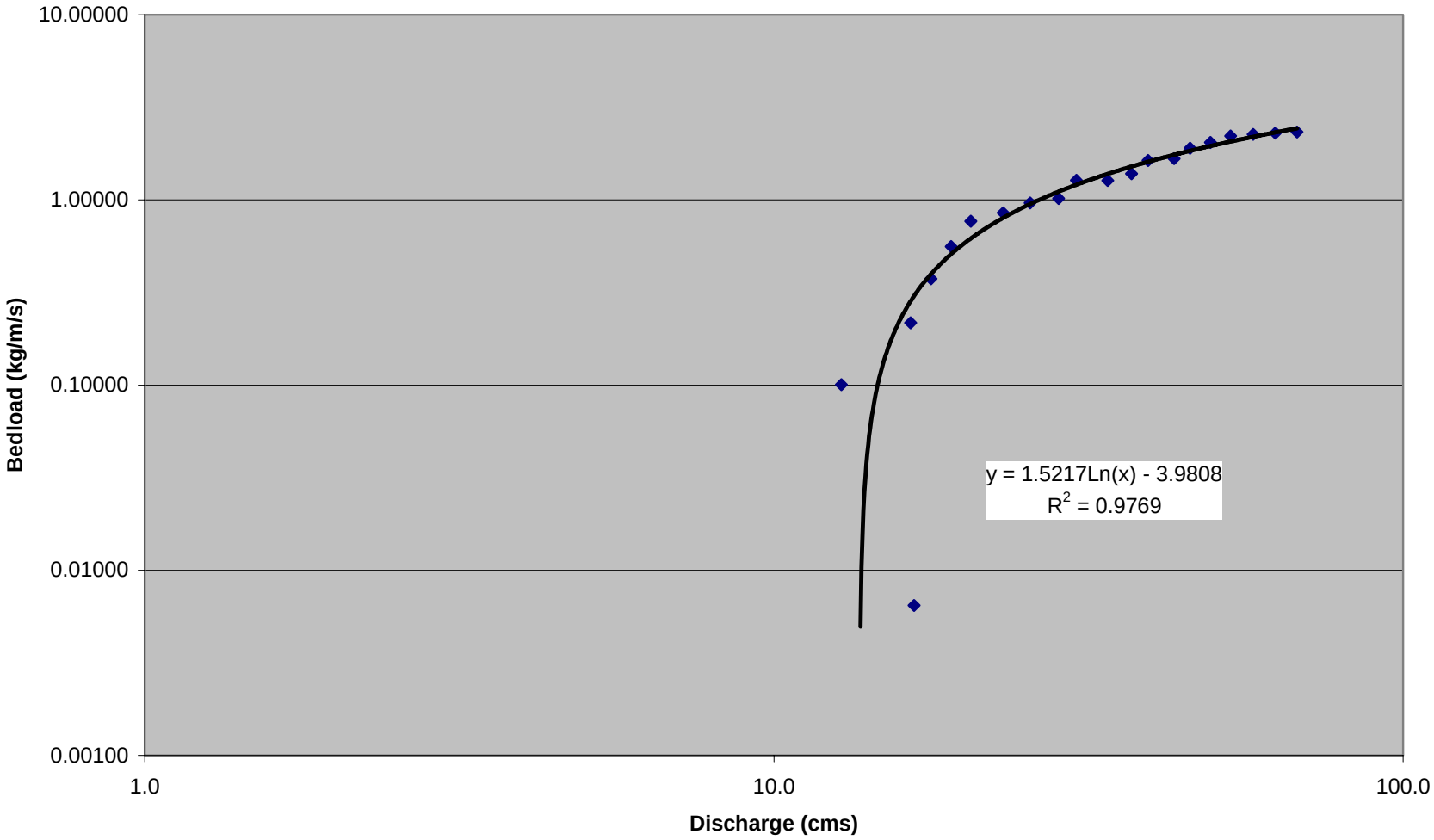

Figure 32: Bedload rating curve (17.25 mm)

Table 42: Bedload discharge per unit width (28.5 mm)

Energy slope (ft/ft)	Y_o (ft)	WSEL	d_s (mm)	d_s (ft)	Calculated Shields parameter	Gravity (ft/s^2)	Shields - Critical	Bedload discharge per unit width (ft^2/s)	Top width (ft)	Volumetric discharge (ft^3/s)	Duration at stage or greater stage (time, seconds)	Total volume transported (ft^3)	Total weight transported (lbs)
0.0055	1.56	97.80	53	0.174	0.030	32.2	-0.017	0.00000	67.1	0.00000	210120	0	0
0.0055	1.66	97.90	53	0.174	0.032	32.2	-0.015	0.00000	67.1	0.00000	199320	0	0
0.0051	1.75	97.99	53	0.174	0.031	32.2	-0.016	0.00000	67.1	0.00000	188520	0	0
0.0050	1.85	98.09	53	0.174	0.033	32.2	-0.014	0.00000	67.1	0.00000	182520	0	0
0.0050	1.94	98.18	53	0.174	0.034	32.2	-0.013	0.00000	67.1	0.00000	178920	0	0
0.0050	2.04	98.28	53	0.174	0.036	32.2	-0.011	0.00000	67.1	0.00000	176520	0	0
0.0050	2.15	98.39	53	0.174	0.038	32.2	-0.009	0.00000	67.1	0.00000	175320	0	0
0.0044	2.25	98.49	53	0.174	0.035	32.2	-0.012	0.00000	67.1	0.00000	164520	0	0
0.0048	2.35	98.59	53	0.174	0.039	32.2	-0.008	0.00000	67.1	0.00000	144120	0	0
0.0047	2.45	98.69	53	0.174	0.040	32.2	-0.007	0.00000	67.1	0.00000	123720	0	0
0.0045	2.55	98.79	53	0.174	0.040	32.2	-0.007	0.00000	67.1	0.00000	92520	0	0
0.0046	2.65	98.89	53	0.174	0.043	32.2	-0.004	0.00000	67.1	0.00000	70920	0	0
0.0043	2.75	98.99	53	0.174	0.041	32.2	-0.006	0.00000	67.1	0.00000	66120	0	0
0.0045	2.85	99.09	53	0.174	0.044	32.2	-0.003	0.00000	67.1	0.00000	64920	0	0
0.0045	2.95	99.19	53	0.174	0.046	32.2	-0.001	0.00000	67.1	0.00000	57720	0	0
0.0045	3.05	99.29	53	0.174	0.047	32.2	0.000	0.00004	67.1	0.00247	52920	131	21581
0.0045	3.15	99.39	53	0.174	0.049	32.2	0.002	0.00037	67.1	0.02495	46920	1171	193177
0.0044	3.26	99.50	53	0.174	0.050	32.2	0.003	0.00055	67.1	0.03678	40920	1505	248323
0.0043	3.36	99.60	53	0.174	0.050	32.2	0.003	0.00080	67.1	0.05397	34920	1885	310944
0.0042	3.45	99.69	53	0.174	0.051	32.2	0.004	0.00094	67.1	0.06286	32520	2044	337290
0.0042	3.56	99.80	53	0.174	0.052	32.2	0.005	0.00162	67.1	0.10873	30120	3275	540390
0.0041	3.66	99.90	53	0.174	0.052	32.2	0.005	0.00161	67.1	0.10814	25320	2738	451781
0.0040	3.76	100.00	53	0.174	0.053	32.2	0.006	0.00193	67.1	0.12924	22920	2962	488761
0.0040	3.86	100.10	53	0.174	0.054	32.2	0.007	0.00265	67.1	0.17795	21720	3865	637737
0.0039	3.96	100.20	53	0.174	0.055	32.2	0.008	0.00276	67.1	0.18529	19320	3580	590667
0.0039	4.05	100.29	53	0.174	0.056	32.2	0.009	0.00347	67.1	0.23287	16920	3940	650115
0.0039	4.15	100.39	53	0.174	0.057	32.2	0.010	0.00392	67.1	0.26314	16920	4452	734626
0.0039	4.26	100.50	53	0.174	0.057	32.2	0.010	0.00446	67.1	0.29912	15720	4702	775846
0.0038	4.36	100.60	53	0.174	0.058	32.2	0.011	0.00461	67.1	0.30952	12120	3751	618969
0.0037	4.46	100.70	53	0.174	0.058	32.2	0.011	0.00474	67.1	0.31779	12120	3852	635507
0.0036	4.56	100.80	53	0.174	0.058	32.2	0.011	0.00483	67.1	0.32387	10920	3537	583541
0.0035	4.66	100.90	53	0.174	0.057	32.2	0.010	0.00427	67.1	0.28636	8520	2440	402564
0.0034	4.76	101.00	53	0.174	0.056	32.2	0.009	0.00368	67.1	0.24670	8520	2102	346813
0.0034	4.86	101.10	53	0.174	0.057	32.2	0.010	0.00441	67.1	0.29608	6120	1812	298986
0.0033	4.96	101.20	53	0.174	0.057	32.2	0.010	0.00412	67.1	0.27649	4920	1360	224451
0.0032	5.06	101.30	53	0.174	0.057	32.2	0.010	0.00432	67.1	0.28967	3720	1078	177801
0.0032	5.16	101.40	53	0.174	0.057	32.2	0.010	0.00450	67.1	0.30163	120	36	5972
												sum =	9,275,842 lbs

Table 43: Mass transport per unit of channel width (28.5 mm)

W.S. Elev.	Upstream Yo	Downstream WSEL	Stage	Discharge Q	Volumetric transport rate of sediment per unit stream width q_b	Specific weight of Sediment	Dry weight of sediment transported per unit width and time g_b	Gravitational acceleration g	Mass transport rate per unit of channel width	Mass transport rate per unit of channel width
(ft)	(ft)	(ft)	(ft)	(m^3/s)	(ft^2/s)	(lbs/ft^3)	(lbs/s/ft)	(ft/s^2)	($Slugs*s^{-1}*ft^{-1}$)	($kg*m^{-1}*s^{-1}$)
97.80	1.56	94.05	3.16	2.5	0.00000	165	0.00000	32.2	0.00000	0.00000
97.90	1.66	94.15	3.26	2.8	0.00000	165	0.00000	32.2	0.00000	0.00000
97.99	1.75	94.47	3.58	4.0	0.00000	165	0.00000	32.2	0.00000	0.00000
98.09	1.85	94.64	3.75	4.8	0.00000	165	0.00000	32.2	0.00000	0.00000
98.18	1.94	94.74	3.85	5.3	0.00000	165	0.00000	32.2	0.00000	0.00000
98.28	2.04	94.84	3.95	5.9	0.00000	165	0.00000	32.2	0.00000	0.00000
98.39	2.15	94.94	4.05	6.5	0.00000	165	0.00000	32.2	0.00000	0.00000
98.49	2.25	95.46	4.57	10.4	0.00000	165	0.00000	32.2	0.00000	0.00000
98.59	2.35	95.32	4.43	9.2	0.00000	165	0.00000	32.2	0.00000	0.00000
98.69	2.45	95.47	4.58	10.4	0.00000	165	0.00000	32.2	0.00000	0.00000
98.79	2.55	95.69	4.80	12.5	0.00000	165	0.00000	32.2	0.00000	0.00000
98.89	2.65	95.71	4.82	12.8	0.00000	165	0.00000	32.2	0.00000	0.00000
98.99	2.75	96.06	5.17	16.7	0.00000	165	0.00000	32.2	0.00000	0.00000
99.09	2.85	96.04	5.15	16.5	0.00000	165	0.00000	32.2	0.00000	0.00000
99.19	2.95	96.14	5.25	17.8	0.00000	165	0.00000	32.2	0.00000	0.00000
99.29	3.05	96.24	5.35	19.1	0.00004	165	0.00608	32.2	0.00019	0.00904
99.39	3.15	96.34	5.45	20.6	0.00037	165	0.06137	32.2	0.00191	0.09125
99.50	3.26	96.51	5.62	23.1	0.00055	165	0.09045	32.2	0.00281	0.13450
99.60	3.36	96.65	5.76	25.5	0.00080	165	0.13272	32.2	0.00412	0.19736
99.69	3.45	96.81	5.92	28.4	0.00094	165	0.15459	32.2	0.00480	0.22988
99.80	3.56	96.91	6.02	30.3	0.00162	165	0.26742	32.2	0.00830	0.39764
99.90	3.66	97.09	6.20	33.9	0.00161	165	0.26595	32.2	0.00826	0.39546
100.00	3.76	97.23	6.34	37.0	0.00193	165	0.31785	32.2	0.00987	0.47263
100.10	3.86	97.33	6.44	39.3	0.00265	165	0.43765	32.2	0.01359	0.65076
100.20	3.96	97.49	6.60	43.3	0.00276	165	0.45570	32.2	0.01415	0.67761
100.29	4.05	97.59	6.70	45.9	0.00347	165	0.57271	32.2	0.01779	0.85159
100.39	4.15	97.72	6.83	49.4	0.00392	165	0.64715	32.2	0.02010	0.96229
100.50	4.26	97.85	6.96	53.2	0.00446	165	0.73564	32.2	0.02285	1.09387
100.60	4.36	98.00	7.11	57.8	0.00461	165	0.76122	32.2	0.02364	1.13190
100.70	4.46	98.15	7.26	62.6	0.00474	165	0.78156	32.2	0.02427	1.16214
100.80	4.56	98.30	7.41	67.8	0.00483	165	0.79651	32.2	0.02474	1.18438
100.90	4.66	98.49	7.60	74.8	0.00427	165	0.70427	32.2	0.02187	1.04722
101.00	4.76	98.68	7.79	82.4	0.00368	165	0.60673	32.2	0.01884	0.90219
101.10	4.86	98.78	7.89	86.6	0.00441	165	0.72819	32.2	0.02261	1.08278
101.20	4.96	98.94	8.05	93.8	0.00412	165	0.67999	32.2	0.02112	1.01111
101.30	5.06	99.08	8.19	99.9	0.00432	165	0.71242	32.2	0.02212	1.05934
101.40	5.16	99.21	8.32	106.4	0.00450	165	0.74182	32.2	0.02304	1.10305

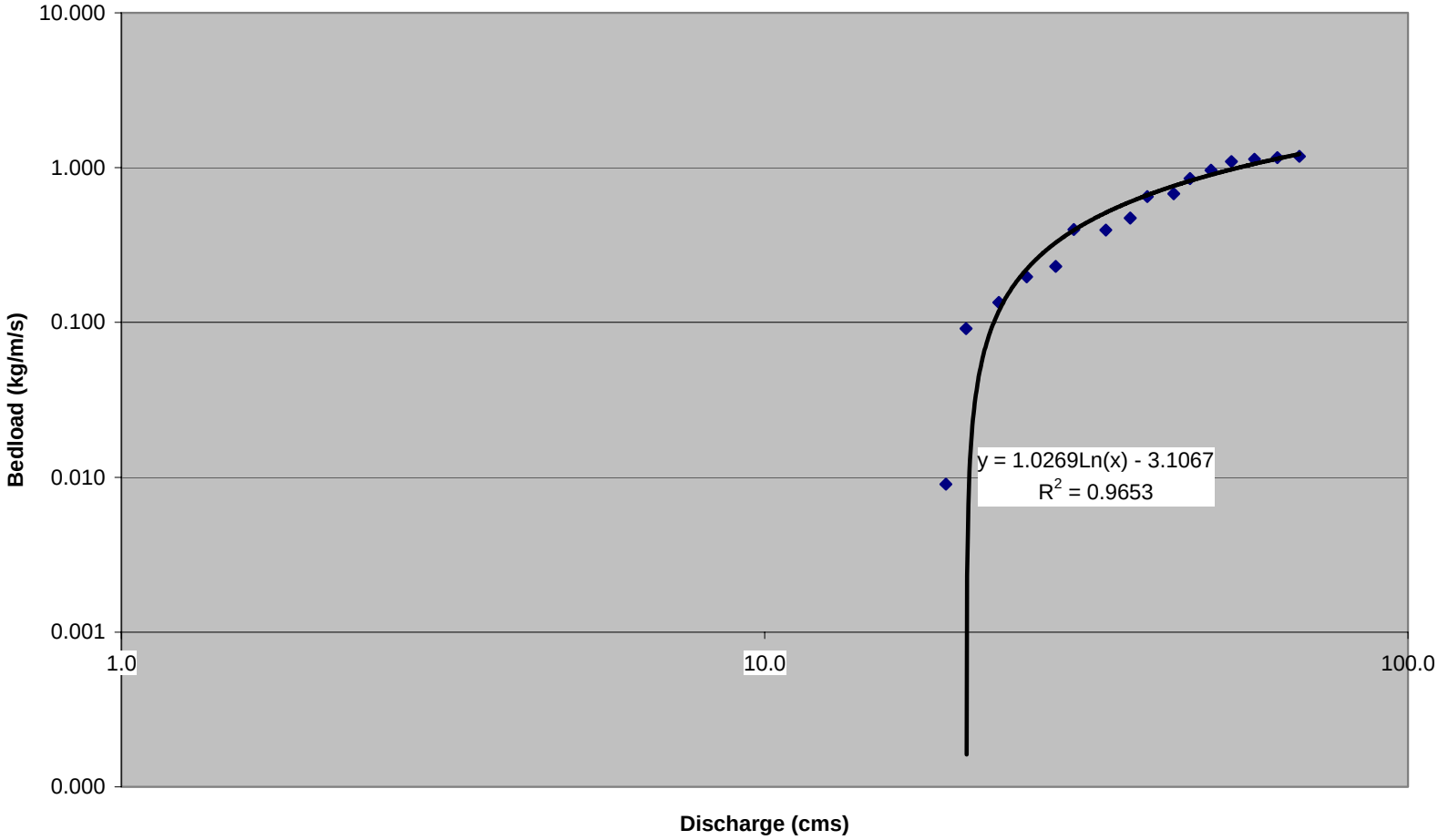

Figure 33: Bedload rating curve (28.5 mm)

Table 44: Bedload discharge per unit width (41.5 mm)

Energy slope (ft/ft)	Y_o (ft)	WSEL	d_s (mm)	d_s (ft)	Calculated Shields parameter	Gravity (ft/s^2)	Shields - Critical	Bedload discharge per unit width (ft^2/s)	Top width (ft)	Volumetric discharge (ft^3/s)	Duration at stage or greater stage (time, seconds)	Total volume transported (ft^3)	Total weight transported (lbs)
0.0055	1.56	97.80	59	0.194	0.027	32.2	-0.020	0.00000	67.1	0.00000	210120	0	0
0.0055	1.66	97.90	59	0.194	0.028	32.2	-0.019	0.00000	67.1	0.00000	199320	0	0
0.0051	1.75	97.99	59	0.194	0.028	32.2	-0.019	0.00000	67.1	0.00000	188520	0	0
0.0050	1.85	98.09	59	0.194	0.029	32.2	-0.018	0.00000	67.1	0.00000	182520	0	0
0.0050	1.94	98.18	59	0.194	0.031	32.2	-0.016	0.00000	67.1	0.00000	178920	0	0
0.0050	2.04	98.28	59	0.194	0.032	32.2	-0.015	0.00000	67.1	0.00000	176520	0	0
0.0050	2.15	98.39	59	0.194	0.034	32.2	-0.013	0.00000	67.1	0.00000	175320	0	0
0.0044	2.25	98.49	59	0.194	0.031	32.2	-0.016	0.00000	67.1	0.00000	164520	0	0
0.0048	2.35	98.59	59	0.194	0.035	32.2	-0.012	0.00000	67.1	0.00000	144120	0	0
0.0047	2.45	98.69	59	0.194	0.036	32.2	-0.011	0.00000	67.1	0.00000	123720	0	0
0.0045	2.55	98.79	59	0.194	0.036	32.2	-0.011	0.00000	67.1	0.00000	92520	0	0
0.0046	2.65	98.89	59	0.194	0.039	32.2	-0.008	0.00000	67.1	0.00000	70920	0	0
0.0043	2.75	98.99	59	0.194	0.037	32.2	-0.010	0.00000	67.1	0.00000	66120	0	0
0.0045	2.85	99.09	59	0.194	0.040	32.2	-0.007	0.00000	67.1	0.00000	64920	0	0
0.0045	2.95	99.19	59	0.194	0.041	32.2	-0.006	0.00000	67.1	0.00000	57720	0	0
0.0045	3.05	99.29	59	0.194	0.043	32.2	-0.004	0.00000	67.1	0.00000	52920	0	0
0.0045	3.15	99.39	59	0.194	0.044	32.2	-0.003	0.00000	67.1	0.00000	46920	0	0
0.0044	3.26	99.50	59	0.194	0.045	32.2	-0.002	0.00000	67.1	0.00000	40920	0	0
0.0043	3.36	99.60	59	0.194	0.045	32.2	-0.002	0.00000	67.1	0.00000	34920	0	0
0.0042	3.45	99.69	59	0.194	0.046	32.2	-0.001	0.00000	67.1	0.00000	32520	0	0
0.0042	3.56	99.80	59	0.194	0.047	32.2	0.000	0.00000	67.1	0.00000	30120	0	0
0.0041	3.66	99.90	59	0.194	0.047	32.2	0.000	0.00000	67.1	0.00000	25320	0	0
0.0040	3.76	100.00	59	0.194	0.048	32.2	0.001	0.00006	67.1	0.00419	22920	96	15829
0.0040	3.86	100.10	59	0.194	0.049	32.2	0.002	0.00038	67.1	0.02554	21720	555	91524
0.0039	3.96	100.20	59	0.194	0.049	32.2	0.002	0.00044	67.1	0.02945	19320	569	93877
0.0039	4.05	100.29	59	0.194	0.050	32.2	0.003	0.00086	67.1	0.05743	16920	972	160333
0.0039	4.15	100.39	59	0.194	0.051	32.2	0.004	0.00115	67.1	0.07699	16920	1303	214952
0.0039	4.26	100.50	59	0.194	0.052	32.2	0.005	0.00151	67.1	0.10151	15720	1596	263299
0.0038	4.36	100.60	59	0.194	0.052	32.2	0.005	0.00162	67.1	0.10881	12120	1319	217595
0.0037	4.46	100.70	59	0.194	0.052	32.2	0.005	0.00171	67.1	0.11467	12120	1390	229319
0.0036	4.56	100.80	59	0.194	0.052	32.2	0.005	0.00177	67.1	0.11901	10920	1300	214438
0.0035	4.66	100.90	59	0.194	0.051	32.2	0.004	0.00138	67.1	0.09268	8520	790	130293
0.0034	4.76	101.00	59	0.194	0.050	32.2	0.003	0.00099	67.1	0.06623	8520	564	93111
0.0034	4.86	101.10	59	0.194	0.051	32.2	0.004	0.00148	67.1	0.09940	6120	608	100375
0.0033	4.96	101.20	59	0.194	0.051	32.2	0.004	0.00128	67.1	0.08595	4920	423	69773
0.0032	5.06	101.30	59	0.194	0.051	32.2	0.004	0.00142	67.1	0.09496	3720	353	58288
0.0032	5.16	101.40	59	0.194	0.052	32.2	0.005	0.00154	67.1	0.10327	120	12	2045
												sum =	1,955,048 lbs

Table 45: Mass transport per unit of channel width (41.5 mm)

W.S. Elev.	Upstream Yo	Downstream WSEL	Stage	Discharge Q	Volumetric transport rate of sediment per unit stream width q_b	Specific weight of Sediment	Dry weight of sediment transported per unit width and time g_b	Gravitational acceleration g	Mass transport rate per unit of channel width	Mass transport rate per unit of channel width
(ft)	(ft)	(ft)	(ft)	(m^3/s)	(ft^2/s)	(lbs/ft^3)	(lbs/s/ft)	(ft/s^2)	($Slugs*s^{-1}*ft^{-1}$)	($kg*m^{-1}*s^{-1}$)
97.80	1.56	94.05	3.16	2.5	0.00000	165	0.00000	32.2	0.00000	0.00000
97.90	1.66	94.15	3.26	2.8	0.00000	165	0.00000	32.2	0.00000	0.00000
97.99	1.75	94.47	3.58	4.0	0.00000	165	0.00000	32.2	0.00000	0.00000
98.09	1.85	94.64	3.75	4.8	0.00000	165	0.00000	32.2	0.00000	0.00000
98.18	1.94	94.74	3.85	5.3	0.00000	165	0.00000	32.2	0.00000	0.00000
98.28	2.04	94.84	3.95	5.9	0.00000	165	0.00000	32.2	0.00000	0.00000
98.39	2.15	94.94	4.05	6.5	0.00000	165	0.00000	32.2	0.00000	0.00000
98.49	2.25	95.46	4.57	10.4	0.00000	165	0.00000	32.2	0.00000	0.00000
98.59	2.35	95.32	4.43	9.2	0.00000	165	0.00000	32.2	0.00000	0.00000
98.69	2.45	95.47	4.58	10.4	0.00000	165	0.00000	32.2	0.00000	0.00000
98.79	2.55	95.69	4.80	12.5	0.00000	165	0.00000	32.2	0.00000	0.00000
98.89	2.65	95.71	4.82	12.8	0.00000	165	0.00000	32.2	0.00000	0.00000
98.99	2.75	96.06	5.17	16.7	0.00000	165	0.00000	32.2	0.00000	0.00000
99.09	2.85	96.04	5.15	16.5	0.00000	165	0.00000	32.2	0.00000	0.00000
99.19	2.95	96.14	5.25	17.8	0.00000	165	0.00000	32.2	0.00000	0.00000
99.29	3.05	96.24	5.35	19.1	0.00000	165	0.00000	32.2	0.00000	0.00000
99.39	3.15	96.34	5.45	20.6	0.00000	165	0.00000	32.2	0.00000	0.00000
99.50	3.26	96.51	5.62	23.1	0.00000	165	0.00000	32.2	0.00000	0.00000
99.60	3.36	96.65	5.76	25.5	0.00000	165	0.00000	32.2	0.00000	0.00000
99.69	3.45	96.81	5.92	28.4	0.00000	165	0.00000	32.2	0.00000	0.00000
99.80	3.56	96.91	6.02	30.3	0.00000	165	0.00000	32.2	0.00000	0.00000
99.90	3.66	97.09	6.20	33.9	0.00000	165	0.00000	32.2	0.00000	0.00000
100.00	3.76	97.23	6.34	37.0	0.00006	165	0.01029	32.2	0.00032	0.01531
100.10	3.86	97.33	6.44	39.3	0.00038	165	0.06281	32.2	0.00195	0.09339
100.20	3.96	97.49	6.60	43.3	0.00044	165	0.07243	32.2	0.00225	0.10769
100.29	4.05	97.59	6.70	45.9	0.00086	165	0.14124	32.2	0.00439	0.21002
100.39	4.15	97.72	6.83	49.4	0.00115	165	0.18936	32.2	0.00588	0.28157
100.50	4.26	97.85	6.96	53.2	0.00151	165	0.24965	32.2	0.00775	0.37123
100.60	4.36	98.00	7.11	57.8	0.00162	165	0.26760	32.2	0.00831	0.39791
100.70	4.46	98.15	7.26	62.6	0.00171	165	0.28202	32.2	0.00876	0.41935
100.80	4.56	98.30	7.41	67.8	0.00177	165	0.29270	32.2	0.00909	0.43523
100.90	4.66	98.49	7.60	74.8	0.00138	165	0.22794	32.2	0.00708	0.33894
101.00	4.76	98.68	7.79	82.4	0.00099	165	0.16289	32.2	0.00506	0.24222
101.10	4.86	98.78	7.89	86.6	0.00148	165	0.24446	32.2	0.00759	0.36351
101.20	4.96	98.94	8.05	93.8	0.00128	165	0.21138	32.2	0.00656	0.31431
101.30	5.06	99.08	8.19	99.9	0.00142	165	0.23355	32.2	0.00725	0.34728
101.40	5.16	99.21	8.32	106.4	0.00154	165	0.25397	32.2	0.00789	0.37764

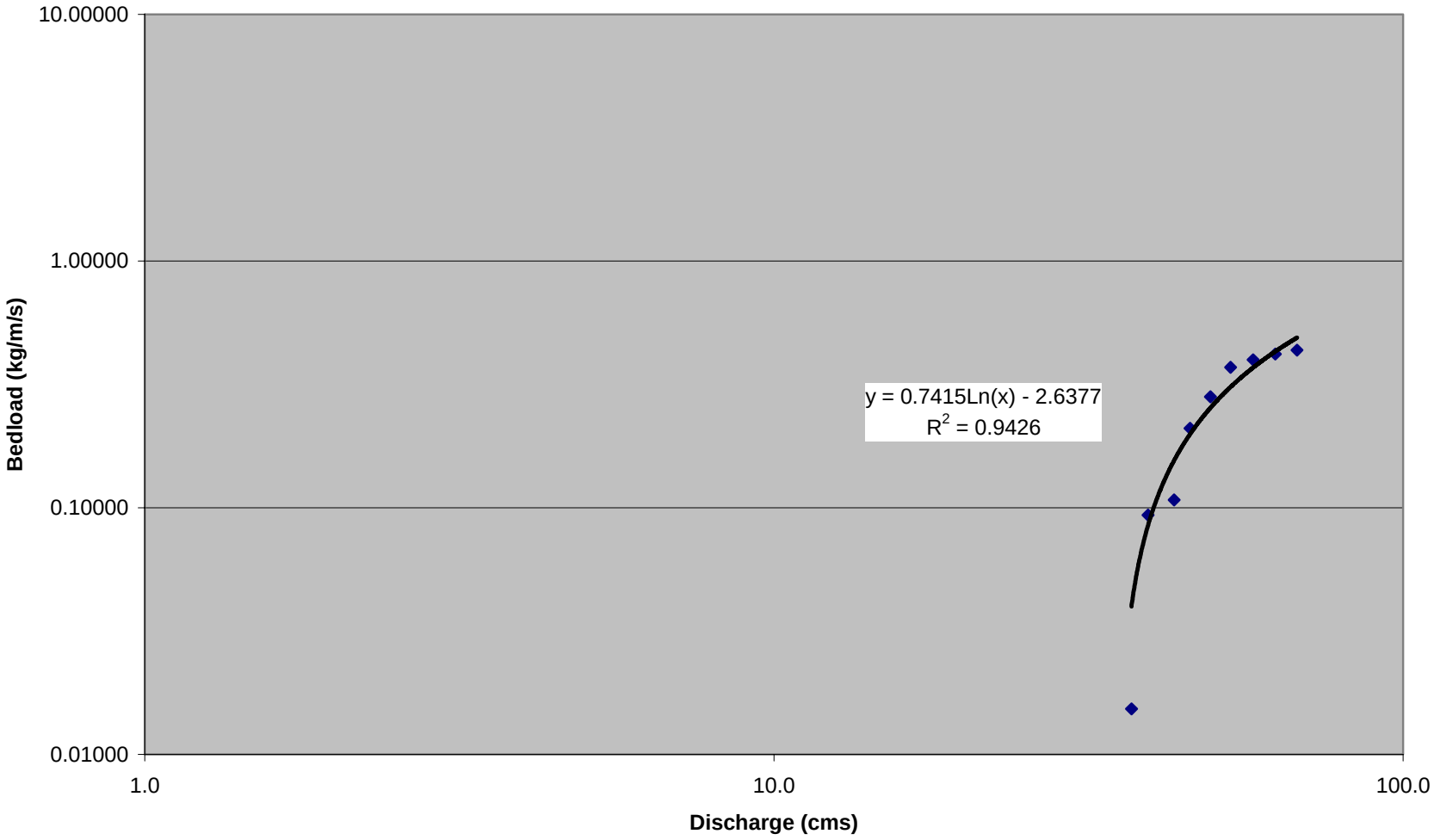

Figure 34: Bedload rating curve (41.5 mm)

Table 46: Bedload discharge per unit width (54 mm)

Energy slope (ft/ft)	Y_o (ft)	WSEL	d_s (mm)	d_s (ft)	Calculated Shields parameter	Gravity (ft/s^2)	Shields - Critical	Bedload discharge per unit width (ft^2/s)	Top width (ft)	Volumetric discharge (ft^3/s)	Duration at stage or greater stage (time, seconds)	Total volume transported (ft^3)	Total weight transported (lbs)
0.0055	1.56	97.80	64	0.210	0.025	32.2	-0.022	0.00000	67.1	0.00000	210120	0	0
0.0055	1.66	97.90	64	0.210	0.026	32.2	-0.021	0.00000	67.1	0.00000	199320	0	0
0.0051	1.75	97.99	64	0.210	0.026	32.2	-0.021	0.00000	67.1	0.00000	188520	0	0
0.0050	1.85	98.09	64	0.210	0.027	32.2	-0.020	0.00000	67.1	0.00000	182520	0	0
0.0050	1.94	98.18	64	0.210	0.028	32.2	-0.019	0.00000	67.1	0.00000	178920	0	0
0.0050	2.04	98.28	64	0.210	0.030	32.2	-0.017	0.00000	67.1	0.00000	176520	0	0
0.0050	2.15	98.39	64	0.210	0.031	32.2	-0.016	0.00000	67.1	0.00000	175320	0	0
0.0044	2.25	98.49	64	0.210	0.029	32.2	-0.018	0.00000	67.1	0.00000	164520	0	0
0.0048	2.35	98.59	64	0.210	0.032	32.2	-0.015	0.00000	67.1	0.00000	144120	0	0
0.0047	2.45	98.69	64	0.210	0.033	32.2	-0.014	0.00000	67.1	0.00000	123720	0	0
0.0045	2.55	98.79	64	0.210	0.033	32.2	-0.014	0.00000	67.1	0.00000	92520	0	0
0.0046	2.65	98.89	64	0.210	0.036	32.2	-0.011	0.00000	67.1	0.00000	70920	0	0
0.0043	2.75	98.99	64	0.210	0.034	32.2	-0.013	0.00000	67.1	0.00000	66120	0	0
0.0045	2.85	99.09	64	0.210	0.037	32.2	-0.010	0.00000	67.1	0.00000	64920	0	0
0.0045	2.95	99.19	64	0.210	0.038	32.2	-0.009	0.00000	67.1	0.00000	57720	0	0
0.0045	3.05	99.29	64	0.210	0.039	32.2	-0.008	0.00000	67.1	0.00000	52920	0	0
0.0045	3.15	99.39	64	0.210	0.041	32.2	-0.006	0.00000	67.1	0.00000	46920	0	0
0.0044	3.26	99.50	64	0.210	0.041	32.2	-0.006	0.00000	67.1	0.00000	40920	0	0
0.0043	3.36	99.60	64	0.210	0.042	32.2	-0.005	0.00000	67.1	0.00000	34920	0	0
0.0042	3.45	99.69	64	0.210	0.042	32.2	-0.005	0.00000	67.1	0.00000	32520	0	0
0.0042	3.56	99.80	64	0.210	0.043	32.2	-0.004	0.00000	67.1	0.00000	30120	0	0
0.0041	3.66	99.90	64	0.210	0.043	32.2	-0.004	0.00000	67.1	0.00000	25320	0	0
0.0040	3.76	100.00	64	0.210	0.044	32.2	-0.003	0.00000	67.1	0.00000	22920	0	0
0.0040	3.86	100.10	64	0.210	0.045	32.2	-0.002	0.00000	67.1	0.00000	21720	0	0
0.0039	3.96	100.20	64	0.210	0.045	32.2	-0.002	0.00000	67.1	0.00000	19320	0	0
0.0039	4.05	100.29	64	0.210	0.046	32.2	-0.001	0.00000	67.1	0.00000	16920	0	0
0.0039	4.15	100.39	64	0.210	0.047	32.2	0.000	0.00000	67.1	0.00000	16920	0	0
0.0039	4.26	100.50	64	0.210	0.048	32.2	0.001	0.00006	67.1	0.00425	15720	67	334
0.0038	4.36	100.60	64	0.210	0.048	32.2	0.001	0.00010	67.1	0.00698	12120	85	423
0.0037	4.46	100.70	64	0.210	0.048	32.2	0.001	0.00014	67.1	0.00944	12120	114	572
0.0036	4.56	100.80	64	0.210	0.048	32.2	0.001	0.00017	67.1	0.01137	10920	124	621
0.0035	4.66	100.90	64	0.210	0.047	32.2	0.000	0.00002	67.1	0.00156	8520	13	66
0.0034	4.76	101.00	64	0.210	0.046	32.2	-0.001	0.00000	67.1	0.00000	8520	0	0
0.0034	4.86	101.10	64	0.210	0.047	32.2	0.000	0.00005	67.1	0.00354	6120	22	108
0.0033	4.96	101.20	64	0.210	0.047	32.2	0.000	0.00000	67.1	0.00020	4920	1	5
0.0032	5.06	101.30	64	0.210	0.047	32.2	0.000	0.00003	67.1	0.00217	3720	8	40
0.0032	5.16	101.40	64	0.210	0.048	32.2	0.001	0.00007	67.1	0.00487	120	1	3
												sum =	2,173 lbs

Table 47: Mass transport per unit of channel width (54 mm)

W.S. Elev.	Upstream Yo	Downstream WSEL	Stage	Discharge Q	Volumetric transport rate of sediment per unit stream width q_b	Specific weight of Sediment	Dry weight of sediment transported per unit width and time g_b	Gravitational acceleration g	Mass transport rate per unit of channel width	Mass transport rate per unit of channel width
(ft)	(ft)	(ft)	(ft)	(m^3/s)	(ft^2/s)	(lbs/ft^3)	(lbs/s/ft)	(ft/s^2)	($Slugs*s^{-1}*ft^{-1}$)	($kg*m^{-1}*s^{-1}$)
97.80	1.56	94.05	3.16	2.5	0.00000	165	0.00000	32.2	0.00000	0.00000
97.90	1.66	94.15	3.26	2.8	0.00000	165	0.00000	32.2	0.00000	0.00000
97.99	1.75	94.47	3.58	4.0	0.00000	165	0.00000	32.2	0.00000	0.00000
98.09	1.85	94.64	3.75	4.8	0.00000	165	0.00000	32.2	0.00000	0.00000
98.18	1.94	94.74	3.85	5.3	0.00000	165	0.00000	32.2	0.00000	0.00000
98.28	2.04	94.84	3.95	5.9	0.00000	165	0.00000	32.2	0.00000	0.00000
98.39	2.15	94.94	4.05	6.5	0.00000	165	0.00000	32.2	0.00000	0.00000
98.49	2.25	95.46	4.57	10.4	0.00000	165	0.00000	32.2	0.00000	0.00000
98.59	2.35	95.32	4.43	9.2	0.00000	165	0.00000	32.2	0.00000	0.00000
98.69	2.45	95.47	4.58	10.4	0.00000	165	0.00000	32.2	0.00000	0.00000
98.79	2.55	95.69	4.80	12.5	0.00000	165	0.00000	32.2	0.00000	0.00000
98.89	2.65	95.71	4.82	12.8	0.00000	165	0.00000	32.2	0.00000	0.00000
98.99	2.75	96.06	5.17	16.7	0.00000	165	0.00000	32.2	0.00000	0.00000
99.09	2.85	96.04	5.15	16.5	0.00000	165	0.00000	32.2	0.00000	0.00000
99.19	2.95	96.14	5.25	17.8	0.00000	165	0.00000	32.2	0.00000	0.00000
99.29	3.05	96.24	5.35	19.1	0.00000	165	0.00000	32.2	0.00000	0.00000
99.39	3.15	96.34	5.45	20.6	0.00000	165	0.00000	32.2	0.00000	0.00000
99.50	3.26	96.51	5.62	23.1	0.00000	165	0.00000	32.2	0.00000	0.00000
99.60	3.36	96.65	5.76	25.5	0.00000	165	0.00000	32.2	0.00000	0.00000
99.69	3.45	96.81	5.92	28.4	0.00000	165	0.00000	32.2	0.00000	0.00000
99.80	3.56	96.91	6.02	30.3	0.00000	165	0.00000	32.2	0.00000	0.00000
99.90	3.66	97.09	6.20	33.9	0.00000	165	0.00000	32.2	0.00000	0.00000
100.00	3.76	97.23	6.34	37.0	0.00000	165	0.00000	32.2	0.00000	0.00000
100.10	3.86	97.33	6.44	39.3	0.00000	165	0.00000	32.2	0.00000	0.00000
100.20	3.96	97.49	6.60	43.3	0.00000	165	0.00000	32.2	0.00000	0.00000
100.29	4.05	97.59	6.70	45.9	0.00000	165	0.00000	32.2	0.00000	0.00000
100.39	4.15	97.72	6.83	49.4	0.00000	165	0.00000	32.2	0.00000	0.00000
100.50	4.26	97.85	6.96	53.2	0.00006	165	0.01045	32.2	0.00032	0.01554
100.60	4.36	98.00	7.11	57.8	0.00010	165	0.01718	32.2	0.00053	0.02554
100.70	4.46	98.15	7.26	62.6	0.00014	165	0.02321	32.2	0.00072	0.03451
100.80	4.56	98.30	7.41	67.8	0.00017	165	0.02797	32.2	0.00087	0.04160
100.90	4.66	98.49	7.60	74.8	0.00002	165	0.00383	32.2	0.00012	0.00569
101.00	4.76	98.68	7.79	82.4	0.00000	165	0.00000	32.2	0.00000	0.00000
101.10	4.86	98.78	7.89	86.6	0.00005	165	0.00869	32.2	0.00027	0.01293
101.20	4.96	98.94	8.05	93.8	0.00000	165	0.00048	32.2	0.00002	0.00072
101.30	5.06	99.08	8.19	99.9	0.00003	165	0.00534	32.2	0.00017	0.00794
101.40	5.16	99.21	8.32	106.4	0.00007	165	0.01198	32.2	0.00037	0.01781

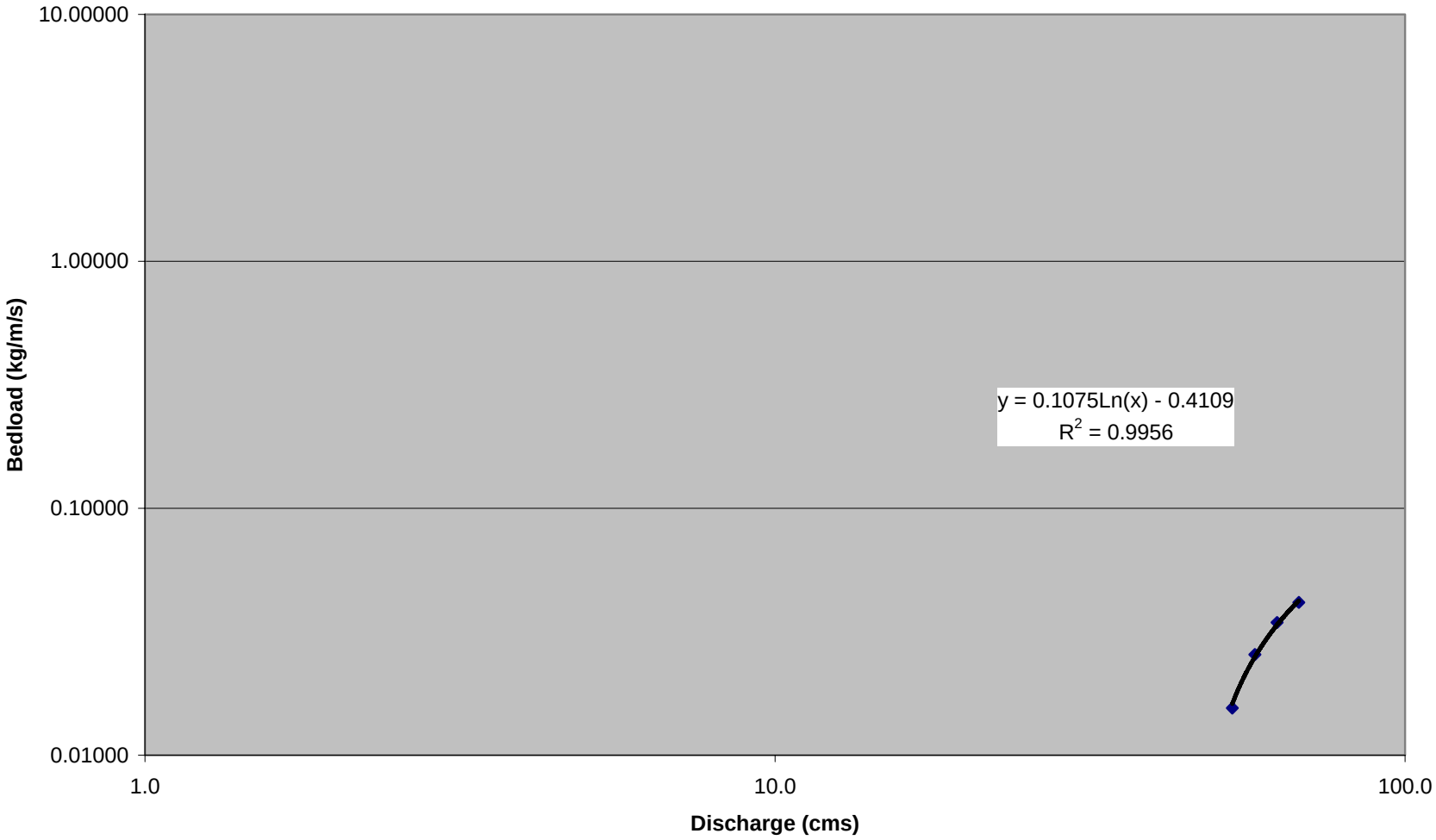

Figure 35: Bedload rating curve (54 mm)

Table 48: Bedload discharge per unit width (67.5 mm)

Energy slope (ft/ft)	Y_o (ft)	WSEL	d_s (mm)	d_s (ft)	Calculated Shields parameter	Gravity (ft/s^2)	Shields - Critical	Bedload discharge per unit width (ft^2/s)	Top width (ft)	Volumetric discharge (ft^3/s)	Duration at stage or greater stage (time, seconds)	Total volume transported (ft^3)	Total weight transported (lbs)
0.0055	1.56	97.80	69	0.226	0.023	32.2	-0.024	0.00000	67.1	0.00000	210120	0	0
0.0055	1.66	97.90	69	0.226	0.024	32.2	-0.023	0.00000	67.1	0.00000	199320	0	0
0.0051	1.75	97.99	69	0.226	0.024	32.2	-0.023	0.00000	67.1	0.00000	188520	0	0
0.0050	1.85	98.09	69	0.226	0.025	32.2	-0.022	0.00000	67.1	0.00000	182520	0	0
0.0050	1.94	98.18	69	0.226	0.026	32.2	-0.021	0.00000	67.1	0.00000	178920	0	0
0.0050	2.04	98.28	69	0.226	0.028	32.2	-0.019	0.00000	67.1	0.00000	176520	0	0
0.0050	2.15	98.39	69	0.226	0.029	32.2	-0.018	0.00000	67.1	0.00000	175320	0	0
0.0044	2.25	98.49	69	0.226	0.027	32.2	-0.020	0.00000	67.1	0.00000	164520	0	0
0.0048	2.35	98.59	69	0.226	0.030	32.2	-0.017	0.00000	67.1	0.00000	144120	0	0
0.0047	2.45	98.69	69	0.226	0.031	32.2	-0.016	0.00000	67.1	0.00000	123720	0	0
0.0045	2.55	98.79	69	0.226	0.031	32.2	-0.016	0.00000	67.1	0.00000	92520	0	0
0.0046	2.65	98.89	69	0.226	0.033	32.2	-0.014	0.00000	67.1	0.00000	70920	0	0
0.0043	2.75	98.99	69	0.226	0.032	32.2	-0.015	0.00000	67.1	0.00000	66120	0	0
0.0045	2.85	99.09	69	0.226	0.034	32.2	-0.013	0.00000	67.1	0.00000	64920	0	0
0.0045	2.95	99.19	69	0.226	0.035	32.2	-0.012	0.00000	67.1	0.00000	57720	0	0
0.0045	3.05	99.29	69	0.226	0.036	32.2	-0.011	0.00000	67.1	0.00000	52920	0	0
0.0045	3.15	99.39	69	0.226	0.038	32.2	-0.009	0.00000	67.1	0.00000	46920	0	0
0.0044	3.26	99.50	69	0.226	0.038	32.2	-0.009	0.00000	67.1	0.00000	40920	0	0
0.0043	3.36	99.60	69	0.226	0.039	32.2	-0.008	0.00000	67.1	0.00000	34920	0	0
0.0042	3.45	99.69	69	0.226	0.039	32.2	-0.008	0.00000	67.1	0.00000	32520	0	0
0.0042	3.56	99.80	69	0.226	0.040	32.2	-0.007	0.00000	67.1	0.00000	30120	0	0
0.0041	3.66	99.90	69	0.226	0.040	32.2	-0.007	0.00000	67.1	0.00000	25320	0	0
0.0040	3.76	100.00	69	0.226	0.041	32.2	-0.006	0.00000	67.1	0.00000	22920	0	0
0.0040	3.86	100.10	69	0.226	0.042	32.2	-0.005	0.00000	67.1	0.00000	21720	0	0
0.0039	3.96	100.20	69	0.226	0.042	32.2	-0.005	0.00000	67.1	0.00000	19320	0	0
0.0039	4.05	100.29	69	0.226	0.043	32.2	-0.004	0.00000	67.1	0.00000	16920	0	0
0.0039	4.15	100.39	69	0.226	0.043	32.2	-0.004	0.00000	67.1	0.00000	16920	0	0
0.0039	4.26	100.50	69	0.226	0.044	32.2	-0.003	0.00000	67.1	0.00000	15720	0	0
0.0038	4.36	100.60	69	0.226	0.044	32.2	-0.003	0.00000	67.1	0.00000	12120	0	0
0.0037	4.46	100.70	69	0.226	0.044	32.2	-0.003	0.00000	67.1	0.00000	12120	0	0
0.0036	4.56	100.80	69	0.226	0.044	32.2	-0.003	0.00000	67.1	0.00000	10920	0	0
0.0035	4.66	100.90	69	0.226	0.044	32.2	-0.003	0.00000	67.1	0.00000	8520	0	0
0.0034	4.76	101.00	69	0.226	0.043	32.2	-0.004	0.00000	67.1	0.00000	8520	0	0
0.0034	4.86	101.10	69	0.226	0.044	32.2	-0.003	0.00000	67.1	0.00000	6120	0	0
0.0033	4.96	101.20	69	0.226	0.044	32.2	-0.003	0.00000	67.1	0.00000	4920	0	0
0.0032	5.06	101.30	69	0.226	0.044	32.2	-0.003	0.00000	67.1	0.00000	3720	0	0
0.0032	5.16	101.40	69	0.226	0.044	32.2	-0.003	0.00000	67.1	0.00000	120	0	0
												sum =	0 lbs

Table 49: Mass transport per unit of channel width (67.5 mm)

W.S. Elev.	Upstream Yo	Downstream WSEL	Stage	Discharge Q	Volumetric transport rate of sediment per unit stream width q_b	Specific weight of Sediment	Dry weight of sediment transported per unit width and time g_b	Gravitational acceleration g	Mass transport rate per unit of channel width	Mass transport rate per unit of channel width
(ft)	(ft)	(ft)	(ft)	(m^3/s)	(ft^2/s)	(lbs/ft^3)	(lbs/s/ft)	(ft/s^2)	($Slugs*s^{-1}*ft^{-1}$)	($kg*m^{-1}*s^{-1}$)
97.80	1.56	94.05	3.16	2.5	0.00000	165	0.00000	32.2	0.00000	0.00000
97.90	1.66	94.15	3.26	2.8	0.00000	165	0.00000	32.2	0.00000	0.00000
97.99	1.75	94.47	3.58	4.0	0.00000	165	0.00000	32.2	0.00000	0.00000
98.09	1.85	94.64	3.75	4.8	0.00000	165	0.00000	32.2	0.00000	0.00000
98.18	1.94	94.74	3.85	5.3	0.00000	165	0.00000	32.2	0.00000	0.00000
98.28	2.04	94.84	3.95	5.9	0.00000	165	0.00000	32.2	0.00000	0.00000
98.39	2.15	94.94	4.05	6.5	0.00000	165	0.00000	32.2	0.00000	0.00000
98.49	2.25	95.46	4.57	10.4	0.00000	165	0.00000	32.2	0.00000	0.00000
98.59	2.35	95.32	4.43	9.2	0.00000	165	0.00000	32.2	0.00000	0.00000
98.69	2.45	95.47	4.58	10.4	0.00000	165	0.00000	32.2	0.00000	0.00000
98.79	2.55	95.69	4.80	12.5	0.00000	165	0.00000	32.2	0.00000	0.00000
98.89	2.65	95.71	4.82	12.8	0.00000	165	0.00000	32.2	0.00000	0.00000
98.99	2.75	96.06	5.17	16.7	0.00000	165	0.00000	32.2	0.00000	0.00000
99.09	2.85	96.04	5.15	16.5	0.00000	165	0.00000	32.2	0.00000	0.00000
99.19	2.95	96.14	5.25	17.8	0.00000	165	0.00000	32.2	0.00000	0.00000
99.29	3.05	96.24	5.35	19.1	0.00000	165	0.00000	32.2	0.00000	0.00000
99.39	3.15	96.34	5.45	20.6	0.00000	165	0.00000	32.2	0.00000	0.00000
99.50	3.26	96.51	5.62	23.1	0.00000	165	0.00000	32.2	0.00000	0.00000
99.60	3.36	96.65	5.76	25.5	0.00000	165	0.00000	32.2	0.00000	0.00000
99.69	3.45	96.81	5.92	28.4	0.00000	165	0.00000	32.2	0.00000	0.00000
99.80	3.56	96.91	6.02	30.3	0.00000	165	0.00000	32.2	0.00000	0.00000
99.90	3.66	97.09	6.20	33.9	0.00000	165	0.00000	32.2	0.00000	0.00000
100.00	3.76	97.23	6.34	37.0	0.00000	165	0.00000	32.2	0.00000	0.00000
100.10	3.86	97.33	6.44	39.3	0.00000	165	0.00000	32.2	0.00000	0.00000
100.20	3.96	97.49	6.60	43.3	0.00000	165	0.00000	32.2	0.00000	0.00000
100.29	4.05	97.59	6.70	45.9	0.00000	165	0.00000	32.2	0.00000	0.00000
100.39	4.15	97.72	6.83	49.4	0.00000	165	0.00000	32.2	0.00000	0.00000
100.50	4.26	97.85	6.96	53.2	0.00000	165	0.00000	32.2	0.00000	0.00000
100.60	4.36	98.00	7.11	57.8	0.00000	165	0.00000	32.2	0.00000	0.00000
100.70	4.46	98.15	7.26	62.6	0.00000	165	0.00000	32.2	0.00000	0.00000
100.80	4.56	98.30	7.41	67.8	0.00000	165	0.00000	32.2	0.00000	0.00000
100.90	4.66	98.49	7.60	74.8	0.00000	165	0.00000	32.2	0.00000	0.00000
101.00	4.76	98.68	7.79	82.4	0.00000	165	0.00000	32.2	0.00000	0.00000
101.10	4.86	98.78	7.89	86.6	0.00000	165	0.00000	32.2	0.00000	0.00000
101.20	4.96	98.94	8.05	93.8	0.00000	165	0.00000	32.2	0.00000	0.00000
101.30	5.06	99.08	8.19	99.9	0.00000	165	0.00000	32.2	0.00000	0.00000
101.40	5.16	99.21	8.32	106.4	0.00000	165	0.00000	32.2	0.00000	0.00000

Table 50: Bedload rating curve summary

Time (Seconds)	Flow Discharge (cms)	Bedload discharge ($kg*m^{-1}*s^{-1}$)				
		Size Class 2	Size Class 3	Size Class 4	Size Class 5	Size Class 6
		8.25mm	17.25mm	28.5mm	41.5mm	54mm
0	2.4	0.000	0.000	0.000	0.000	0.000
1200	2.4	0.000	0.000	0.000	0.000	0.000
2400	2.5	0.000	0.000	0.000	0.000	0.000
3600	2.5	0.000	0.000	0.000	0.000	0.000
4800	2.5	0.000	0.000	0.000	0.000	0.000
6000	2.6	0.000	0.000	0.000	0.000	0.000
7200	2.6	0.000	0.000	0.000	0.000	0.000
8400	2.6	0.000	0.000	0.000	0.000	0.000
9600	2.6	0.000	0.000	0.000	0.000	0.000
10800	2.6	0.000	0.000	0.000	0.000	0.000
12000	2.7	0.000	0.000	0.000	0.000	0.000
13200	2.8	0.000	0.000	0.000	0.000	0.000
14400	2.9	0.000	0.000	0.000	0.000	0.000
15600	3.1	0.000	0.000	0.000	0.000	0.000
16800	4.2	0.000	0.000	0.000	0.000	0.000
18000	13.4	1.381	0.000	0.000	0.000	0.000
18873	14.0	1.468	0.039	0.000	0.000	0.000
20040	14.3	1.496	0.063	0.000	0.000	0.000
21240	14.5	1.525	0.086	0.000	0.000	0.000
22440	14.6	1.539	0.098	0.000	0.000	0.000
23640	14.6	1.539	0.098	0.000	0.000	0.000
24840	14.4	1.511	0.075	0.000	0.000	0.000
26040	14.0	1.468	0.039	0.000	0.000	0.000
27240	14.3	1.496	0.063	0.000	0.000	0.000
28440	14.3	1.496	0.063	0.000	0.000	0.000
29640	14.3	1.496	0.063	0.000	0.000	0.000
30840	14.1	1.482	0.051	0.000	0.000	0.000
32040	14.0	1.468	0.039	0.000	0.000	0.000
33240	13.3	1.366	0.000	0.000	0.000	0.000
34440	13.1	1.337	0.000	0.000	0.000	0.000
35640	11.1	1.038	0.000	0.000	0.000	0.000
36840	13.9	1.453	0.027	0.000	0.000	0.000
38040	15.9	1.694	0.227	0.000	0.000	0.000
39240	16.6	1.777	0.296	0.000	0.000	0.000
40440	16.7	1.791	0.308	0.000	0.000	0.000
41640	18.2	1.941	0.432	0.000	0.000	0.000
42840	19.1	2.034	0.510	0.000	0.000	0.000
44040	25.3	2.547	0.936	0.212	0.000	0.000
45240	55.6	3.985	2.133	1.019	0.342	0.021
46440	85.3	4.348	2.326	1.184	0.435	0.042
47640	102.0	4.348	2.326	1.184	0.435	0.042
48840	106.4	4.348	2.326	1.184	0.435	0.042
50040	105.9	4.348	2.326	1.184	0.435	0.042
51240	104.9	4.348	2.326	1.184	0.435	0.042

Table 48: Bedload rating curve summary (continued)

Time (Seconds)	Flow Discharge (cms)	Bedload discharge ($kg*m^{-1}*s^{-1}$)				
		Size Class 2	Size Class 3	Size Class 4	Size Class 5	Size Class 6
		8.25mm	17.25mm	28.5mm	41.5mm	54mm
52440	96.8	4.348	2.326	1.184	0.435	0.042
53640	89.6	4.348	2.326	1.184	0.435	0.042
54840	82.4	4.348	2.326	1.184	0.435	0.042
56040	75.6	4.348	2.326	1.184	0.435	0.042
57240	70.0	4.348	2.326	1.184	0.435	0.042
58440	65.0	4.272	2.326	1.180	0.435	0.038
59640	59.0	4.095	2.225	1.081	0.386	0.027
60840	55.6	3.985	2.133	1.019	0.342	0.021
62040	52.0	3.863	2.032	0.951	0.292	0.014
63240	46.7	3.665	1.867	0.840	0.212	0.002
64440	44.3	3.569	1.787	0.786	0.173	0.000
65640	42.0	3.472	1.707	0.731	0.134	0.000
66840	40.5	3.407	1.652	0.695	0.107	0.000
68040	38.4	3.308	1.570	0.639	0.067	0.000
69240	36.8	3.230	1.505	0.595	0.035	0.000
70440	35.0	3.139	1.429	0.544	0.000	0.000
71640	33.9	3.082	1.382	0.512	0.000	0.000
72840	32.9	3.025	1.334	0.480	0.000	0.000
74040	31.6	2.955	1.276	0.441	0.000	0.000
75240	30.3	2.873	1.208	0.395	0.000	0.000
76440	29.5	2.825	1.168	0.368	0.000	0.000
77640	28.5	2.766	1.119	0.335	0.000	0.000
78840	27.4	2.693	1.059	0.294	0.000	0.000
80040	26.5	2.633	1.008	0.260	0.000	0.000
81240	25.8	2.584	0.967	0.232	0.000	0.000
82440	25.0	2.522	0.916	0.198	0.000	0.000
83640	24.3	2.472	0.874	0.170	0.000	0.000
84840	23.6	2.422	0.833	0.142	0.000	0.000
86040	23.0	2.371	0.791	0.113	0.000	0.000
87240	22.4	2.321	0.748	0.085	0.000	0.000
88440	21.9	2.282	0.717	0.063	0.000	0.000
89640	21.3	2.231	0.674	0.034	0.000	0.000
90840	20.9	2.192	0.641	0.012	0.000	0.000
92040	20.4	2.153	0.609	0.000	0.000	0.000
93240	20.0	2.113	0.576	0.000	0.000	0.000
94440	19.4	2.061	0.532	0.000	0.000	0.000
95640	19.1	2.034	0.510	0.000	0.000	0.000
96840	18.7	1.994	0.477	0.000	0.000	0.000
98040	18.6	1.981	0.466	0.000	0.000	0.000
99240	17.9	1.914	0.410	0.000	0.000	0.000
100440	17.6	1.887	0.387	0.000	0.000	0.000
101640	17.3	1.846	0.353	0.000	0.000	0.000
102840	17.0	1.818	0.331	0.000	0.000	0.000
104040	16.7	1.791	0.308	0.000	0.000	0.000
105240	16.4	1.750	0.273	0.000	0.000	0.000

Table 48: Bedload rating curve summary (continued)

Time (Seconds)	Flow Discharge (cms)	Bedload discharge ($kg*m^{-1}*s^{-1}$)				
		Size Class 2	Size Class 3	Size Class 4	Size Class 5	Size Class 6
		8.25mm	17.25mm	28.5mm	41.5mm	54mm
106440	16.0	1.708	0.239	0.000	0.000	0.000
107640	15.8	1.680	0.216	0.000	0.000	0.000
108840	15.5	1.652	0.192	0.000	0.000	0.000
110040	15.2	1.610	0.157	0.000	0.000	0.000
111240	14.9	1.582	0.134	0.000	0.000	0.000
112440	14.7	1.553	0.110	0.000	0.000	0.000
113640	14.5	1.525	0.086	0.000	0.000	0.000
114840	14.1	1.482	0.051	0.000	0.000	0.000
116040	13.9	1.453	0.027	0.000	0.000	0.000
117240	13.9	1.453	0.027	0.000	0.000	0.000
118440	13.7	1.424	0.003	0.000	0.000	0.000
119640	13.4	1.381	0.000	0.000	0.000	0.000
120840	13.2	1.352	0.000	0.000	0.000	0.000
122040	12.9	1.308	0.000	0.000	0.000	0.000
123240	12.7	1.278	0.000	0.000	0.000	0.000
124440	12.4	1.248	0.000	0.000	0.000	0.000
125640	12.1	1.189	0.000	0.000	0.000	0.000
126840	12.0	1.174	0.000	0.000	0.000	0.000
128040	12.1	1.189	0.000	0.000	0.000	0.000
129240	11.9	1.159	0.000	0.000	0.000	0.000
130440	11.0	1.022	0.000	0.000	0.000	0.000
131640	11.1	1.038	0.000	0.000	0.000	0.000
132840	10.9	1.007	0.000	0.000	0.000	0.000
134040	10.5	0.930	0.000	0.000	0.000	0.000
135240	10.1	0.868	0.000	0.000	0.000	0.000
136440	10.4	0.914	0.000	0.000	0.000	0.000
137640	11.2	1.053	0.000	0.000	0.000	0.000
138840	11.1	1.038	0.000	0.000	0.000	0.000
140040	10.9	1.007	0.000	0.000	0.000	0.000
141240	10.7	0.976	0.000	0.000	0.000	0.000
142440	10.6	0.961	0.000	0.000	0.000	0.000
143640	10.5	0.945	0.000	0.000	0.000	0.000
144840	10.4	0.914	0.000	0.000	0.000	0.000
146040	10.3	0.899	0.000	0.000	0.000	0.000
147240	10.2	0.883	0.000	0.000	0.000	0.000
148440	10.2	0.883	0.000	0.000	0.000	0.000
149640	10.0	0.852	0.000	0.000	0.000	0.000
150840	10.0	0.852	0.000	0.000	0.000	0.000
152040	9.8	0.805	0.000	0.000	0.000	0.000
153240	9.8	0.805	0.000	0.000	0.000	0.000
154440	9.7	0.789	0.000	0.000	0.000	0.000
155640	9.7	0.789	0.000	0.000	0.000	0.000
156840	9.4	0.741	0.000	0.000	0.000	0.000
158040	9.4	0.741	0.000	0.000	0.000	0.000
159240	9.4	0.741	0.000	0.000	0.000	0.000

Table 48: Bedload rating curve summary (continued)

Time (Seconds)	Flow Discharge (cms)	Bedload discharge ($kg*m^{-1}*s^{-1}$)				
		Size Class 2	Size Class 3	Size Class 4	Size Class 5	Size Class 6
		8.25mm	17.25mm	28.5mm	41.5mm	54mm
160440	9.4	0.741	0.000	0.000	0.000	0.000
161640	9.1	0.677	0.000	0.000	0.000	0.000
162840	9.1	0.677	0.000	0.000	0.000	0.000
164040	9.0	0.661	0.000	0.000	0.000	0.000
165240	9.0	0.661	0.000	0.000	0.000	0.000
166440	8.9	0.629	0.000	0.000	0.000	0.000
167640	8.7	0.596	0.000	0.000	0.000	0.000
168840	8.7	0.596	0.000	0.000	0.000	0.000
170040	8.6	0.580	0.000	0.000	0.000	0.000
171240	8.6	0.580	0.000	0.000	0.000	0.000
172440	8.6	0.580	0.000	0.000	0.000	0.000
173640	8.6	0.564	0.000	0.000	0.000	0.000
174840	8.6	0.564	0.000	0.000	0.000	0.000
176040	8.3	0.514	0.000	0.000	0.000	0.000
177240	8.3	0.514	0.000	0.000	0.000	0.000
178440	8.3	0.514	0.000	0.000	0.000	0.000
179640	8.3	0.514	0.000	0.000	0.000	0.000
180840	8.3	0.514	0.000	0.000	0.000	0.000
182040	8.3	0.514	0.000	0.000	0.000	0.000
183240	8.4	0.531	0.000	0.000	0.000	0.000
184440	8.4	0.531	0.000	0.000	0.000	0.000
185640	8.3	0.514	0.000	0.000	0.000	0.000
186840	8.4	0.531	0.000	0.000	0.000	0.000
188040	8.3	0.514	0.000	0.000	0.000	0.000
189240	8.3	0.514	0.000	0.000	0.000	0.000
190440	8.1	0.465	0.000	0.000	0.000	0.000
191640	7.6	0.348	0.000	0.000	0.000	0.000
192840	7.2	0.246	0.000	0.000	0.000	0.000
194040	6.3	0.003	0.000	0.000	0.000	0.000
195240	5.8	0.000	0.000	0.000	0.000	0.000
196440	5.3	0.000	0.000	0.000	0.000	0.000
197640	5.4	0.000	0.000	0.000	0.000	0.000
198840	5.0	0.000	0.000	0.000	0.000	0.000
200040	5.2	0.000	0.000	0.000	0.000	0.000
201240	4.2	0.000	0.000	0.000	0.000	0.000
202440	4.2	0.000	0.000	0.000	0.000	0.000
203640	4.2	0.000	0.000	0.000	0.000	0.000
204840	4.4	0.000	0.000	0.000	0.000	0.000
206040	4.5	0.000	0.000	0.000	0.000	0.000
207240	4.4	0.000	0.000	0.000	0.000	0.000
207720	4.4	0.000	0.000	0.000	0.000	0.000
208920	4.4	0.000	0.000	0.000	0.000	0.000
210120	4.3	0.000	0.000	0.000	0.000	0.000
211320	4.3	0.000	0.000	0.000	0.000	0.000

Appendix J: CCHE2D boundary condition files

Table 51: Discharge hydrograph data

Time (Seconds)	Discharge (cms)	Time (Seconds)	Discharge (cms)	Time (Seconds)	Discharge (cms)	Time (Seconds)	Discharge (cms)
0	2.383	57240	69.982	114840	14.145	172440	8.639
1200	2.413	58440	65.022	116040	13.924	173640	8.562
2400	2.504	59640	59.035	117240	13.924	174840	8.562
3600	2.535	60840	55.583	118440	13.706	176040	8.335
4800	2.535	62040	51.992	119640	13.384	177240	8.335
6000	2.566	63240	46.661	120840	13.172	178440	8.335
7200	2.566	64440	44.283	122040	12.859	179640	8.335
8400	2.566	65640	41.996	123240	12.653	180840	8.335
9600	2.566	66840	40.521	124440	12.450	182040	8.335
10800	2.629	68040	38.381	125640	12.051	183240	8.410
12000	2.693	69240	36.776	126840	11.952	184440	8.410
13200	2.792	70440	35.002	128040	12.051	185640	8.335
14400	2.893	71640	33.927	129240	11.855	186840	8.410
15600	3.067	72840	32.876	130440	11.002	188040	8.335
16800	4.239	74040	31.647	131640	11.095	189240	8.335
18000	13.384	75240	30.257	132840	10.910	190440	8.112
18873	14.034	76440	29.484	134040	10.460	191640	7.610
20040	14.256	77640	28.537	135240	10.109	192840	7.198
21240	14.481	78840	27.432	136440	10.371	194040	6.302
22440	14.594	80040	26.535	137640	11.188	195240	5.771
23640	14.594	81240	25.833	138840	11.095	196440	5.274
24840	14.368	82440	24.976	140040	10.910	197640	5.436
26040	14.034	83640	24.305	141240	10.728	198840	5.012
27240	14.256	84840	23.648	142440	10.638	200040	5.221
28440	14.256	86040	23.004	143640	10.549	201240	4.239
29640	14.256	87240	22.373	144840	10.371	202440	4.194
30840	14.145	88440	21.909	146040	10.283	203640	4.194
32040	14.034	89640	21.301	147240	10.196	204840	4.377
33240	13.277	90840	20.853	148440	10.196	206040	4.518
34440	13.067	92040	20.412	149640	10.023	207240	4.377
35640	11.095	93240	19.978	150840	10.023	207720	4.423
36840	13.924	94440	19.410	152040	9.767	208920	4.377
38040	15.885	95640	19.131	153240	9.767	210120	4.330
39240	16.623	96840	18.717	154440	9.683	211320	4.330
40440	16.749	98040	18.581	155640	9.683		
41640	18.176	99240	17.910	156840	9.434		
42840	19.131	100440	17.647	158040	9.434		
44040	25.316	101640	17.258	159240	9.434		
45240	55.583	102840	17.002	160440	9.434		
46440	85.283	104040	16.749	161640	9.110		
47640	101.972	105240	16.374	162840	9.110		
48840	106.374	106440	16.006	164040	9.030		
50040	105.878	107640	15.764	165240	9.030		
51240	104.891	108840	15.525	166440	8.872		
52440	96.778	110040	15.171	167640	8.716		
53640	89.576	111240	14.938	168840	8.716		
54840	82.369	112440	14.708	170040	8.639		
56040	75.602	113640	14.481	171240	8.639		

Table 52: Stage hydrograph data

Time (Seconds)	Stage (m)	Time (Seconds)	Stage (m)	Time (Seconds)	Stage (m)	Time (Seconds)	Stage (m)
0	28.657	57240	29.980	114840	29.212	172440	29.032
1200	28.660	58440	29.937	116040	29.206	173640	29.029
2400	28.669	59640	29.883	117240	29.206	174840	29.029
3600	28.673	60840	29.849	118440	29.200	176040	29.020
4800	28.673	62040	29.812	119640	29.191	177240	29.020
6000	28.676	63240	29.755	120840	29.185	178440	29.020
7200	28.676	64440	29.727	122040	29.175	179640	29.020
8400	28.676	65640	29.700	123240	29.169	180840	29.020
9600	28.676	66840	29.681	124440	29.163	182040	29.020
10800	28.682	68040	29.654	125640	29.151	183240	29.023
12000	28.688	69240	29.633	126840	29.148	184440	29.023
13200	28.697	70440	29.608	128040	29.151	185640	29.020
14400	28.706	71640	29.593	129240	29.145	186840	29.023
15600	28.721	72840	29.578	130440	29.118	188040	29.020
16800	28.810	74040	29.560	131640	29.121	189240	29.020
18000	29.191	75240	29.538	132840	29.114	190440	29.011
18873	29.209	76440	29.526	134040	29.099	191640	28.990
20040	29.215	77640	29.511	135240	29.087	192840	28.971
21240	29.221	78840	29.492	136440	29.096	194040	28.929
22440	29.224	80040	29.477	137640	29.124	195240	28.901
23640	29.224	81240	29.465	138840	29.121	196440	28.874
24840	29.218	82440	29.450	140040	29.114	197640	28.883
26040	29.209	83640	29.438	141240	29.108	198840	28.858
27240	29.215	84840	29.425	142440	29.105	200040	28.871
28440	29.215	86040	29.413	143640	29.102	201240	28.810
29640	29.215	87240	29.401	144840	29.096	202440	28.807
30840	29.212	88440	29.392	146040	29.093	203640	28.807
32040	29.209	89640	29.380	147240	29.090	204840	28.819
33240	29.188	90840	29.371	148440	29.090	206040	28.828
34440	29.182	92040	29.361	149640	29.084	207240	28.819
35640	29.121	93240	29.352	150840	29.084	207720	28.822
36840	29.206	94440	29.340	152040	29.075	208920	28.819
38040	29.258	95640	29.334	153240	29.075	210120	28.816
39240	29.276	96840	29.325	154440	29.072	211320	28.816
40440	29.279	98040	29.322	155640	29.072		
41640	29.313	99240	29.307	156840	29.063		
42840	29.334	100440	29.300	158040	29.063		
44040	29.456	101640	29.291	159240	29.063		
45240	29.849	102840	29.285	160440	29.063		
46440	30.099	104040	29.279	161640	29.050		
47640	30.212	105240	29.270	162840	29.050		
48840	30.239	106440	29.261	164040	29.047		
50040	30.236	107640	29.255	165240	29.047		
51240	30.230	108840	29.249	166440	29.041		
52440	30.178	110040	29.239	167640	29.035		
53640	30.129	111240	29.233	168840	29.035		
54840	30.078	112440	29.227	170040	29.032		
56040	30.026	113640	29.221	171240	29.032		

Table 53: Bedload rating curve data

Time (s)	Bedload discharge ($kg*m^{-1}*s^{-1}$)	Size Class 1	Size Class 2	Size Class 3	Size Class 4	Size Class 5	Size Class 6	Size Class 7	Size Class 8	Size Class 9	Size Class 10
0	0.000	1.00	0.00	0.00	0.00	0.00	0.00	0.00	0.00	0.00	0.00
1200	0.000	1.00	0.00	0.00	0.00	0.00	0.00	0.00	0.00	0.00	0.00
2400	0.000	1.00	0.00	0.00	0.00	0.00	0.00	0.00	0.00	0.00	0.00
3600	0.000	1.00	0.00	0.00	0.00	0.00	0.00	0.00	0.00	0.00	0.00
4800	0.000	1.00	0.00	0.00	0.00	0.00	0.00	0.00	0.00	0.00	0.00
6000	0.000	1.00	0.00	0.00	0.00	0.00	0.00	0.00	0.00	0.00	0.00
7200	0.000	1.00	0.00	0.00	0.00	0.00	0.00	0.00	0.00	0.00	0.00
8400	0.000	1.00	0.00	0.00	0.00	0.00	0.00	0.00	0.00	0.00	0.00
9600	0.000	1.00	0.00	0.00	0.00	0.00	0.00	0.00	0.00	0.00	0.00
10800	0.000	1.00	0.00	0.00	0.00	0.00	0.00	0.00	0.00	0.00	0.00
12000	0.000	1.00	0.00	0.00	0.00	0.00	0.00	0.00	0.00	0.00	0.00
13200	0.000	1.00	0.00	0.00	0.00	0.00	0.00	0.00	0.00	0.00	0.00
14400	0.000	1.00	0.00	0.00	0.00	0.00	0.00	0.00	0.00	0.00	0.00
15600	0.000	1.00	0.00	0.00	0.00	0.00	0.00	0.00	0.00	0.00	0.00
16800	0.000	1.00	0.00	0.00	0.00	0.00	0.00	0.00	0.00	0.00	0.00
18000	1.381	0.00	1.00	0.00	0.00	0.00	0.00	0.00	0.00	0.00	0.00
18873	1.506	0.00	0.97	0.03	0.00	0.00	0.00	0.00	0.00	0.00	0.00
20040	1.559	0.00	0.96	0.04	0.00	0.00	0.00	0.00	0.00	0.00	0.00
21240	1.611	0.00	0.95	0.05	0.00	0.00	0.00	0.00	0.00	0.00	0.00
22440	1.637	0.00	0.94	0.06	0.00	0.00	0.00	0.00	0.00	0.00	0.00
23640	1.637	0.00	0.94	0.06	0.00	0.00	0.00	0.00	0.00	0.00	0.00
24840	1.585	0.00	0.95	0.05	0.00	0.00	0.00	0.00	0.00	0.00	0.00
26040	1.506	0.00	0.97	0.03	0.00	0.00	0.00	0.00	0.00	0.00	0.00
27240	1.559	0.00	0.96	0.04	0.00	0.00	0.00	0.00	0.00	0.00	0.00
28440	1.559	0.00	0.96	0.04	0.00	0.00	0.00	0.00	0.00	0.00	0.00
29640	1.559	0.00	0.96	0.04	0.00	0.00	0.00	0.00	0.00	0.00	0.00
30840	1.533	0.00	0.97	0.03	0.00	0.00	0.00	0.00	0.00	0.00	0.00
32040	1.506	0.00	0.97	0.03	0.00	0.00	0.00	0.00	0.00	0.00	0.00
33240	1.366	0.00	1.00	0.00	0.00	0.00	0.00	0.00	0.00	0.00	0.00
34440	1.337	0.00	1.00	0.00	0.00	0.00	0.00	0.00	0.00	0.00	0.00
35640	1.038	0.00	1.00	0.00	0.00	0.00	0.00	0.00	0.00	0.00	0.00
36840	1.480	0.00	0.98	0.02	0.00	0.00	0.00	0.00	0.00	0.00	0.00
38040	1.921	0.00	0.88	0.12	0.00	0.00	0.00	0.00	0.00	0.00	0.00
39240	2.074	0.00	0.86	0.14	0.00	0.00	0.00	0.00	0.00	0.00	0.00
40440	2.099	0.00	0.85	0.15	0.00	0.00	0.00	0.00	0.00	0.00	0.00
41640	2.373	0.00	0.82	0.18	0.00	0.00	0.00	0.00	0.00	0.00	0.00
42840	2.544	0.00	0.80	0.20	0.00	0.00	0.00	0.00	0.00	0.00	0.00
44040	3.695	0.00	0.69	0.25	0.06	0.00	0.00	0.00	0.00	0.00	0.00
45240	7.500	0.00	0.53	0.28	0.14	0.05	0.00	0.00	0.00	0.00	0.00
46440	8.335	0.00	0.52	0.28	0.14	0.05	0.00	0.00	0.00	0.00	0.00
47640	8.335	0.00	0.52	0.28	0.14	0.05	0.00	0.00	0.00	0.00	0.00
48840	8.335	0.00	0.52	0.28	0.14	0.05	0.00	0.00	0.00	0.00	0.00
50040	8.335	0.00	0.52	0.28	0.14	0.05	0.00	0.00	0.00	0.00	0.00
51240	8.335	0.00	0.52	0.28	0.14	0.05	0.00	0.00	0.00	0.00	0.00
52440	8.335	0.00	0.52	0.28	0.14	0.05	0.00	0.00	0.00	0.00	0.00
53640	8.335	0.00	0.52	0.28	0.14	0.05	0.00	0.00	0.00	0.00	0.00
54840	8.335	0.00	0.52	0.28	0.14	0.05	0.00	0.00	0.00	0.00	0.00
56040	8.335	0.00	0.52	0.28	0.14	0.05	0.00	0.00	0.00	0.00	0.00
57240	8.335	0.00	0.52	0.28	0.14	0.05	0.00	0.00	0.00	0.00	0.00

Table 53: Bedload rating curve data (continued)

Time (s)	Bedload discharge ($kg*m^{-1}*s^{-1}$)	Size Class 1	Size Class 2	Size Class 3	Size Class 4	Size Class 5	Size Class 6	Size Class 7	Size Class 8	Size Class 9	Size Class 10
58440	8.251	0.00	0.52	0.28	0.14	0.05	0.00	0.00	0.00	0.00	0.00
59640	7.815	0.00	0.52	0.28	0.14	0.05	0.00	0.00	0.00	0.00	0.00
60840	7.500	0.00	0.53	0.28	0.14	0.05	0.00	0.00	0.00	0.00	0.00
62040	7.151	0.00	0.54	0.28	0.13	0.04	0.00	0.00	0.00	0.00	0.00
63240	6.586	0.00	0.56	0.28	0.13	0.03	0.00	0.00	0.00	0.00	0.00
64440	6.316	0.00	0.57	0.28	0.12	0.03	0.00	0.00	0.00	0.00	0.00
65640	6.044	0.00	0.57	0.28	0.12	0.02	0.00	0.00	0.00	0.00	0.00
66840	5.861	0.00	0.58	0.28	0.12	0.02	0.00	0.00	0.00	0.00	0.00
68040	5.583	0.00	0.59	0.28	0.11	0.01	0.00	0.00	0.00	0.00	0.00
69240	5.365	0.00	0.60	0.28	0.11	0.01	0.00	0.00	0.00	0.00	0.00
70440	5.113	0.00	0.61	0.28	0.11	0.00	0.00	0.00	0.00	0.00	0.00
71640	4.976	0.00	0.62	0.28	0.10	0.00	0.00	0.00	0.00	0.00	0.00
72840	4.839	0.00	0.63	0.28	0.10	0.00	0.00	0.00	0.00	0.00	0.00
74040	4.672	0.00	0.63	0.27	0.09	0.00	0.00	0.00	0.00	0.00	0.00
75240	4.475	0.00	0.64	0.27	0.09	0.00	0.00	0.00	0.00	0.00	0.00
76440	4.362	0.00	0.65	0.27	0.08	0.00	0.00	0.00	0.00	0.00	0.00
77640	4.219	0.00	0.66	0.27	0.08	0.00	0.00	0.00	0.00	0.00	0.00
78840	4.046	0.00	0.67	0.26	0.07	0.00	0.00	0.00	0.00	0.00	0.00
80040	3.901	0.00	0.67	0.26	0.07	0.00	0.00	0.00	0.00	0.00	0.00
81240	3.783	0.00	0.68	0.26	0.06	0.00	0.00	0.00	0.00	0.00	0.00
82440	3.636	0.00	0.69	0.25	0.05	0.00	0.00	0.00	0.00	0.00	0.00
83640	3.516	0.00	0.70	0.25	0.05	0.00	0.00	0.00	0.00	0.00	0.00
84840	3.396	0.00	0.71	0.25	0.04	0.00	0.00	0.00	0.00	0.00	0.00
86040	3.276	0.00	0.72	0.24	0.03	0.00	0.00	0.00	0.00	0.00	0.00
87240	3.154	0.00	0.74	0.24	0.03	0.00	0.00	0.00	0.00	0.00	0.00
88440	3.062	0.00	0.75	0.23	0.02	0.00	0.00	0.00	0.00	0.00	0.00
89640	2.939	0.00	0.76	0.23	0.01	0.00	0.00	0.00	0.00	0.00	0.00
90840	2.846	0.00	0.77	0.23	0.00	0.00	0.00	0.00	0.00	0.00	0.00
92040	2.762	0.00	0.78	0.22	0.00	0.00	0.00	0.00	0.00	0.00	0.00
93240	2.690	0.00	0.79	0.21	0.00	0.00	0.00	0.00	0.00	0.00	0.00
94440	2.593	0.00	0.79	0.21	0.00	0.00	0.00	0.00	0.00	0.00	0.00
95640	2.544	0.00	0.80	0.20	0.00	0.00	0.00	0.00	0.00	0.00	0.00
96840	2.471	0.00	0.81	0.19	0.00	0.00	0.00	0.00	0.00	0.00	0.00
98040	2.447	0.00	0.81	0.19	0.00	0.00	0.00	0.00	0.00	0.00	0.00
99240	2.324	0.00	0.82	0.18	0.00	0.00	0.00	0.00	0.00	0.00	0.00
100440	2.274	0.00	0.83	0.17	0.00	0.00	0.00	0.00	0.00	0.00	0.00
101640	2.199	0.00	0.84	0.16	0.00	0.00	0.00	0.00	0.00	0.00	0.00
102840	2.149	0.00	0.85	0.15	0.00	0.00	0.00	0.00	0.00	0.00	0.00
104040	2.099	0.00	0.85	0.15	0.00	0.00	0.00	0.00	0.00	0.00	0.00
105240	2.023	0.00	0.86	0.14	0.00	0.00	0.00	0.00	0.00	0.00	0.00
106440	1.947	0.00	0.88	0.12	0.00	0.00	0.00	0.00	0.00	0.00	0.00
107640	1.896	0.00	0.89	0.11	0.00	0.00	0.00	0.00	0.00	0.00	0.00
108840	1.845	0.00	0.90	0.10	0.00	0.00	0.00	0.00	0.00	0.00	0.00
110040	1.767	0.00	0.91	0.09	0.00	0.00	0.00	0.00	0.00	0.00	0.00
111240	1.716	0.00	0.92	0.08	0.00	0.00	0.00	0.00	0.00	0.00	0.00
112440	1.664	0.00	0.93	0.07	0.00	0.00	0.00	0.00	0.00	0.00	0.00
113640	1.611	0.00	0.95	0.05	0.00	0.00	0.00	0.00	0.00	0.00	0.00
114840	1.533	0.00	0.97	0.03	0.00	0.00	0.00	0.00	0.00	0.00	0.00
116040	1.480	0.00	0.98	0.02	0.00	0.00	0.00	0.00	0.00	0.00	0.00
117240	1.480	0.00	0.98	0.02	0.00	0.00	0.00	0.00	0.00	0.00	0.00

Table 53: Bedload rating curve data (continued)

Time (s)	Bedload discharge ($kg*m^{-1}*s^{-1}$)	Size Class 1	Size Class 2	Size Class 3	Size Class 4	Size Class 5	Size Class 6	Size Class 7	Size Class 8	Size Class 9	Size Class 10
118440	1.427	0.00	1.00	0.00	0.00	0.00	0.00	0.00	0.00	0.00	0.00
119640	1.381	0.00	1.00	0.00	0.00	0.00	0.00	0.00	0.00	0.00	0.00
120840	1.352	0.00	1.00	0.00	0.00	0.00	0.00	0.00	0.00	0.00	0.00
122040	1.308	0.00	1.00	0.00	0.00	0.00	0.00	0.00	0.00	0.00	0.00
123240	1.278	0.00	1.00	0.00	0.00	0.00	0.00	0.00	0.00	0.00	0.00
124440	1.248	0.00	1.00	0.00	0.00	0.00	0.00	0.00	0.00	0.00	0.00
125640	1.189	0.00	1.00	0.00	0.00	0.00	0.00	0.00	0.00	0.00	0.00
126840	1.174	0.00	1.00	0.00	0.00	0.00	0.00	0.00	0.00	0.00	0.00
128040	1.189	0.00	1.00	0.00	0.00	0.00	0.00	0.00	0.00	0.00	0.00
129240	1.159	0.00	1.00	0.00	0.00	0.00	0.00	0.00	0.00	0.00	0.00
130440	1.022	0.00	1.00	0.00	0.00	0.00	0.00	0.00	0.00	0.00	0.00
131640	1.038	0.00	1.00	0.00	0.00	0.00	0.00	0.00	0.00	0.00	0.00
132840	1.007	0.00	1.00	0.00	0.00	0.00	0.00	0.00	0.00	0.00	0.00
134040	0.930	0.00	1.00	0.00	0.00	0.00	0.00	0.00	0.00	0.00	0.00
135240	0.868	0.00	1.00	0.00	0.00	0.00	0.00	0.00	0.00	0.00	0.00
136440	0.914	0.00	1.00	0.00	0.00	0.00	0.00	0.00	0.00	0.00	0.00
137640	1.053	0.00	1.00	0.00	0.00	0.00	0.00	0.00	0.00	0.00	0.00
138840	1.038	0.00	1.00	0.00	0.00	0.00	0.00	0.00	0.00	0.00	0.00
140040	1.007	0.00	1.00	0.00	0.00	0.00	0.00	0.00	0.00	0.00	0.00
141240	0.976	0.00	1.00	0.00	0.00	0.00	0.00	0.00	0.00	0.00	0.00
142440	0.961	0.00	1.00	0.00	0.00	0.00	0.00	0.00	0.00	0.00	0.00
143640	0.945	0.00	1.00	0.00	0.00	0.00	0.00	0.00	0.00	0.00	0.00
144840	0.914	0.00	1.00	0.00	0.00	0.00	0.00	0.00	0.00	0.00	0.00
146040	0.899	0.00	1.00	0.00	0.00	0.00	0.00	0.00	0.00	0.00	0.00
147240	0.883	0.00	1.00	0.00	0.00	0.00	0.00	0.00	0.00	0.00	0.00
148440	0.883	0.00	1.00	0.00	0.00	0.00	0.00	0.00	0.00	0.00	0.00
149640	0.852	0.00	1.00	0.00	0.00	0.00	0.00	0.00	0.00	0.00	0.00
150840	0.852	0.00	1.00	0.00	0.00	0.00	0.00	0.00	0.00	0.00	0.00
152040	0.805	0.00	1.00	0.00	0.00	0.00	0.00	0.00	0.00	0.00	0.00
153240	0.805	0.00	1.00	0.00	0.00	0.00	0.00	0.00	0.00	0.00	0.00
154440	0.789	0.00	1.00	0.00	0.00	0.00	0.00	0.00	0.00	0.00	0.00
155640	0.789	0.00	1.00	0.00	0.00	0.00	0.00	0.00	0.00	0.00	0.00
156840	0.741	0.00	1.00	0.00	0.00	0.00	0.00	0.00	0.00	0.00	0.00
158040	0.741	0.00	1.00	0.00	0.00	0.00	0.00	0.00	0.00	0.00	0.00
159240	0.741	0.00	1.00	0.00	0.00	0.00	0.00	0.00	0.00	0.00	0.00
160440	0.741	0.00	1.00	0.00	0.00	0.00	0.00	0.00	0.00	0.00	0.00
161640	0.677	0.00	1.00	0.00	0.00	0.00	0.00	0.00	0.00	0.00	0.00
162840	0.677	0.00	1.00	0.00	0.00	0.00	0.00	0.00	0.00	0.00	0.00
164040	0.661	0.00	1.00	0.00	0.00	0.00	0.00	0.00	0.00	0.00	0.00
165240	0.661	0.00	1.00	0.00	0.00	0.00	0.00	0.00	0.00	0.00	0.00
166440	0.629	0.00	1.00	0.00	0.00	0.00	0.00	0.00	0.00	0.00	0.00
167640	0.596	0.00	1.00	0.00	0.00	0.00	0.00	0.00	0.00	0.00	0.00
168840	0.596	0.00	1.00	0.00	0.00	0.00	0.00	0.00	0.00	0.00	0.00
170040	0.580	0.00	1.00	0.00	0.00	0.00	0.00	0.00	0.00	0.00	0.00
171240	0.580	0.00	1.00	0.00	0.00	0.00	0.00	0.00	0.00	0.00	0.00
172440	0.580	0.00	1.00	0.00	0.00	0.00	0.00	0.00	0.00	0.00	0.00
173640	0.564	0.00	1.00	0.00	0.00	0.00	0.00	0.00	0.00	0.00	0.00
174840	0.564	0.00	1.00	0.00	0.00	0.00	0.00	0.00	0.00	0.00	0.00
176040	0.514	0.00	1.00	0.00	0.00	0.00	0.00	0.00	0.00	0.00	0.00
177240	0.514	0.00	1.00	0.00	0.00	0.00	0.00	0.00	0.00	0.00	0.00

Table 53: Bedload rating curve data (continued)

Time (s)	Bedload discharge ($kg*m^{-1}*s^{-1}$)	Size Class 1	Size Class 2	Size Class 3	Size Class 4	Size Class 5	Size Class 6	Size Class 7	Size Class 8	Size Class 9	Size Class 10
178440	0.514	0.00	1.00	0.00	0.00	0.00	0.00	0.00	0.00	0.00	0.00
179640	0.514	0.00	1.00	0.00	0.00	0.00	0.00	0.00	0.00	0.00	0.00
180840	0.514	0.00	1.00	0.00	0.00	0.00	0.00	0.00	0.00	0.00	0.00
182040	0.514	0.00	1.00	0.00	0.00	0.00	0.00	0.00	0.00	0.00	0.00
183240	0.531	0.00	1.00	0.00	0.00	0.00	0.00	0.00	0.00	0.00	0.00
184440	0.531	0.00	1.00	0.00	0.00	0.00	0.00	0.00	0.00	0.00	0.00
185640	0.514	0.00	1.00	0.00	0.00	0.00	0.00	0.00	0.00	0.00	0.00
186840	0.531	0.00	1.00	0.00	0.00	0.00	0.00	0.00	0.00	0.00	0.00
188040	0.514	0.00	1.00	0.00	0.00	0.00	0.00	0.00	0.00	0.00	0.00
189240	0.514	0.00	1.00	0.00	0.00	0.00	0.00	0.00	0.00	0.00	0.00
190440	0.465	0.00	1.00	0.00	0.00	0.00	0.00	0.00	0.00	0.00	0.00
191640	0.348	0.00	1.00	0.00	0.00	0.00	0.00	0.00	0.00	0.00	0.00
192840	0.246	0.00	1.00	0.00	0.00	0.00	0.00	0.00	0.00	0.00	0.00
194040	0.003	0.00	1.00	0.00	0.00	0.00	0.00	0.00	0.00	0.00	0.00
195240	0.000	1.00	0.00	0.00	0.00	0.00	0.00	0.00	0.00	0.00	0.00
196440	0.000	1.00	0.00	0.00	0.00	0.00	0.00	0.00	0.00	0.00	0.00
197640	0.000	1.00	0.00	0.00	0.00	0.00	0.00	0.00	0.00	0.00	0.00
198840	0.000	1.00	0.00	0.00	0.00	0.00	0.00	0.00	0.00	0.00	0.00
200040	0.000	1.00	0.00	0.00	0.00	0.00	0.00	0.00	0.00	0.00	0.00
201240	0.000	1.00	0.00	0.00	0.00	0.00	0.00	0.00	0.00	0.00	0.00
202440	0.000	1.00	0.00	0.00	0.00	0.00	0.00	0.00	0.00	0.00	0.00
203640	0.000	1.00	0.00	0.00	0.00	0.00	0.00	0.00	0.00	0.00	0.00
204840	0.000	1.00	0.00	0.00	0.00	0.00	0.00	0.00	0.00	0.00	0.00
206040	0.000	1.00	0.00	0.00	0.00	0.00	0.00	0.00	0.00	0.00	0.00
207240	0.000	1.00	0.00	0.00	0.00	0.00	0.00	0.00	0.00	0.00	0.00
207720	0.000	1.00	0.00	0.00	0.00	0.00	0.00	0.00	0.00	0.00	0.00
208920	0.000	1.00	0.00	0.00	0.00	0.00	0.00	0.00	0.00	0.00	0.00
210120	0.000	1.00	0.00	0.00	0.00	0.00	0.00	0.00	0.00	0.00	0.00
211320	0.000	1.00	0.00	0.00	0.00	0.00	0.00	0.00	0.00	0.00	0.00

Table 54: Suspended load rating curve data

Time (s)	Suspended Sediment (kg/m^3)	Size Class 1	Size Class 2	Size Class 3	Size Class 4	Size Class 5	Size Class 6	Size Class 7	Size Class 8	Size Class 9	Size Class 10
0	0.055	1	0	0	0	0	0	0	0	0	0
1200	0.056	1	0	0	0	0	0	0	0	0	0
2400	0.058	1	0	0	0	0	0	0	0	0	0
3600	0.059	1	0	0	0	0	0	0	0	0	0
4800	0.059	1	0	0	0	0	0	0	0	0	0
6000	0.06	1	0	0	0	0	0	0	0	0	0
7200	0.06	1	0	0	0	0	0	0	0	0	0
8400	0.06	1	0	0	0	0	0	0	0	0	0
9600	0.06	1	0	0	0	0	0	0	0	0	0
10800	0.062	1	0	0	0	0	0	0	0	0	0
12000	0.064	1	0	0	0	0	0	0	0	0	0
13200	0.067	1	0	0	0	0	0	0	0	0	0
14400	0.069	1	0	0	0	0	0	0	0	0	0
15600	0.075	1	0	0	0	0	0	0	0	0	0
16800	0.111	1	0	0	0	0	0	0	0	0	0
18000	0.451	1	0	0	0	0	0	0	0	0	0
18873	0.467	1	0	0	0	0	0	0	0	0	0
20040	0.471	1	0	0	0	0	0	0	0	0	0
21240	0.474	1	0	0	0	0	0	0	0	0	0
22440	0.476	1	0	0	0	0	0	0	0	0	0
23640	0.476	1	0	0	0	0	0	0	0	0	0
24840	0.472	1	0	0	0	0	0	0	0	0	0
26040	0.467	1	0	0	0	0	0	0	0	0	0
27240	0.471	1	0	0	0	0	0	0	0	0	0
28440	0.471	1	0	0	0	0	0	0	0	0	0
29640	0.471	1	0	0	0	0	0	0	0	0	0
30840	0.469	1	0	0	0	0	0	0	0	0	0
32040	0.467	1	0	0	0	0	0	0	0	0	0
33240	0.447	1	0	0	0	0	0	0	0	0	0
34440	0.438	1	0	0	0	0	0	0	0	0	0
35640	0.359	1	0	0	0	0	0	0	0	0	0
36840	0.465	1	0	0	0	0	0	0	0	0	0
38040	0.497	1	0	0	0	0	0	0	0	0	0
39240	0.509	1	0	0	0	0	0	0	0	0	0
40440	0.511	1	0	0	0	0	0	0	0	0	0
41640	0.532	1	0	0	0	0	0	0	0	0	0
42840	0.546	1	0	0	0	0	0	0	0	0	0
44040	0.63	1	0	0	0	0	0	0	0	0	0
45240	0.939	1	0	0	0	0	0	0	0	0	0
46440	1.166	1	0	0	0	0	0	0	0	0	0
47640	1.277	1	0	0	0	0	0	0	0	0	0
48840	1.305	1	0	0	0	0	0	0	0	0	0
50040	1.302	1	0	0	0	0	0	0	0	0	0
51240	1.295	1	0	0	0	0	0	0	0	0	0
52440	1.244	1	0	0	0	0	0	0	0	0	0
53640	1.196	1	0	0	0	0	0	0	0	0	0
54840	1.146	1	0	0	0	0	0	0	0	0	0

Table 54: Suspended load rating curve data (continued)

Time (s)	Suspended Sediment (kg/m^3)	Size Class 1	Size Class 2	Size Class 3	Size Class 4	Size Class 5	Size Class 6	Size Class 7	Size Class 8	Size Class 9	Size Class 10
56040	1.097	1	0	0	0	0	0	0	0	0	0
57240	1.055	1	0	0	0	0	0	0	0	0	0
58440	1.016	1	0	0	0	0	0	0	0	0	0
59640	0.968	1	0	0	0	0	0	0	0	0	0
60840	0.939	1	0	0	0	0	0	0	0	0	0
62040	0.907	1	0	0	0	0	0	0	0	0	0
63240	0.859	1	0	0	0	0	0	0	0	0	0
64440	0.836	1	0	0	0	0	0	0	0	0	0
65640	0.814	1	0	0	0	0	0	0	0	0	0
66840	0.8	1	0	0	0	0	0	0	0	0	0
68040	0.778	1	0	0	0	0	0	0	0	0	0
69240	0.761	1	0	0	0	0	0	0	0	0	0
70440	0.742	1	0	0	0	0	0	0	0	0	0
71640	0.731	1	0	0	0	0	0	0	0	0	0
72840	0.719	1	0	0	0	0	0	0	0	0	0
74040	0.705	1	0	0	0	0	0	0	0	0	0
75240	0.689	1	0	0	0	0	0	0	0	0	0
76440	0.68	1	0	0	0	0	0	0	0	0	0
77640	0.669	1	0	0	0	0	0	0	0	0	0
78840	0.656	1	0	0	0	0	0	0	0	0	0
80040	0.645	1	0	0	0	0	0	0	0	0	0
81240	0.636	1	0	0	0	0	0	0	0	0	0
82440	0.625	1	0	0	0	0	0	0	0	0	0
83640	0.617	1	0	0	0	0	0	0	0	0	0
84840	0.608	1	0	0	0	0	0	0	0	0	0
86040	0.6	1	0	0	0	0	0	0	0	0	0
87240	0.592	1	0	0	0	0	0	0	0	0	0
88440	0.585	1	0	0	0	0	0	0	0	0	0
89640	0.577	1	0	0	0	0	0	0	0	0	0
90840	0.571	1	0	0	0	0	0	0	0	0	0
92040	0.565	1	0	0	0	0	0	0	0	0	0
93240	0.558	1	0	0	0	0	0	0	0	0	0
94440	0.55	1	0	0	0	0	0	0	0	0	0
95640	0.546	1	0	0	0	0	0	0	0	0	0
96840	0.54	1	0	0	0	0	0	0	0	0	0
98040	0.538	1	0	0	0	0	0	0	0	0	0
99240	0.528	1	0	0	0	0	0	0	0	0	0
100440	0.524	1	0	0	0	0	0	0	0	0	0
101640	0.519	1	0	0	0	0	0	0	0	0	0
102840	0.515	1	0	0	0	0	0	0	0	0	0
104040	0.511	1	0	0	0	0	0	0	0	0	0
105240	0.505	1	0	0	0	0	0	0	0	0	0
106440	0.499	1	0	0	0	0	0	0	0	0	0
107640	0.495	1	0	0	0	0	0	0	0	0	0
108840	0.491	1	0	0	0	0	0	0	0	0	0
110040	0.486	1	0	0	0	0	0	0	0	0	0
111240	0.482	1	0	0	0	0	0	0	0	0	0
112440	0.478	1	0	0	0	0	0	0	0	0	0
113640	0.474	1	0	0	0	0	0	0	0	0	0
114840	0.469	1	0	0	0	0	0	0	0	0	0

Table 54: Suspended load rating curve data (continued)

Time (s)	Suspended Sediment (kg/m^3)	Size Class 1	Size Class 2	Size Class 3	Size Class 4	Size Class 5	Size Class 6	Size Class 7	Size Class 8	Size Class 9	Size Class 10
116040	0.465	1	0	0	0	0	0	0	0	0	0
117240	0.465	1	0	0	0	0	0	0	0	0	0
118440	0.461	1	0	0	0	0	0	0	0	0	0
119640	0.451	1	0	0	0	0	0	0	0	0	0
120840	0.442	1	0	0	0	0	0	0	0	0	0
122040	0.43	1	0	0	0	0	0	0	0	0	0
123240	0.421	1	0	0	0	0	0	0	0	0	0
124440	0.413	1	0	0	0	0	0	0	0	0	0
125640	0.397	1	0	0	0	0	0	0	0	0	0
126840	0.393	1	0	0	0	0	0	0	0	0	0
128040	0.397	1	0	0	0	0	0	0	0	0	0
129240	0.389	1	0	0	0	0	0	0	0	0	0
130440	0.355	1	0	0	0	0	0	0	0	0	0
131640	0.359	1	0	0	0	0	0	0	0	0	0
132840	0.351	1	0	0	0	0	0	0	0	0	0
134040	0.334	1	0	0	0	0	0	0	0	0	0
135240	0.32	1	0	0	0	0	0	0	0	0	0
136440	0.33	1	0	0	0	0	0	0	0	0	0
137640	0.362	1	0	0	0	0	0	0	0	0	0
138840	0.359	1	0	0	0	0	0	0	0	0	0
140040	0.351	1	0	0	0	0	0	0	0	0	0
141240	0.344	1	0	0	0	0	0	0	0	0	0
142440	0.341	1	0	0	0	0	0	0	0	0	0
143640	0.337	1	0	0	0	0	0	0	0	0	0
144840	0.33	1	0	0	0	0	0	0	0	0	0
146040	0.327	1	0	0	0	0	0	0	0	0	0
147240	0.324	1	0	0	0	0	0	0	0	0	0
148440	0.324	1	0	0	0	0	0	0	0	0	0
149640	0.317	1	0	0	0	0	0	0	0	0	0
150840	0.317	1	0	0	0	0	0	0	0	0	0
152040	0.307	1	0	0	0	0	0	0	0	0	0
153240	0.307	1	0	0	0	0	0	0	0	0	0
154440	0.304	1	0	0	0	0	0	0	0	0	0
155640	0.304	1	0	0	0	0	0	0	0	0	0
156840	0.294	1	0	0	0	0	0	0	0	0	0
158040	0.294	1	0	0	0	0	0	0	0	0	0
159240	0.294	1	0	0	0	0	0	0	0	0	0
160440	0.294	1	0	0	0	0	0	0	0	0	0
161640	0.282	1	0	0	0	0	0	0	0	0	0
162840	0.282	1	0	0	0	0	0	0	0	0	0
164040	0.279	1	0	0	0	0	0	0	0	0	0
165240	0.279	1	0	0	0	0	0	0	0	0	0
166440	0.273	1	0	0	0	0	0	0	0	0	0
167640	0.267	1	0	0	0	0	0	0	0	0	0
168840	0.267	1	0	0	0	0	0	0	0	0	0
170040	0.264	1	0	0	0	0	0	0	0	0	0
171240	0.264	1	0	0	0	0	0	0	0	0	0
172440	0.264	1	0	0	0	0	0	0	0	0	0
173640	0.261	1	0	0	0	0	0	0	0	0	0
174840	0.261	1	0	0	0	0	0	0	0	0	0

Table 54: Suspended load rating curve data (continued)

Time (s)	Suspended Sediment (kg/m^3)	Size Class 1	Size Class 2	Size Class 3	Size Class 4	Size Class 5	Size Class 6	Size Class 7	Size Class 8	Size Class 9	Size Class 10
176040	0.253	1	0	0	0	0	0	0	0	0	0
177240	0.253	1	0	0	0	0	0	0	0	0	0
178440	0.253	1	0	0	0	0	0	0	0	0	0
179640	0.253	1	0	0	0	0	0	0	0	0	0
180840	0.253	1	0	0	0	0	0	0	0	0	0
182040	0.253	1	0	0	0	0	0	0	0	0	0
183240	0.256	1	0	0	0	0	0	0	0	0	0
184440	0.256	1	0	0	0	0	0	0	0	0	0
185640	0.253	1	0	0	0	0	0	0	0	0	0
186840	0.256	1	0	0	0	0	0	0	0	0	0
188040	0.253	1	0	0	0	0	0	0	0	0	0
189240	0.253	1	0	0	0	0	0	0	0	0	0
190440	0.245	1	0	0	0	0	0	0	0	0	0
191640	0.226	1	0	0	0	0	0	0	0	0	0
192840	0.211	1	0	0	0	0	0	0	0	0	0
194040	0.18	1	0	0	0	0	0	0	0	0	0
195240	0.161	1	0	0	0	0	0	0	0	0	0
196440	0.145	1	0	0	0	0	0	0	0	0	0
197640	0.15	1	0	0	0	0	0	0	0	0	0
198840	0.136	1	0	0	0	0	0	0	0	0	0
200040	0.143	1	0	0	0	0	0	0	0	0	0
201240	0.111	1	0	0	0	0	0	0	0	0	0
202440	0.109	1	0	0	0	0	0	0	0	0	0
203640	0.109	1	0	0	0	0	0	0	0	0	0
204840	0.115	1	0	0	0	0	0	0	0	0	0
206040	0.12	1	0	0	0	0	0	0	0	0	0
207240	0.115	1	0	0	0	0	0	0	0	0	0
207720	0.117	1	0	0	0	0	0	0	0	0	0
208920	0.115	1	0	0	0	0	0	0	0	0	0
210120	0.114	1	0	0	0	0	0	0	0	0	0
211320	0.114	1	0	0	0	0	0	0	0	0	0

Vita

Daniel Johnson was born and raised in Columbia, South Carolina. He attended Brookland Cayce High School and graduated in 2001, after which he attended Clemson University. At Clemson he majored in Civil Engineering and minored in Environmental Engineering and Science, graduating in the spring of 2005. After graduation, Daniel pursued a career in Charlotte, North Carolina providing technical support in the preliminary assessment, design, construction, and monitoring of stream and wetland restoration projects, preparing FEMA letters of map revision, preparing no-rise certifications, and designing urban stormwater and best management practices. In the fall of 2008, he started the graduate program at the University of Tennessee. Daniel's graduate research, sponsored by a grant from the Office of Surface Mining, involved the application of a one-dimensional sediment transport model to four streams located in East Tennessee. Daniel's thesis research was concerned with the application of a two-dimensional sediment transport model to a stream with coarse bed substrate and complex morphology to predict reach, local, and point scale bed elevation change. Daniel graduated with a 4.0 GPA and earned a Master's of Science in Environmental Engineering in December of 2008.